



universität
wien

MASTERARBEIT

Titel der Masterarbeit

„Establishment and evaluation of a
feline foamy virus subviral particle-based vaccine strategy
for induction of
neutralizing antibodies against HIV-1“

verfasst von

Gerald Schneikart, BSc

angestrebter akademischer Grad

Master of Science (MSc)

Wien, 2014

Studienkennzahl lt. Studienblatt:

A 066 834

Studienrichtung lt. Studienblatt:

Masterstudium Molekulare Biologie

Betreut von:

ao. Univ. Prof. Dr. Timothy Skern

ROBERT KOCH INSTITUT



Supervisors at the FG 18, „Zentrum für HIV und andere Retroviren“

Robert Koch-Institute

Nordufer 20, 13353 Berlin, Germany

Head of the FG 18 Priv.-Doz. Dr. Norbert Bannert

Group leader Dr. Joachim Denner

PhD student Dipl.-Ing. Michael Mühle

Acknowledgements

I hereby want to express my honest gratitude to Dr. Joachim Denner. He offered me the terrific opportunity to carry out my Master's thesis in the fields of HIV vaccine research at the Robert Koch-Institute and he always provided unrestrained support.

I would particularly like to thank my firsthand supervisor Dipl.-Ing. Michael Mühle for professionally teaching me scientific working. Without his unfailing dedication to his job, my thesis would have developed another outcome. Especially his persistent patience as a mentor was eminent and allowed the achievement of rapid progress and many goals. He did a great job as a teacher and made a lot of time for explanations and demonstrations on experimental work. All in all, he was the most influential person to me during the nine months of working that constituted an outstanding work experience.

I also want to thank Priv.-Doz. Dr. Norbert Bannert. I really appreciate his reliable support as a supervisor.

Thank you to ao. Univ. Prof. Dr. Timothy Skern for being my supervisor in Vienna.

I owe special thanks to Fr. Regina Staszuck of the DLE Internationale Beziehungen Universität Wien. She was responsible for the scholarship Kurzfristige Auslandsstipendien – KWA. She was incredibly committed and helpful despite complications during the application process thanks to colleagues in Vienna.

I hereby want to take a chance and say a big Thank You to my beloved parents, Inge and Friedrich Schneikart. Without their financial support and all their support during my life so far, I would not be working on my Master's thesis these days. They always believe in me and keep me encouraged in achieving my goals.

And finally, I also say Thank You to my dearest friends, Martina Zawodnik and Thomas Blank. As a personal fitness coach, Martina provided physical education to me that kept me balanced during all the years of studying. Since I am an only child, the close long-term friendship with Thomas gave rise to a brotherhood-like relationship over the years.

Abstract

35 million people died due to the acquired immunodeficiency syndrome (AIDS) since the outbreak of the HIV pandemic. Despite intensive research, developing an immunogen to induce broadly neutralizing antibodies (bnAbs) against HIV remains a challenge, although about 10 - 30 % of infected individuals develop bnAbs against HIV-1 on average 2.5 years after infection. Two of them are 2F5 and 4E10, targeting the membrane proximal external region (MPER) of the transmembrane envelope protein (TM) gp41. Previous studies on the non-pathogenic retrovirus feline foamy virus (FFV) revealed immunogenic regions with a bipartite motif in its TM protein, gp48, equivalent to the locations of the 2F5 and 4E10 epitopes in HIV gp41. In order to use the FFV TM protein as HIV epitope scaffold, the 2F5 and 4E10 epitopes were integrated into the full-length FFV Env backbone by replacing the equivalent sequences. After transfection of HEK293T cells, it could be shown that the chimeric FFV/HIV-1 proteins are produced and released into the cell culture supernatants. Furthermore, the secreted material has properties typical for subviral particles (SVPs). This is in line with the finding that FFV Env protein expression is sufficient to induce budding in absence of any other FV proteins. In order to allow evaluation of the potential of those hybrid SVPs as HIV-1 vaccines by administration in a DNA-prime/SVP-boost regimen in rats, sufficient amounts were required. In the frame of this thesis, efficient protocols for large-scale production of SVPs were established. This was achieved by subcloning the respective sequences into retroviral transfer vectors and systematic optimization of transfection, virus production and concentration protocols to obtain high titer stocks of infectious vesicular stomatitis virus protein G (VSV-G) pseudo-typed viruses. Transduction of various cell lines revealed CRFK cells as suitable producer cells for the production of the intended SVPs. Immunoprecipitation of the native antigens with mAb 2F5 and mAb 4E10 demonstrated that the respective epitopes are accessible. Application of transmission electron microscopy using the method of negative staining confirmed successful SVP production which was further optimized by testing different commercially available expression media. First steps to scale up the production process using Corning® HYPERFlasks® have also been accomplished. The established protocols for large-scale production of hybrid FFV/HIV-1 SVPs carrying the 2F5 and 4E10 epitopes allow testing the potential of a novel recombinant vaccine strategy against HIV-1 infections.

Table of contents

1	Introduction	1
1.1	Human immunodeficiency virus-1	1
1.1.1	HIV and AIDS	1
1.1.2	Genome	3
1.1.3	Replication	4
1.1.4	HIV-1 Env and broadly neutralizing antibodies against the MPER of gp41	6
1.2	Feline foamy virus	9
1.2.1	Foamy viruses	9
1.2.2	Feline foamy virus genome and Env	10
1.3	Goal of this thesis	12
2	Materials	17
2.1	Equipment	17
2.2	Consumables	18
2.3	Chemicals	18
2.4	Kits	19
2.5	Buffers and solutions	19
2.5.1	SDS-PAGE and immunoblotting	19
2.5.2	Agarose gel-electrophoresis	20
2.5.3	Lysis buffers	20
2.5.4	Other buffers	20
2.6	Protein and DNA ladders	20
2.7	Enzymes	20
2.7.1	Restriction enzymes	20
2.7.2	Polymerases	21
2.7.3	Other enzymes	21
2.8	Primers	21
2.9	Probe for real-time PCR	22
2.10	Plasmids	22
2.11	Antibodies and antisera	23
2.11.1	Primary antibodies	23
2.11.2	Antisera	23

2.11.3	Secondary antibodies	23
2.12	Media	23
2.12.1	Media for bacteria	23
2.12.2	Media for cell cultures	24
2.12.3	Freezing media for eukaryotic cells	24
2.13	Prokaryotic strains	24
2.14	Eukaryotic strains	25
2.15	Software	25
3	Methods	26
3.1	Molecular biological methods	26
3.1.1	PCR for subcloning	26
3.1.2	Mutagenesis-PCR	26
3.1.3	Colony PCR	27
3.1.4	Reverse transcription-PCR (RT-PCR)	28
3.1.5	Real-time PCR	28
3.1.6	Subcloning with the In-Fusion® HD Protocol from Clontech	29
3.1.7	Ligation and self-circularization	31
3.1.8	Restriction digestion	31
3.1.9	Isolation of plasmid DNA from E.coli	31
3.1.10	Isolation of genomic DNA from eukaryotic cells	31
3.1.11	Isolation of RNA from eukaryotic cells	32
3.1.12	Determination of DNA concentrations	32
3.1.13	Sequencing and analysis of cloned plasmid constructs	32
3.1.14	Agarose gel-electrophoresis	32
3.1.15	Extraction and purification of DNA fragments from agarose gels	33
3.1.16	Transformation of competent bacteria	33
3.1.17	Preparation of glycerol stocks of single clones for long- term storage	33
3.2	Cell cultural methods	33
3.2.1	Thawing and establishing of eukaryotic cells	33
3.2.2	Subculturing of cells	34
3.2.3	Determination of cell numbers and viabilities	34
3.2.4	Freezing cells	35
3.2.5	Transfection of cells	35
3.2.6	Transduction of cells	35
3.2.7	Concentration of virus particles	36
3.2.8	Concentration of cell culture supernatants containing subviral particles	36
3.2.9	Large-scale production of subviral particles	36

3.3	Biochemical and immunological methods.....	37
3.3.1	Preparation of cell lysates.....	37
3.3.2	Determination of protein concentrations	37
3.3.3	SDS-PAGE	37
3.3.4	Immunoblot.....	38
3.3.5	Blot stripping.....	38
3.3.6	Immunoprecipitation of subviral particles.....	39
3.4	Negative staining electron microscopy.....	39
4	Results.....	40
4.1	Subcloning of the FFV EnvG2 and chimeric FFV/HIV-1 EnvG2 x MPER1 and MPER2 DNA sequences into a retroviral vector	40
4.1.1	Generation of MP71 FFV EnvG2 and chimeric MP71 FFV/HIV-1 MPER1 and MPER2 expression plasmids.....	43
4.1.2	Testing the FFV EnvG2 and chimeric FFV/HIV-1 MPER1 and MPER2 expression constructs for protein expression	45
4.2	Establishment of efficient protocols for virus production	47
4.2.1	Transfection optimization for virus production	47
4.2.2	Testing additives for enhanced virus production.....	50
4.2.3	Testing methods to concentrate virus.....	52
4.3	Optimization of retroviral infection.....	53
4.4	Testing the established protocols for virus production and infection for applicability on the FFV EnvG2 and chimeric FFV/HIV-1 MPER1 and MPER2 constructs.....	57
4.4.1	Real-time PCR for determination of virus titers.....	57
4.4.2	Applicability of the established protocols on the MP71- EnvG2 and pLenti-EnvG2 constructs	60
4.5	Production of subviral particles.....	63
4.5.1	Finding a suitable target cell line for stable FFV EnvG2 and chimeric FFV/HIV-1 MPER1 and MPER2 protein expression	63
4.5.2	CRFK cells transduced with MP71-EnvG2, MPER1 and MPER2 virus release subviral particles	66
4.5.3	Characterization of EnvG2, MPER1 and MPER2 subviral particles by immunoprecipitation	67
4.5.4	Transmission electron microscopy of concentrated cell culture supernatants supposed to contain subviral particles	70
4.5.5	Optimization of subviral particle production	72
4.5.6	Do lysine-to-arginine mutations in FFV E1p increase SVP-release?	75

5	Discussion.....	79
5.1	Transfection optimization for high virus titers	79
5.2	MP71-infection of CRFK cells seemed to be most suitable for the establishment of cell lines stably expressing EnvG2, MPER1 and MPER2 protein.....	81
5.3	Transduced CRFK cells release chimeric FFV/HIV-1 MPER1 and MPER2 SVPs that are recognized by 2F5 and 4E10	83
5.4	Some expression media increase EnvG2 protein expression	84
5.5	Lysine-to-arginine mutations in FFV Elp decrease subviral particle release.....	85
5.6	Immunization studies will reveal the potential of hybrid FFV/HIV-1 SVPs to induce neutralizing antibodies against HIV-1.....	86
6	Zusammenfassung	87
7	References.....	88

1 Introduction

1.1 Human immunodeficiency virus-1

1.1.1 HIV and AIDS

Most likely, the acquired immunodeficiency syndrome (AIDS) was present in Africa for many decades. In 1981, it emerged in the human population as an outbreak of *Pneumocystis carinii pneumonia* among homosexual men in the United States [1]. AIDS is caused by the lentivirus HIV that belongs to the member of *Retroviridae*. The equivalent agent in apes and monkeys is the simian immunodeficiency virus (SIV). HIV is transmitted primarily by sexual intercourse, injection of infected blood or blood-derived products and by mother-to-child transmission [2, 3].

After an acute infection in which CD4⁺ T-cells are massively depleted in the genital tissue and the gut-associated lymphoid tissue (GALT), replication starts in resting CD4⁺ T-cells of the genital mucosa in the case of sexual transmission [4]. A chronic infection characterized by a progressively dying immune system follows [5].

The first 10 days represent the initial phase or eclipse phase, when viral RNA is below detection level in the blood circulation. It is followed by the acute phase which is characterized by high virus production in activated CD4⁺ T-cells (Figure 1) [6]. When control by the cellular immune system sets in, infection proceeds to an asymptomatic period in which CD4⁺ T-cell numbers slowly but steadily decline [3]. HIV-1 infection is associated by a chronic immune stimulation increasing T-cell turnover, production of pro-inflammatory cytokines and chemokines and activation of cytotoxic T-cells (CTLs) and polyclonal B-cells [5, 7]. As a consequence, the humoral immune response begins to show weeks after infection, resulting in seropositivity. Together, CTL and antibody responses against HIV reduce the plasma viral load to a stable level, called the viral set point, at which patients are less infective than during the acute phase of infection [8]. However, virus is never completely neutralized due to escape mutations of HIV. The asymptomatic phase can last from several months to more than 10 years before patients develop AIDS and finally die because of opportunistic infections with usually harmless pathogens [9].

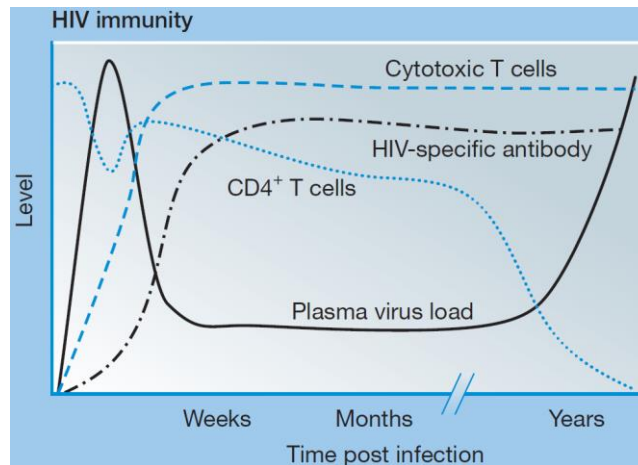


Figure 1: Time course of a HIV infection [3]

During the acute phase of infection, the plasma viral load is highest because of ongoing replication in CD4⁺ T-cells. A chronic infection of the immune system follows where CD4⁺ T-cells continually die. Weeks after infection, the plasma viral load is reduced to a stable level because cytotoxic T-cells are activated and the humoral immune system sets in. Patients develop antibodies against HIV and become seropositive. However, escape mutations prevent complete clearance of HIV. The chronic asymptomatic phase can last more than 10 years before opportunistic infections occur due to AIDS.

Since the beginning of the epidemic, approximately 70 million people have been infected and 35 million have died of AIDS. In 2011, 1.7 million people died of AIDS-related illnesses worldwide and about 34 million people were living with HIV that constitutes 0.8 % of the world population (Figure 2). However, sub-Saharan Africa remains most severely affected as nearly 1 in every 20 adults (4.9 %) lives with HIV which accounts for 69 % of the people living with HIV worldwide [10].

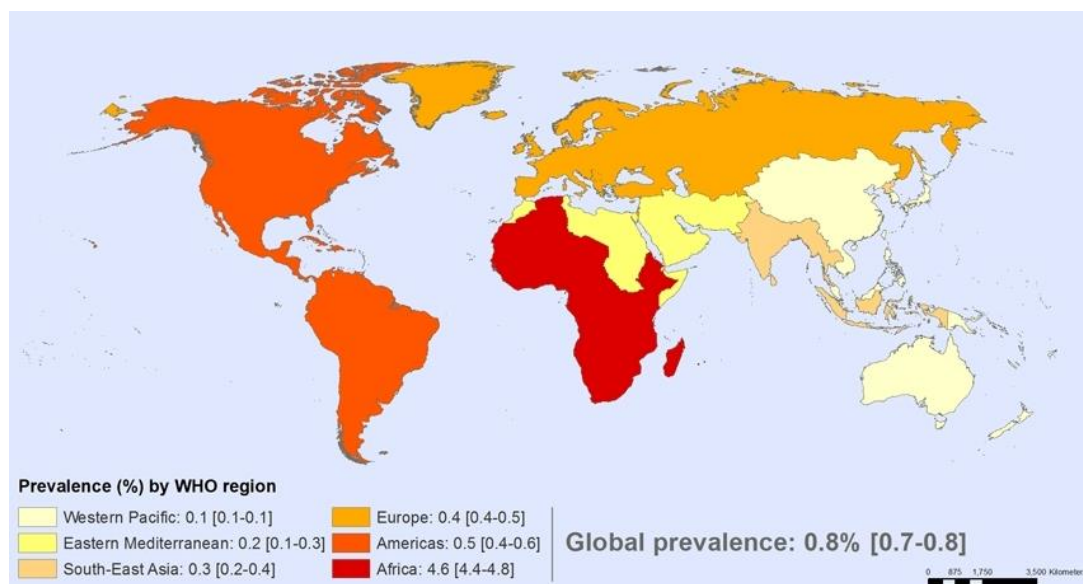


Figure 2: Worldwide prevalence of HIV [10]

1.1.2 Genome

HIV is an enveloped single-stranded positive sense RNA virus with a genome of 9.5 kb in length. Like all retroviruses, the genome encodes Gag (further cleaved into matrix, capsid and nucleocapsid), Pol (cleaved into protease, reverse transcriptase and integrase) and Env (processed into gp120 and gp41) (Figure 3).

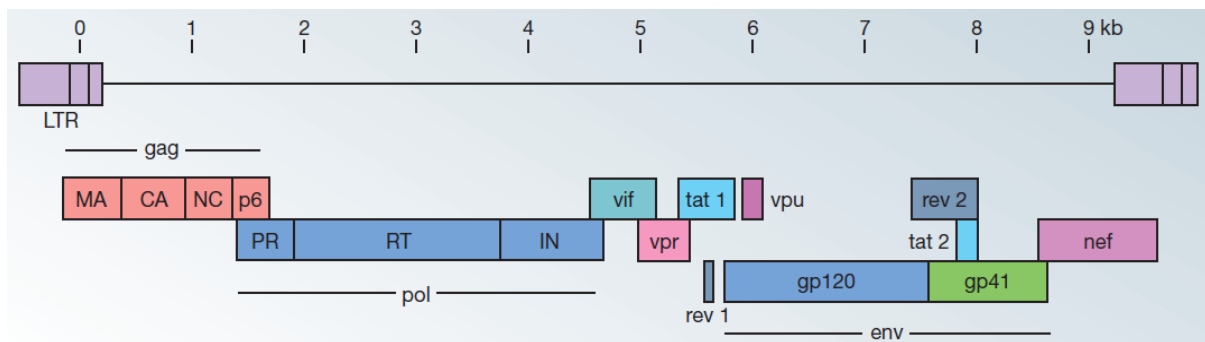


Figure 3: HIV-1 genome organization [3]

LTR: long terminal repeat, gag: group specific antigen, pol: polymerase, env: envelope protein, MA: matrix protein, CA: capsid protein, NC: nucleocapsid protein, PR: protease, RT: reverse transcriptase, IN: integrase, vif: viral infectivity factor, vpr: viral protein R, tat: transactivator of transcription, rev: regulator of virion, vpu: viral protein U, gp120/41: glycoprotein120/41, nef: negative factor

In addition, the HIV-1 genome encodes several accessory and regulatory proteins:

Tat (trans-activator of transcription) increases the production of full length HIV-1 mRNA transcripts that are packaged into viral particles. Transcriptional elongation is accomplished by binding to an RNA stem-loop structure (Tat activation region, TAR) at the 5'-terminus of the viral mRNA [11].

Rev (regulator of virion) facilitates the transport of unspliced viral mRNAs encoding Gag, Pol and Env from the nucleus to the cytoplasm by binding to the Rev-response element (RRE). It is responsible for regulating the switch from early transcription of regulatory proteins to late structural proteins [12].

Nef (negative factor) contributes to high viral loads and promotes activation of resting T-cells [13]. In uninfected bystander CD4⁺ T-cells it induces apoptosis [14, 15] and down-regulates CD4 and MHC-I. Therefore, infected cells can evade the immune system [16].

Vif (viral infectivity factor) recruits ubiquitinating proteins to apolipoprotein B mRNA-editing enzyme catalytic polypeptide 3 (APOBEC3G) and thereby predestines it for

proteasomal degradation [17]. Human APOBEC3G is a cytidine deaminase that induces multiple C-to-U deaminations in minus-strands of HIV-1 proviral DNA derived from viral particles carrying that enzyme [18].

Vpr (viral protein R) induces cell cycle arrest in G2 and apoptosis. Furthermore, it allows entry of the viral pre-integration complex into the nucleus of non-dividing cells [19].

Vpu (viral protein U) antagonizes tetherin which inhibits the release of fully assembled virions at the cell membrane [20]. Additionally, it targets CD4 to proteasomes for degradation [21].

1.1.3 Replication

Primary targets of HIV-1 are CD4⁺ T-cells [22] and cells of the macrophage and monocyte lineage [4]. Binding of gp120 to the CD4 receptor triggers conformational changes leading to the exposure of the CCR5 or CXCR4 co-receptor binding sites. Which co-receptor is actually bound depends on the amino acid sequence of the V3 loop of the SU domain (gp120). Further conformational changes in gp41 lead to the six-helix bundle-formation that initiates the fusion of the cellular and viral membranes (Figure 4) [23].

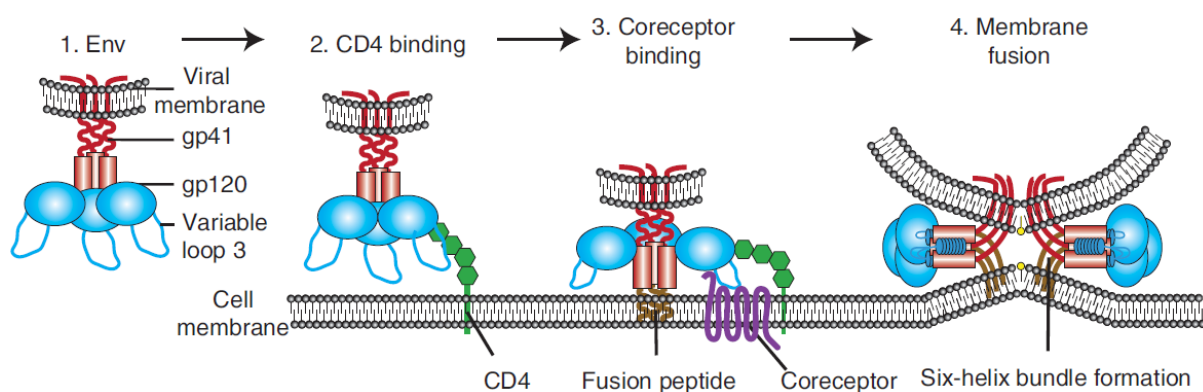


Figure 4: HIV-1 entry [24]

Gp120 binds the CD4 receptor that triggers conformational changes resulting in co-receptor binding. The V3 loop of SU plays a role at the decision between the co-receptors, CCR5 or CXCR4. The fusion peptide of gp41 inserts into the host membrane. The subsequent sex-helix bundle-formation of gp41 brings the viral and host membrane into close proximity and induces them to fuse.

After release into the cytoplasm, active reverse transcriptase (RT) transforms the RNA genome into one pro-viral DNA copy (Figure 5). The provirus migrates into the host cell nucleus where it randomly integrates into the host cell genome. The cellular machinery transcribes the proviral DNA into spliced mRNAs for viral protein expression and into full-length single stranded RNA. Viral proteins and two copies of full-length RNA are assembled to viral particles at the cell surface where they are released as immature and noninfectious virions [2]. Only after cleavage of Gag by viral protease, HIV particles acquire infectivity [25].

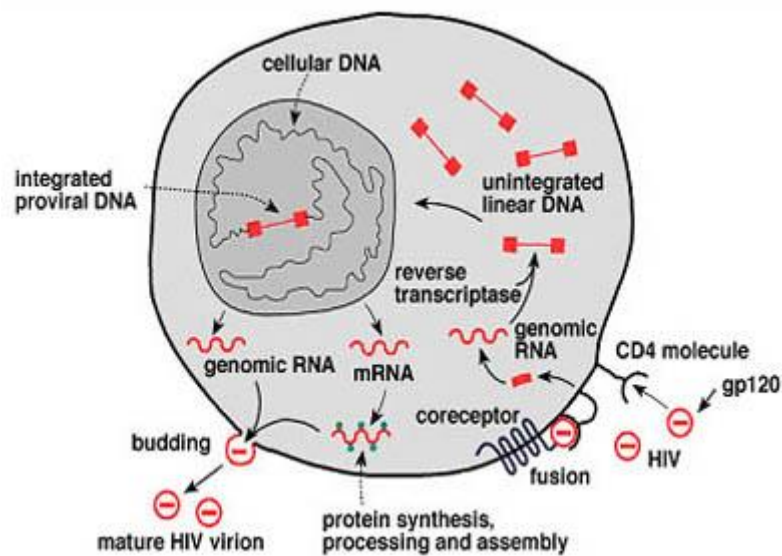


Figure 5: Simplified replication cycle of HIV-1 [26]

Binding of gp120 to CD4 receptor triggers the fusion process. After release of the viral RNA genome into the cytoplasm, reverse transcriptase produces proviral DNA that randomly integrates into the host cell genome. The cell machinery starts viral protein expression and the production of two full-length single stranded RNA copies. Virus particles are assembled at the cytoplasm membrane and bud as noninfectious virions. Viral protease cleaves Gag and thereby infectivity is acquired.

Single HIV-1 particles (Figure 6) comprise an internal cone-shaped capsid (p24, CA) surrounded by a lipid membrane that is wrapped on a scaffold of matrix proteins (p17, MA). Approximately 15 trimers of gp160 (gp120 + gp41) form spikes on a single virion's surface [27]. The lipid membrane originates from the virus-producing host cell. As a consequence, membrane proteins are embedded in the viral lipid bilayer. The CA contains two copies of the HIV RNA genome that are associated with the nucleocapsid (p7, NC), reverse transcriptase and regulatory proteins Nef, Vif and Vpr.

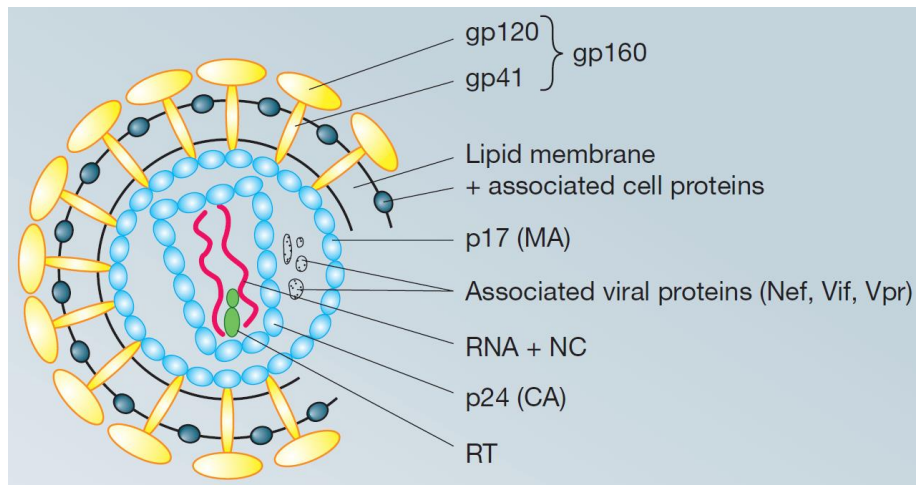


Figure 6: Structure of a single HIV-1 virion [3]

MA: matrix, NC: nucleocapsid, CA: capsid, RT: reverse transcriptase, Nef: negative factor, Vif: viral infectivity factor, Vpr: viral protein R

1.1.4 HIV-1 Env and broadly neutralizing antibodies against the MPER of gp41

The 160 kD glycoprotein Env (gp160) is synthesized in the rough endoplasmic reticulum (Figure 7A) and cleaved into gp120 (SU) and gp41 (TM) by a cellular furin protease in the Golgi apparatus [28, 29]. Gp120 and gp41 assemble into hetero-trimers and form spikes on the viral surface (Figure 7B).

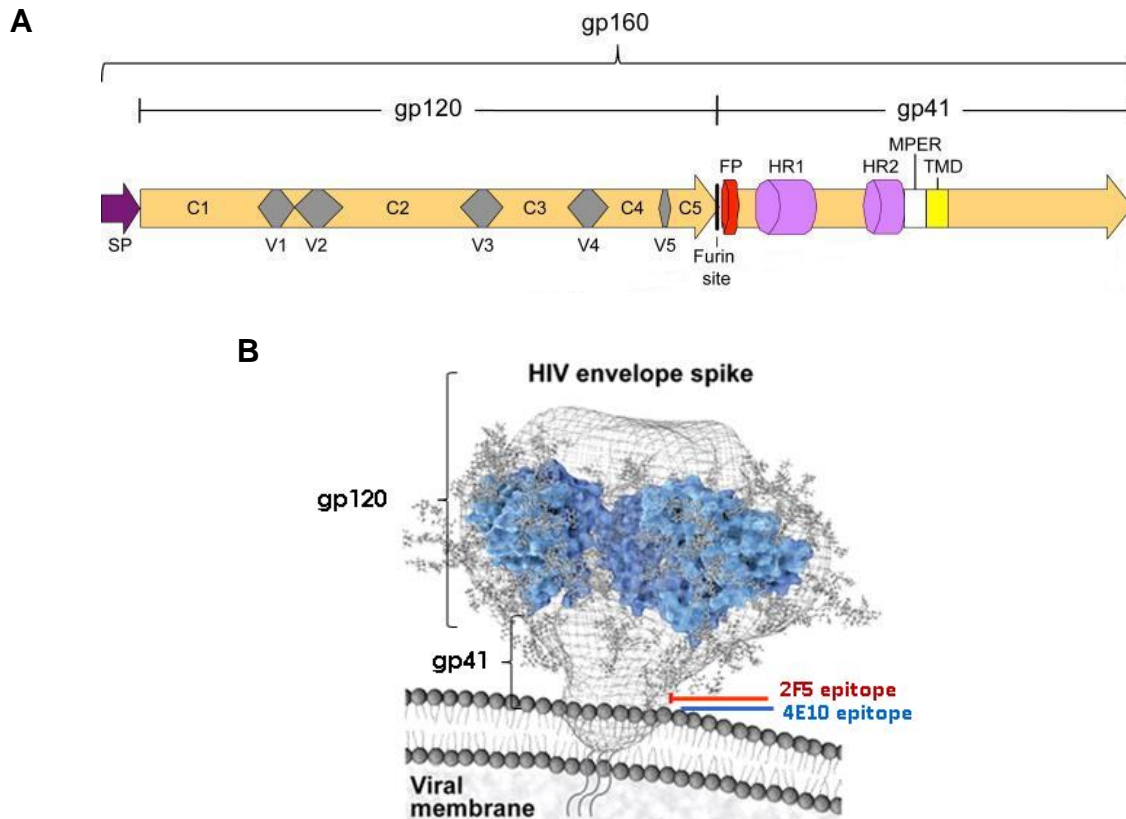


Figure 7: HIV-1 Env (gp160) [30] and a single HIV-1 Env spike [31]

A) Gp160 consists of the surface protein gp120, the transmembrane envelope protein gp41 and the signal peptide (SP). Gp120 and gp41 are cleaved by furin protease at the furin site after transportation to the Golgi apparatus. Depicted are the different regions of gp120 and gp41. Gp120 comprises five constant regions (C1-5) and five variable regions (V1-5). The gp41 protein contains a fusion peptide (FP), two helical regions (HR1, HR2), a membrane proximal external region (MPER) and a transmembrane domain (TMD). **B)** 3-dimensional structure of a single heterotrimeric HIV-1 envelope spike consisting of gp120 and gp41. The approximate locations of the 2F5 (red) and 4E10 (blue) epitopes in the viral spike are indicated.

After binding of gp120 to CD4 and the co-receptor, conformational changes of gp41 cause the fusion peptide to intrude into the host cell membrane (Figure 4). The N-terminal helical region (NHR) and the C-terminal helical region (CHR) interact to form the six-helix bundle formation (Figure 4 and 8) where the viral and host cell membranes are in close proximity, immediately before fusion.

So far, the development of an effective HIV-1 vaccine remained unsuccessful. Antiviral immune mechanisms fail to clear the virus, although neutralizing antibodies (nAbs) are induced weeks after infection [32]. The viral load is merely reduced to a lower stable level (viral set-point, Figure 1). This is due to the fact that the virus latently infects memory T-cells by integrating into host chromosomes [7]. Another rea-

son is the high mutation rate of HIV-1 that produces escape mutations [33]. Nevertheless, minimally accessible epitopes targeted by broadly neutralizing antibodies (bnAbs) exist and 10 - 30 % of infected patients even develop bnAbs [34, 35] on average 2.5 years after infection [36-38]. Targets of bnAbs are the glycan structure, the V2/V3 loop, the CD4 binding site of the SU domain or regions of the TM domain. The conserved membrane proximal external region (MPER) [39] contains the epitopes recognized by four such bnAbs: Z13, 10E8, 2F5 and 4E10 with a neutralization breadth of <20 %, 97 %, 48 % and 88 %, respectively [40]. The relative positions of the 2F5 (ELDKWAS) and 4E10 (WFNITNWLW) epitope sequences [41] in the MPER are depicted in Figure 8. They neutralize HIV-1 in different stages of infection by interacting with fusion intermediates of gp41. Accordingly, neutralization by 2F5 and 4E10 occurs mainly after receptor binding because their epitopes are undisclosed in free virions. Furthermore, binding of the 2F5 and 4E10 epitopes hinders membrane fusion [42-44].

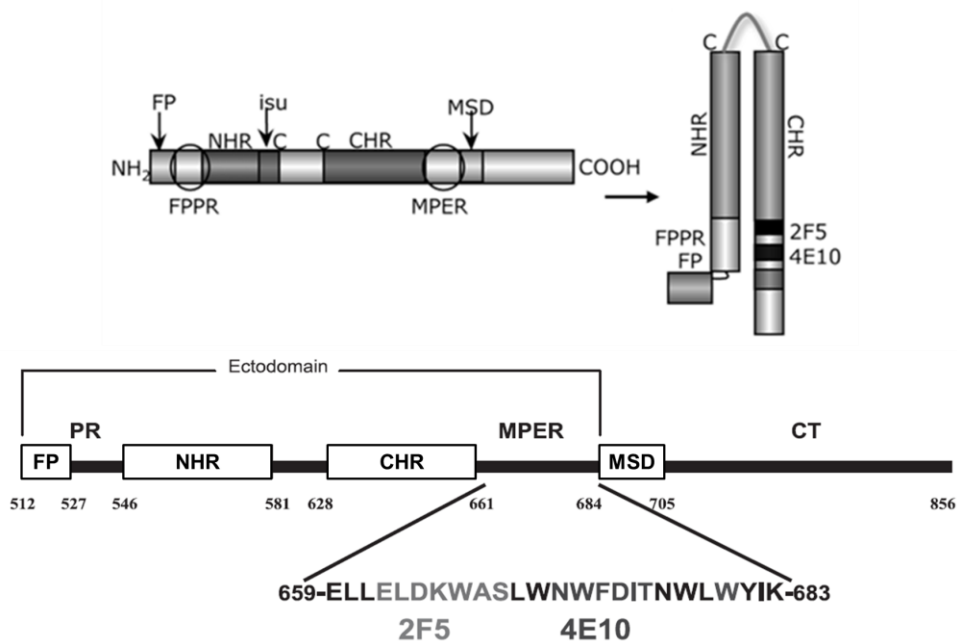


Figure 8: Functional domains of gp41 (TM) and their conformational changes during infection [41, 45]

The gp41 protein consists of the fusion peptide (FP), the fusion peptide proximal region (FPPR), the N-terminal helical region (NHR), the immunosuppressive domain (isu), Cys-Cys-loop (C-C), the C-terminal helical region (CHR) and the membrane proximal external region (MPER). C-terminally of the MPER are the membrane spanning domain (MSD) and the cytoplasmic tail (CT). The conserved epitopes recognized by the broadly neutralizing antibodies 2F5 (ELDKWAS) and 4E10 (WFNITNWLW) are located within the MPER. In order to facilitate the fusion of viral and host cell membranes, gp41 undergoes conformational changes including an interaction of the NHR and CHR. The so called six-helix bundle formation brings both membranes into close proximity initiating fusion pore formation.

The MPER is important for both, the fusion process of the viral and host cell membranes [39, 46, 47] and for the incorporation of Env into virions [39] by a cholesterol binding domain at the C-terminal end of the MPER (LWYIK) [48]. The close proximity of the MPER and the viral membrane implies that 2F5 and 4E10 might interact with the viral membrane during neutralization, thereby turning it into a key component of both epitopes [41]. It was shown that 2F5 and 4E10 have a long complementarity determining region (CDR-H3) [49-52] that may interact with the viral membrane [49, 51]. As the FPPR and MPER interact during infection (Figure 8), they play a crucial role in infectivity [46]. The FPPR supports epitope binding and thereby affinity of 2F5 [47].

Infection mainly occurs via mucosal transmission in pluri-stratified epithelium (e.g., vagina, exocervix, foreskin and anus). Dendritic cells are the first targets of HIV-1 before dissemination in the submucosa follows [4, 53]. Interestingly, peripheral blood mononuclear cells (PBMC) infected with HIV-1 produce virus that is internalized by epithelial cells and cross the epithelial barrier by transcytosis [54]. HIV-1 binds to epithelial cells using the alternative receptor glycosphingolipidgalactosylceramide. This interaction is mediated by the ELDKWA epitope of 2F5 that is also recognized by some IgM or dimeric IgA antibodies induced against Env; such antibodies could block mucosal transmission of HIV-1 [54].

All attempts to induce 2F5- and 4E10-like antibodies by several immunization strategies have been unsuccessful. Antibodies induced by immunization with recombinant antigens presenting the 2F5 and 4E10 epitopes in various protein scaffolds lacked broadly neutralizing activity [55-57]. The characteristics of 2F5 and 4E10 suggest that successful induction requires antigens with the respective epitopes presented in their natural conformation and in an environment that resembles fusion intermediates of the HIV-1 infection after receptor binding.

1.2 Feline foamy virus

1.2.1 Foamy viruses

Foamy viruses (FV) belong to the subfamily of *Spumaretrovirinae*, a genus of *Retroviridae* family. FVs co-evolved with their natural hosts. They are endemic to most non-human primates, cat, cattle and horse [58]; man is not a natural host. In the 70s, prototype foamy virus (PFV) was isolated which was earlier known as human foamy virus (HFV). It shows high sequence homology to chimpanzee foamy viruses

(SFVcpz) suggesting zoonotic transmission from chimpanzee to humans [59-61], although human-to-human transmissions remained undetected [59]. FV infections are persistent [62] but apathogenic in natural hosts as well as in humans [62]. This fact is in stark contrast to the virus' high cytopathic nature in vitro where infection can end in the formation of multinucleated syncytia (cytopathic effect, CPE, Figure 9) followed by death of the target cells [63]. The apathogenicity is thought to be a result of intensive evolutionary adoption of virus and its host [58].

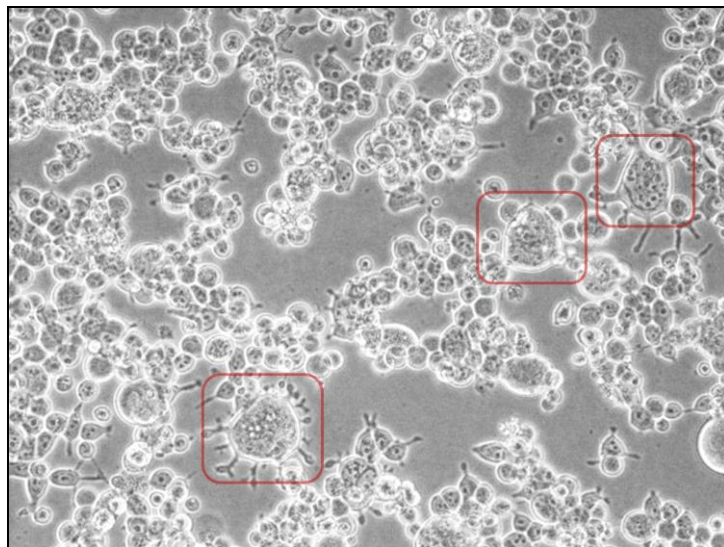


Figure 9: Cytopathic effect (CPE) in 293T cells infected with feline foamy virus (picture kindly provided by Michael Mühle of the Robert Koch-Institute)

Syncytia are framed in red.

FVs are of great interest for the development of retroviral vector systems and gene therapies in view of several reasons. They continuously stimulate the immune system [64] because they persist in the host despite the presence of neutralizing antibodies and they exhibit a broad host range [65]. In addition to that, the genome of FVs offers a high packaging capacity. 9.2 kb of the wild-type SFVcpz-genome with 13.2 kb in size can be supplemented by transgenes [66].

1.2.2 Feline foamy virus genome and Env

Like in other complex retroviruses, the feline foamy virus (FFV) genome (11.7 kb) encodes, in addition to Gag, Env and Pol, accessory and regulatory proteins, as e.g. Bel1/2 and Bet (Figure 10). In contrast to other retroviruses, FV Gag lacks a membrane-targeting signal. Budding and particle release is Env-dependent that impedes

the formation of virus-like particles (VLPs) [67-70]. Interestingly, FV Env contains structural features that allow release of capsid-less subviral particles (SVPs) similar in size and shape to VLPs [71].

The *Bel1* gene encodes transactivator (Tas) that binds to the internal promoter (IP) in *env* and the promoter in the 5'LTR. At lower concentrations, Tas binds the IP that has higher basal activity and thereby increases its own expression. Accumulation of Tas increases binding of the promoter in the 5'LTR which promotes gene expression of structural proteins. The positive feedback-loop regulated by Tas thereby allows the switch from early accessory to late structural gene expression [72-74]. Activation of the IP also induces the gene expression of *bet*. A splicing event that fuses the *bet2* ORF with the 5'end of the *bel1* ORF produces *bet*. Studies showed that Bet protein inhibits APOPEC3 analogously to HIV-1 Vif [75, 76].

The envelope glycoprotein (Env) is translated from a single-spliced mRNA. The Env precursor molecule (gp130) (Figure 10) consisting of the surface (SU, gp80) and transmembrane envelope protein (TM, gp48) is targeted to the rough endoplasmic reticulum by an N-terminal signal peptide.

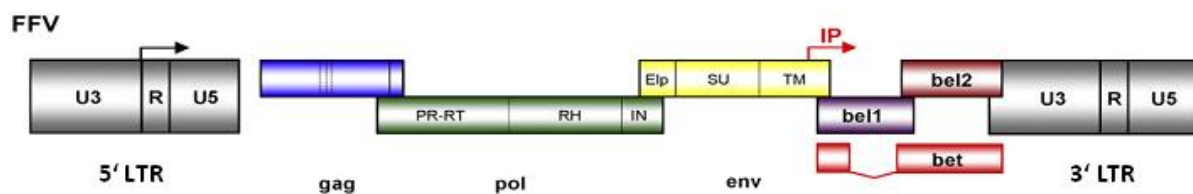


Figure 10: Feline foamy virus genome organization [77]

LTR: long terminal repeat with unique 3' and 5' region (U3, U5) and repeats (R), gag: group specific antigen, pol: polymerase, PR: protease, RT/RH: reverse transcriptase-RNase H domain, IN: integrase, env: envelope, Elp: envelope leader peptide, SU: surface protein, TM: transmembrane envelope protein, IP: internal promoter, bet: between env and LTR.

Different to orthoretroviruses, the envelope leader peptide (Elp) is not cleaved co-translationally but remains attached to the full-length precursor molecule and is incorporated into virus particles [69, 70, 78]. Along its way through the secretory pathway, Env is proteolytically cleaved at the furin-cleavage sites to Elp, SU and TM [69, 70]. Only the SU-TM cleavage is essential for viral infectivity [79-81]. In addition, FV Env is N-glycosylated [79] at several sites. In the case of PFV, 14 to 15 potential glycosylation sites have been predicted of which two conserved sites seem to be critical

for viral infectivity; N8 in gp80 and N13 in gp48 [82]. Similar to HIV Env, FV Env forms heterotrimeric spikes on the viral surface [63, 83]. By applying electron microscopy of negatively stained PFV particles, it was found that those spikes are densely ordered in hexameric rings covering the whole surface of a single virion [83].

Among most FVs, a KKXX di-lysine motif in the C-terminal cytoplasmic domain of TM is conserved [84]. It was shown that in PFV, the KK-motif functions as an endoplasmic reticulum retrieval signal (ERRS) because it retains Env in the endoplasmic reticulum from the Golgi network in the absence of other viral proteins [85]. PFV Env ERRS mutants show augmented syncytia formation probably due to increased transport of Env to the plasma membrane [85, 86].

Additionally, it was shown that PFV Env is ubiquitinated at five lysine residues located in the N-terminal part of its envelope leader peptide. Those ubiquitination sites seem to be nonessential for FV particle-release but obviously affect SVP-release in a negative way. This was shown by lysine-to-arginine mutations of all five ubiquitination sites that resulted in enhanced SVP-release by more than 10-fold [87, 88].

1.3 Goal of this thesis

As mentioned above, some HIV-1 infected patients develop neutralizing antibodies (nAbs) 2 to 3 years after infection [36-38]. From some infected individuals, even antibodies with broadly neutralizing activity could be isolated. Two of those antibodies are 2F5 and 4E10 that bind epitopes in the MPER [41]. Different vaccine strategies were tested for induction of 2F5- and 4E10-like antibodies but all attempts remained without success.

It is still unclear which factors are essential for successful induction of nAb. Studies suggest that the unusually long CDR3s of 2F5 and 4E10 interact with lipids of the viral membrane [49, 51], in addition to their respective epitope sequences (Figure 8). That characteristic implies that the natural conformation of the 2F5 and 4E10 epitopes and positioning close to a lipid membrane play a substantial role in antigenicity. Besides, the long CDR3s, 2F5 and 4E10 were shown to be highly mutated in the framework regions (FWR) of the variable regions. The FWRs maintain the structural integrity of the complementarity determining region (CDR) loops and are thus critical for broadly neutralizing activities and breadths of bnAbs [89]. As a consequence, mutations in the FWR are rarely tolerated and rather selected against [90,

91]. This suggests that long affinity maturation is necessary for nAbs to become broadly neutralizing.

In a previous study, sera of animals that were immunized with recombinant feline foamy virus (FFV) transmembrane envelope protein (gp48) protein and domestic cat sera were screened for antibodies against gp48 [92]. Analysis by use of ELISA and immunoblotting showed that FFV positive sera contained antibodies with reactivity against gp48. Epitope mapping revealed that the reactivity of antibodies in the immunized animals was predominantly against the glycosylated cysteine-rich domain (Figure 11) [84, 92]. In contrast, naturally infected cats contained antibodies preferentially recognizing epitopes in the FPPR and MPER (Figure 11). Most of the epitopes located in the MPER are arranged similarly to the bipartite motif constituted by the 2F5 and 4E10 epitopes in HIV-1 gp41, as depicted above in Figure 8.

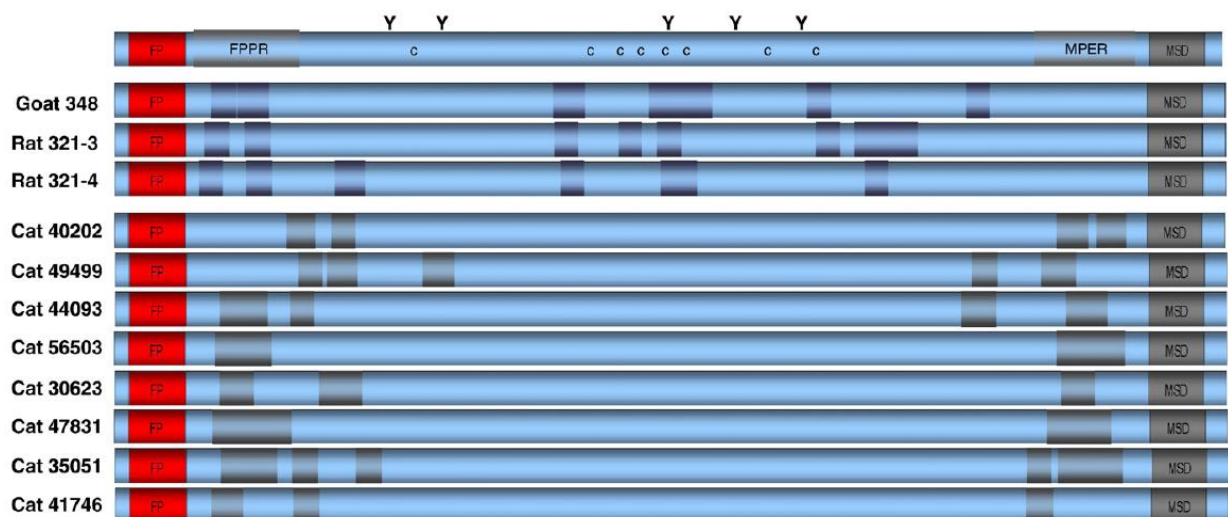


Figure 11. Antigenic regions in the FFV TM detected by epitope mapping of sera from animals that were immunized with the FFV TM and naturally FFV-infected domestic cats [92]

The schematic of the FFV TM is shown on the top. Indicated are the fusion peptide (FP), the fusion peptide proximal region (FPPR), the membrane proximal external region (MPER), the membrane spanning domain (MSD), the cysteines (C) and predicted glycosylation sites (Y). Detected epitopes are depicted in dark blue boxes (immunized animals) and grey boxes (naturally infected cats). Antibodies induced in naturally infected cats target the FPPR and MPER, whereas antibodies in sera from the immunized animals mainly recognized epitopes in the cysteine-rich domain and FPPR.

According to the mentioned characteristics of FFV Env and the bnAbs 2F5 and 4E10, the idea came up to use the FFV Env as a scaffold for the 2F5 and 4E10 epitopes. The strategy was to replace the adjacent immunogenic regions in the FFV MPER with the 2F5 and 4E10 epitope sequences. The fact that FFV Env is released as sub-

viral particles (SVPs) would turn chimeric FFV/HIV-1 SVPs into ideal immunogens because immunogenic reactions against other viral proteins, e.g. FFV Gag [93, 94], would thus be excluded. Such an antigen would also have the advantage that the 2F5 and 4E10 epitopes would be placed in close proximity to a lipid environment just like in their natural context.

This project was based on previous work carried out by my supervisor Michael Mühle, in close cooperation with Anne Bleiholder and Martin Löchelt at the German Cancer Research Center in Heidelberg. Bleiholder generated hybrid FFV/HIV-1 Env expression plasmids that carry the 2F5 and 4E10 epitopes [95]. In her PhD thesis she described the characterization of the hybrid FFV/HIV-1 Env proteins by means of expression, processing, recognition by mAb 2F5 and mAb 4E10 and their ability to promote marker gene transfer (Figure 12A-C) [95]. The MPER1 and MPER2 constructs promoted hybrid FFV/HIV-1 Env protein expression and processing as shown by detection of gp130, gp48 and a cell lysate-associated form of gp48 (TM^{CL}) (Figure 12A). In contrast to gp48, TM^{CL} is truncated and partly glycosylated that also explains their differential electrophoretic mobility [95]; processed gp48 runs above, while TM^{CL} runs below 50 kDa. Immunoprecipitation of hybrid FFV/HIV-1 MPER1 and MPER2 proteins by mAb 2F5 and mAb 4E10 showed that the respective epitopes are accessible (Figure 12B). Furthermore, Bleiholder showed that chimeric FFV/HIV-1 MPER1 and MPER2 proteins did not allow marker gene transfer (Figure 12C). That characteristic prevented them for the generation of replication competent FFV/HIV-1 chimeras for prolonged antigen delivery that could permit antibody affinity maturation. However, FFV EnvG2 and hybrid FFV/HIV-1 MPER1 and MPER2 proteins were released as SVPs (Figure 12D) that turned them into interesting antigens for immunization studies. Bleiholder started with the establishment of protocols for the large-scale production of SVPs by transiently transfecting HEK293T cells with the pBC EnvG2 and hybrid pBC FFV/HIV-1 MPER1 and MPER2 expression plasmids. Unfortunately, she was able to purify only low yields of SVPs (180-440 ng) from the supernatants [95]. For immunization studies in rats, amounts in µg-scale would be necessary.

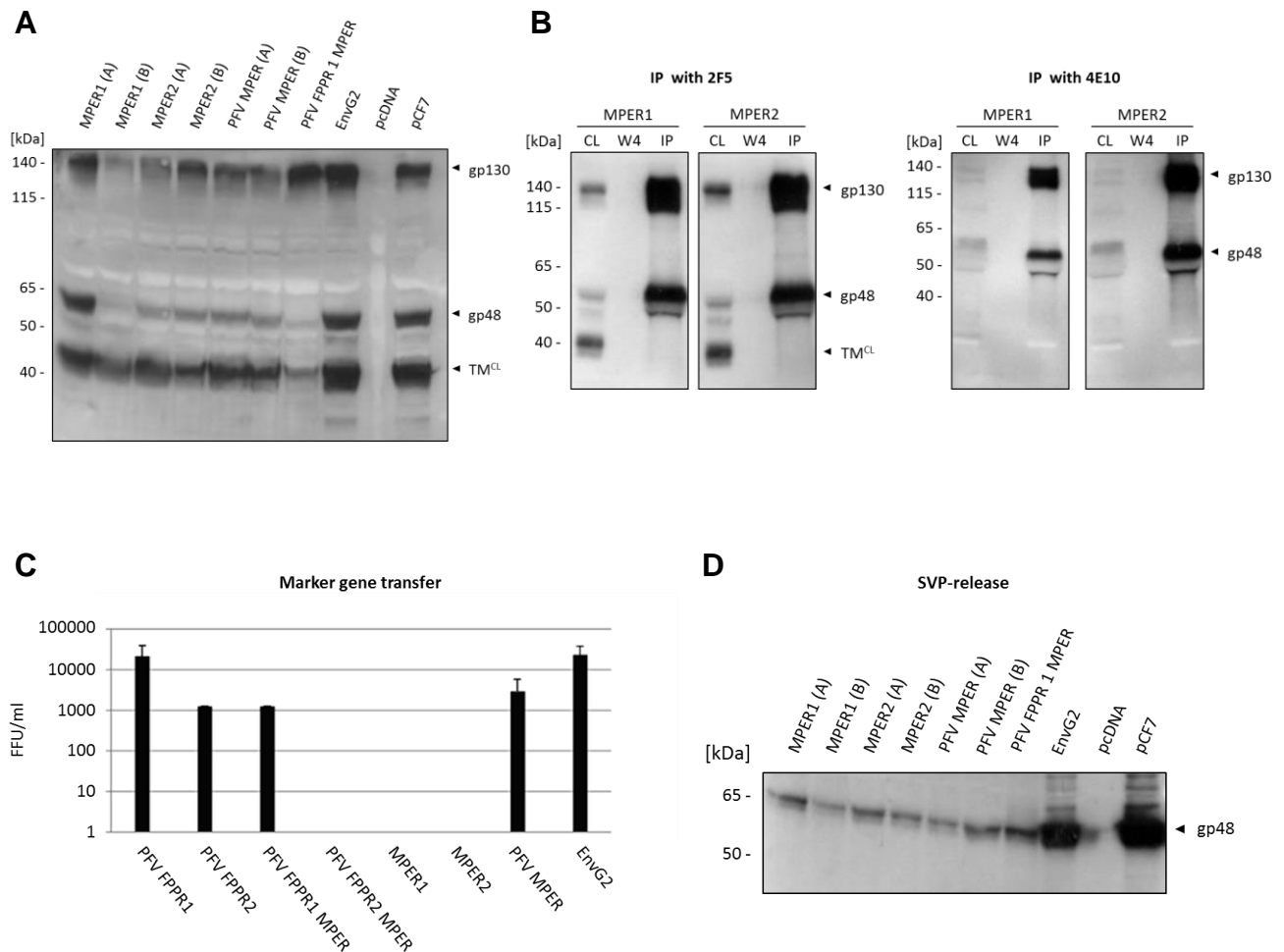


Figure 12. Characterization of hybrid FFV/HIV-1 Env and hybrid FFV/PFV MPER Env protein [95]

A) Immunoblot of HEK293T cell lysates transiently transfected with pBC EnvG2 and hybrid pBC FFV/HIV-1 MPER1 and MPER2 expression constructs (see section 4.1) and hybrid FFV/PFV MPER expression constructs (irrelevant for this project), as indicated. Detection of antigens was performed with goat348 α -TM serum [92]. All recombinant proteins were expressed and processed as shown by the detection of gp48 and TM^{CL}. MPER1 protein was stronger expressed and cleaved by furin protease than MPER2 protein. **B)** Immunoprecipitates of MPER1 and MPER2 proteins from HEK293T cell lysates applied to immunoblotting. Immunoprecipitation was with mAb 2F5 or mAb 4E10, as indicated. Detection of antigens was performed with goat348 α -TM serum [92]. CL: cell lysate; W4: fourth washing fraction; IP: immunoprecipitate. The 2F5 and 4E10 epitopes are accessible, since both hybrid FFV/HIV-1 Env proteins were immunoprecipitated by both antibodies. **C)** Titration of marker gene transfer particles (MGT) on CRFK cells. EnvG2 served as positive control. Fusion incompetent HIV-1 MPER1 and MPER2 proteins were unable to mediate MGT. Also shown are functional PFV hybrids (irrelevant for this project). **D)** Immunoblot of subviral particles released by HEK293T cells transiently transfected with pBC EnvG2 and hybrid pBC FFV/HIV-1 MPER1 and MPER2 expression constructs (see section 4.1), as indicated. Detection of antigens was performed with goat348 α -TM serum [92]. The suffixes (A) and (B) indicate different clones. Chimeric FFV/HIV-1 MPER1 and MPER2 SVPs were released with reduced efficiency in comparison to EnvG2 SVPs. PFV FPPR1 and MPER SVP-releases are also indicated (irrelevant for this project).

The goal of this project (Figure 13) was to establish efficient protocols for large-scale production of chimeric FFV/HIV-1 MPER SVPs to allow testing of their potential to induce neutralizing antibodies against HIV-1 in rats. This should be done by transducing target cells with retroviral vectors in order to allow stable expression of Env. For this purpose, the recombinant FFV/HIV-1 MPER1 and MPER2 sequences [95] should be first subcloned into a retroviral vector. Then protocols for efficient pseudotyping with vesicular stomatitis virus protein G (VSV-G) should be established. Therefore, additives in various concentrations should be screened for increasing virus production. In order to generate transduced cells stably producing SVPs, a suitable target cell line and optimal infection conditions should be found. Native chimeric FFV/HIV-1 SVP antigens should then be tested for the accessibility of the 2F5 and 4E10 epitopes for the respective antibodies. Electron microscopy should be applied to confirm release of SVPs. Finally, different serum-free expression media should be tested for optimal large-scale production and purification of SVP antigens.

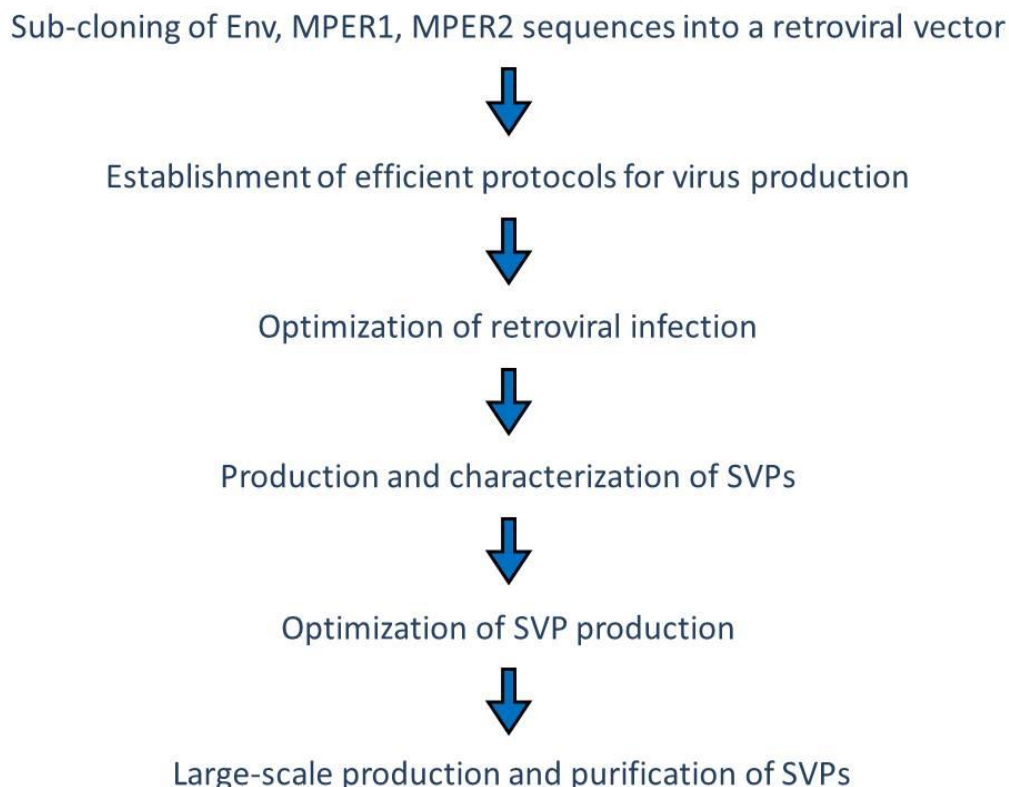


Figure 13. General workflow

2 Materials

2.1 Equipment

Avanti™ J-20XP, centrifuge		Beckman Coulter
Beaker glasses	10 ml, 50 ml, 100 ml, 500 ml	Schott Duran
Charlotte	2-125 µl	Vistalab Technologies
Chemocam		Intas
CO2-Incubator MCO-20AIC		Sanyo
Electrophoresis chamber		Biorad
Eppendorf centrifuge 5415D		Eppendorf
Eppendorf Mastercycler proS		Eppendorf
Eppendorf MiniSpin®		Eppendorf
Eppendorf Research®, variabel	10 µl, 20 µl, 100 µl, 200 µl, 1000 µl	Eppendorf
Eppendorf Research®, multi-channel	30-300 µl	Eppendorf
Erlenmeyer flasks	50 ml, 100 ml, 500 ml, 1 l, 5 l	Schott Duran
FACSCalibur™		BD Biosciences
Finnpipette®	50-300 µl	Thermo Scientific
Fluorescence microscope, Axiovert 100M		Zeiss
Glas flasks	50 ml, 100 ml, 500 ml, 1 l	Schott Duran
Glas pipettes	5 ml, 10 ml	Hirschmann
Guava PCA analysis system		Millipore
Heraeus Multifuge 1S-R Centrifuge		Thermo Scientific
HeraSafe, sterile bench		Thermo Scientific
JA-25.50, rotor		Beckman Coulter
Labotect Inkubator C200		Labotect
Light microscope		Hund Wetzlar
Multiskan™ GO UV/Vis microplate spectrophotometer		Thermo Scientific
Mx30005P™, Real-time PCR-cycler		Stratagene
Nalgene™ Cryo 1 °C Freezing Container		Thermo Scientific
NanoDrop®		peqLab
Neubauer chamber		Celeromics
Optima™L-100K, Ultracentrifuge		Beckman Coulter
pH meter		IKAMAG RET
PIPETMAN® Classic	P2, P10, P20, P100, P200, P1000	Gilson
Pipette boy accu-jet® pro		BrandTech Scientific
SDS electrophoresis chamber		CBS Scientific
Shaker, GFL® 3016		GFL
SW32, rotor for ultracentrifuge		Beckman Coulter
SW41, rotor for ultracentrifuge		Beckman Coulter
Thermomixer comfort		Eppendorf
Transilluminator system and software		Biorad
Type19, rotor for ultracentrifuge		Beckman Coulter
Vortexer, Reax top		Heidolph Instruments
Water bath		Memert

2.2 Consumables

Cell culture flasks	T-25, T-75, T-160	Techno Plastic Products
Cell scraper		Techno Plastic Products
Centrifuge tubes	14 x 89 mm	Beckman Coulter
Centrifuge tubes	25 x 89 mm	Beckman Coulter
Corning® HYPERFlask® Cell Culture Vessels		Corning Life Sciences
Cryotube™ vials	1.5 ml, 1.8 ml	Nunc™
Eppendorf tubes	1,5 ml, 2 ml	Eppendorf
Falcon tubes	15 ml, 50 ml	Techno Plastic Products
Nitrocellulose membrane	0.2 µm	GE Healthcare
Plastic pipettes	1 ml, 2 ml, 5 ml, 10 ml, 25 ml	Techno Plastic Products
Sterile filter	Stericup-Filter 0.22 µm; 0.45 µm	Millipore
Tissue culture dishes	10 cm, 15 cm	Techno Plastic Products
Tissue culture plates	6-, 12-, 24-, 48- or 96-well	Techno Plastic Products

2.3 Chemicals

2-mercaptoethanol	Carl Roth
Acrylamide	Carl Roth
Adenosin triphosphate (ATP)	Thermo Scientific
Agarose	Carl Roth
Ammoniumpersulfat (APS)	Carl Roth
Ampicillin	Carl Roth
Benzonase	Novagen
Big Dye	ABI
Blasticidin S hydrochloride	Sigma-Aldrich
BSA	New England Biolabs
dNTPs	Thermo Scientific
ECL (Enhanced chemiluminescence)	Thermo Scientific
EDTA	Serva
Ethanol	Carl Roth
Ethidium bromide	Sigma-Aldrich
Fetal Calf Serum	Biochrom
Geniticinsulfat (G418)-Lösung	Carl Roth
Glycerin	Carl Roth
Glycin	Carl Roth
Guava® ViaCount® reagent	Millipore
HEPES	Biochrom
Isopropanol	Carl Roth
L-Glutamine	Biochrom
Methanol	Carl Roth
Milk powder, low fat	Carl Roth
Nuclease-free water	QUIAGEN
Orange Loading Dye	Thermo Scientific
Penicillin/Streptomycin	Biochrom
Polybrene	Sigma-Aldrich
Polyethylene glycol 6000	Carl Roth

Materials

Polyethylenimine (PEI)	Sigma-Aldrich
Protease inhibitor	Roche
Rabbit serum	Sigma-Aldrich
Sodium butyrate	Sigma-Aldrich
Sodium chloride	Carl Roth
Sodium dodecyl sulfate (SDS)	Carl Roth
Sodium hydroxide	Carl Roth
Tetramethylethylenediamine (TEMED)	Carl Roth
Tricine	Carl Roth
Tris	Carl Roth
Tris-HCl	Carl Roth
Trypsin	Invitrogen
Tween 20	Carl Roth
Valproic acid	Sigma-Aldrich
Protein G Sepharose™ 4 Fast Flow	GE Healthcare

2.4 Kits

DNeasy® Blood & Tissue Kit (250)	QIAGEN
In-Fusion® HD Cloning Plus	Clontech
Invisorb® Spin DNA Extraction Kit (250)	Invitek
Invisorb® Spin Plasmid Mini Kit Two (250)	Invitek
Nucleobond® AX	Macherey-Nagel
One Step RT-PCR Kit	QIAGEN
Pierce™ BCA Protein Assay Kit	Thermo Scientific
Plasmid Midi/MaxiKit	QIAGEN
RNeasy® Mini Kit (250)	QIAGEN

2.5 Buffers and solutions

2.5.1 SDS-PAGE and immunoblotting

10x Anode buffer	242 g/l Tris, pH 8.9
10x Cathode buffer	121 g/l Tris, 179 g/l tricin, 10 g/l SDS, pH 8.25
Transfer buffer	48 mM Tris, 35 mM glycine, 20 % methanol, 0.03 % SDS
Stripping buffer	92 % [v/v] H ₂ O, 6.25 % [v/v] 1 M Tris-HCl pH 6.7, 2 % [w/v] SDS, 0.7 % [v/v] 2-mercaptoethanol
SDS-Gel buffer	36.3 % [w/v] Tris, 1.5 % [v/v] 20 % SDS, pH 8.4
Blocking solution	3 % [w/v] low-fat milk powder, 1 % rabbit serum, PBS-Tween 20
Washing solution, PBS-Tween 20	0.05 % [v/v] Tween 20
SDS-sample buffer	50 mM Tris-HCl, 12 % glycerol, 4 % SDS, 5 % 2-mercaptoethanol, 0.01 % Coomassie Brilliant Blue G-250

2.5.2 Agarose gel-electrophoresis

Tris-acetate-EDTA (TAE, 50x)	2 M Tris, 50 mM EDTA, 1 M acetate
------------------------------	-----------------------------------

2.5.3 Lysis buffers

SDS-lysis buffer	1 % SDS, 1x PBS
RIPA-buffer	50 mM Tris-HCl pH 7.4, 150 mM NaCl, 1 % NP-40, 0.5 % Sodiumdeoxycholat, 0.1 % SDS, 5 mM EDTA, 1x Protease Inhibitor Cocktail

2.5.4 Other buffers

10x Fast Digest Buffer Green	Thermo Scientific
Buffer HS2, for HotStart Taq DNA-Polymerase	Sengenetic
Buffer C, for AccuProof DNA-Polymerase	Sengenetic
Phusion® GC Reaction Buffer	New England BioLabs
6x Orange Loading Dye	Thermo Scientific

2.6 Protein and DNA ladders

Gene Ruler 1 kb DNA Ladder, Ready-to-use	Thermo Scientific
O'Gene Ruler™ DNA Ladder Mix, Ready-to-use	Thermo Scientific
peqGOLD Protein Marker IV	PEQLAB

2.7 Enzymes

2.7.1 Restriction enzymes

All restriction enzymes were purchased from Thermo Scientific as Fast Digest-enzymes.

<i>Restriction enzyme</i>	<i>Recognition site (5' - 3')</i>
Apal	GGGCC [^] C
BamHI	G [^] GATCC
Bsu36I	CC [^] TNAGG
EcoRI	G [^] AATTC
MunI	C [^] AATTG
NotI	GC [^] GGCCGC
Pdml	GAANN [^] NNTTC
Sall	G [^] TCGAC
XbaI	T [^] CTAGA

2.7.2 Polymerases

AccuProof DNA Polymerase	Sengenetic
Clone Amp HiFi PCR Premix	Clontech
Hot Start Taq DNA-Polymerase	Sengenetic
Pfu DNA-Polymerase	Thermo Scientific
Phusion® Hot Start HD flex	New England BioLabs
AmpliTaq Gold® with GeneAmp®	Roche

2.7.3 Other enzymes

In-Fusion® HD Enzyme Premix	Clontech
Klenow-Fragment	Thermo Scientific
Shrimp alkaline phosphatase (SAP)	Thermo Scientific
T4 DNA-Ligase	Thermo Scientific
T4 Polynucleotide kinase (PNK)	Thermo Scientific
Benzonase	Novagen

2.8 Primers

The primers were designed with gene maps and synthesized by Eurofins MWG Operon.

<i>Primer</i>	<i>Sequence (5'-3')</i>
FFV EnvG2 fwd	ATA GCG GCC GCA TGG AAC AAG AAC ATG TGA TG
FFV EnvG2 rev	TAT GTT TAA ACC TAG TGA TGG TGA TGG TGA TGT TGG TCC TTC TTC
FFV TMH fwd	AGG CAT TCA TGC CTT TTG GAT TCT
FFV TMH rev	CTT CAA AAT ACC CGG AAG AAG GAC CAA
TM seq fwd	TGG AAA TGG AAC TGG TTC AGA CTG C
FFV Int sequencing primer rev	GTC ACC TTG TAA GGA ATG CAG G
FFV SU rev	TGA ATT AGT CAC CTG CCA GCT TAA
FFV FP rev	GCC TAA GCC TGC CTC TTG TAT CCT TCT TA
Elp1 fwd	TGG AAT GCT CAC CGA CAA CTA CAG CGA CTT CAG TCG ACT CAT
Elp1 rev	TTC CAT CCA TTC CCG CAG GGT CAT CAC ATG TTC TTG TTC CAT
Elp2 fwd	CCA GAG CGG GTA CCT TTG CGA ATG AGG ATG CGA TAT AGA TGT
Elp2 rev	TAC TAA AGG AAT ATC CTC AGG TAT GTC AAC ATG CAA CTC AGG
PRE fwd	TTC TGG GAC TTT CGC TTT CC
PRE2 rev	CAT GGA AAG GAC GTC AGC TT
FFV Env Fusion1	CAC TTA CAG GCG GCC GCG CCG CCA CCA TGG AAC AAG AAC ATG TGA
FFV Env Fusion2	TAA GAT GCT CGA ATT CCT AGT GAT GGT GAT GGT GAT GTT GGT CCT

2.9 Probe for real-time PCR

PRE2 Probe fwd	AAC TCA TCG CCG CCT GCC TTG
----------------	-----------------------------

2.10 Plasmids

<i>Plasmids</i>	<i>Description</i>	<i>Reference/vendor</i>
pLenti-GFP	Modified version of the retroviral vector pLenti CMV GFP Puro (658-5).	Addgene, Plasmid 17448
pMDLg/pRRE	Lentiviral vector carrying the HIV-1 structural genes <i>gag</i> and <i>pol</i> .	Addgene, Plasmid 12251
pRSV-Rev	Lentiviral packaging plasmid encoding HIV-1 Rev protein.	Addgene, Plasmid 12253
pMD2.G	Envelope plasmid coding for the vesicular stomatitis virus protein G (VSV-G).	Addgene, Plasmid 12259
MP71-GPRE	MP71-GPRE naturally contains a GFP and has the 856-bp woodchuck hepatitis virus post-transcriptional regulatory element (PRE) (GPRE). It is a retroviral vector with a murine myelo-proliferative sarcoma virus (MPSV) LTR and an improved leader sequence derived from murine embryonic stem cell virus (MESV).	[96]
pBC EnvG2, pBC MPER1, pBC MPER2	FFV EnvG2, FFV EnvG2xHIV-1 MPER1/2 sequences in pBC12 backbone. For details see section 4.1.	[95]
pCF7	Codes for an infectious molecular clone of feline foamy virus.	[97]
pEGFP-N3	Encodes an enhanced variant of GFP that is flanked by Kozak consensus translation initiation sites for increased expression. A multiple cloning site is incorporated between an immediate early CMV promoter and EGFP.	Clontech Laboratories, Inc.

2.11 Antibodies and antisera

2.11.1 Primary antibodies

<i>Antibody</i>	<i>Dilution</i>	<i>Reference/vendor</i>
mAb 4E10	1:20000	The following reagent was obtained through the NIH AIDS Reagent Program, Division of AIDS, NIAID, NIH: HIV-1 gp41 Monoclonal Antibody (4E10) from Dr. Hermann Katinger. [98]
mAb 2F5	1:20000	The following reagent was obtained through the NIH AIDS Reagent Program, Division of AIDS, NIAID, NIH: HIV-1 gp41 Monoclonal Antibody (2F5) from Dr. Hermann Katinger. [99-101]
mouse α -GFP HRP	1:1000	Santa Cruz, SC9996
mouse α - β -actin	1:5000	Sigma-Aldrich

2.11.2 Antisera

<i>Antiserum</i>	<i>Dilution</i>	<i>Reference</i>
goat 348 α -FFV TM	1:1000	[92]
rat 321-3 α -FFV TM	1:1500	[92]

2.11.3 Secondary antibodies

<i>Antibody</i>	<i>Dilution</i>	<i>Vendor</i>
poly rabbit α -mouse HRP	1:3000	Dako
poly rabbit α -human HRP	1:3000	Dako
poly rabbit α -goat HRP	1:3000	Dako

2.12 Media

2.12.1 Media for bacteria

Lysogeny broth (LB)	10 g/L tryptone, 5 g/L yeast extract, 100 mM NaCl, pH 7.0
LB-medium for agar-plates	10 g/l NaCl, 10 g/l tryptone, 5 g/l yeast extract, 15 g/l agar
S.O.C.	Novagen

2.12.2 Media for cell cultures

<i>Medium</i>	<i>Vendor/supplements</i>
Dulbecco's Modified Eagle Medium (DMEM)	GE Healthcare Supplemented before use with: 10 % [v/v] FCS, 2 mM L-glutamine, 10 mM HEPES, 5 mM penicillin/streptomycin
Dulbecco's Modified Eagle Medium (DMEM), High Glucose (4.5 g/l)	GE Healthcare Supplemented before use with: 10 % [v/v] FCS, 2 mM L-glutamine, 10 mM HEPES, 5 mM penicillin/streptomycin
EX-CELL® VPRO, Serum-Free Medium	Sigma-Aldrich
FreeStyle™ 293 Expression Medium	Life Technologies
HyClone™ SFM4HEK293™ Medium	Thermo Scientific
Roswell Park Memorial Institute medium (RPMI)	GE Healthcare Supplemented with: 10 % [v/v] FCS, 2 mM L-glutamine, 10 mM HEPES, 5 mM penicillin/streptomycin

2.12.3 Freezing media for eukaryotic cells

<i>Cell line</i>	<i>Freezing medium</i>
Platinum-GP	70 % DMEM, 20 % FCS, 10 % DMSO
C8166-45	RPMI with 83 % L-glutamine, 10 % FCS, 7 % DMSO
CRFK	10 % DMSO in FCS
FreeStyle™ 293-F Cells	FreeStyle™ 293 Expression Medium with 10 % DMSO
HEK293T	70 % DMEM, 20 % FCS, 10 % DMSO

2.13 Prokaryotic strains

<i>Strain</i>	<i>Genotype</i>	<i>Vendor</i>
NovaBlue GigaSingles™ Competent Cells	endA1 hsdR17 ($r_{K12}^- m_{K12}^+$) supE44 thi-1 recA1 gyrA96 relA1 lac F'[proA ⁺ B ⁺ lacI ^q ZΔM15::Tn 10] (Tet ^R)	Novagen
Stellar™ Competent Cells	F ⁻ , endA1, supE44, thi-1, recA1, relA1, gyrA96, phoA, Φ80d lacZΔ M15, Δ (lacZYA - argF) U169, Δ (mrr - hsdRMS - mcrBC), ΔmcrA, λ ⁻	Clontech Laboratories, Inc.

2.14 Eukaryotic strains

Cell line	Specification	Vendor
C8166-45	C8166 cells are human umbilical cord lymphocytes that contain the poorly infectious HTLV-1 _{CR} virus; increased production of HTLV-1. Morphology is T-lymphoid. C8166 cells are cultured in suspension.	The following reagent was obtained through the NIH AIDS Reagent Program, Division of AIDS, NIAID, NIH: C8166-45 (Cat# 404) from Dr. Robert Gallo.
CRFK cells	The CRFK cells are feline kidney cells with an epithelial morphology.	ATCC
FreeStyle™ 293-F Cells	The 293F cell line that is derived from the 293 cell line is adapted to be grown as suspension cultures in serum-free expression media (e.g., FreeStyle™ 293 Expression Medium).	Life Technologies
HEK293T	The human kidney cell-derived HEK293T cell line is adenovirus immortalized and stably expresses large SV40 T antigen. HEK293T cells are used for transient transfection.	ATCC
Platinum-GP (Plat-GP)	The Plat-GP is a 293T cell line-derived retrovirus packaging cell line which stably expresses retroviral structure proteins (<i>gag</i> and <i>pol</i>) under blasticidin selection.	Cell Biolabs, Inc.

2.15 Software

ClustalW2, EMBL-EBI	Multiple sequence alignment
DNASTAR Lasergene SeqBuilder	Generation of sequence maps
DNASTAR Lasergene SeqMan Pro	Analysis of sequencing data
Expasy translate tool	Translation of nucleotide sequences into amino acid sequences
Oligo Analyzer, Integrated DNA Technologies	Tool for the analysis of designed primers.

3 Methods

3.1 Molecular biological methods

3.1.1 PCR for subcloning

The DNA sequences of FFV EnvG2, FFV EnvG2 x MPER1 and FFV EnvG2 x MPER2 were PCR-amplified (Table 1) with the pBC EnvG2, MPER1 x pBC EnvG2 and MPER2 x pBC EnvG2 expression plasmids [95] as templates. In order to allow subcloning into MP71-GPRE by homologous recombination, the primers FFV Env Fusion1 and FFV Env Fusion2 were designed to add 15 bp extensions 5' and 3' homologous to vector regions confining the GFP gene in MP71-GPRE. In addition, the primer FFV Fusion2 added a Histidine-Tag-encoding sequence 3' of the amplicon.

Table 1: PCR mix with CloneAmp HiFi PCR Premix

<u>Reagent</u>	<u>Volume/amount</u>	<u>Cycler conditions</u>	
CloneAmp HiFi PCR Pre-mix	12.5 µl	95 °C, 5 min	
FFV Env Fusion1	7.5 pmol	98 °C, 30 sec, denaturation	} 30x
FFV Env Fusion2	7.5 pmol	55 °C, 15 sec, annealing	
Template DNA	100 ng	72 °C, 20 sec, elongation	
Nuclease-free H ₂ O	ad 25 µl	72 °C, 5 min	

3.1.2 Mutagenesis-PCR

The mutations K₁₀R, K₂₀R, K₂₄R, K₄₅R and K₄₈R were incorporated into the FFV envelope leader peptide (Elp) of gp48 (Figure 35) by performing two rounds of PCR (Table 2) and self-circularization. pBC EnvG2, MPER1 x pBC EnvG2 and MPER2 x pBC EnvG2 [95] served as templates. Before PCR, the primers Elp1 fwd, Elp1 rev, Elp2 fwd and Elp2 rev carrying the desired mutations were phosphorylated for 1 hour (Table 3) in order to allow subsequent self-circularization of the linear vector amplicons.

Table 2: PCR mix with Phusion® Hot Start HD flex

<u>Reagent</u>	<u>Volume/amount</u>	<u>Cycler conditions</u>	
5x Phusion HF	25 µl	98 °C, 30 sec	
Primer fwd-P	2.5 µl (10 pmol/µl)	98 °C, 10 sec, denaturation	} 35x
Primer rev-P	2.5 µl (10 pmol/µl)	55 °C, 15 sec, annealing	
dNTP	1 µl (10 mM)	72 °C, 3 min, elongation	
Phusion® Hot Start HD flex	0.5 µl	72 °C, 5 min	
Template DNA	10 ng		
Nuclease-free H ₂ O	ad 50 µl		

Table 3: Mixture for primer phosphorylation

<u>Reagent</u>	<u>Volume/amount</u>
Primer (100 pmol/µl)	0.9 µl
10x T4 PNK buffer A	0.9 µl
10 mM ATP	0.9 µl
T4 PNK	0.8 µl
Nuclease-free H ₂ O	5.5 µl

3.1.3 Colony PCR

Colony PCR was used to screen transformed bacteria for positive clones. For this purpose, single colonies were directly picked from an agar plate with a pipette tip. Before mixing with the PCR reaction mix (Table 4), the single clones were put onto a back-up plate.

Table 4: PCR mix with Hot Start Taq DNA-Polymerase

<u>Reagent</u>	<u>Volume/amount</u>	<u>Cycler conditions</u>	
10 x buffer	1.5 µl	94 °C, 10 min	
MgCl ₂	1.2 µl	95 °C, 30 sec, denaturation	} 25x
dNTPs	0.3 µl (10 mM)	52 °C, 30 sec, annealing	
5'-primer	0.3 µl (10 pmol/µl)	72 °C, 1 min 20 sec, elongation	
3'-primer	0.3 µl (10 pmol/µl)	72 °C, 5 min	
Hot Start Taq DNA-Polymerase	0.2 µl		
Template	single clone		
Nuclease-free H ₂ O	ad 15 µl		

3.1.4 Reverse transcription-PCR (RT-PCR)

After isolation of RNA from transfected cells, RNA transcripts were first reverse transcribed to cDNA and subsequently amplified by RT-PCR (Table 5) using the OneStep RT-PCR kit from QIAGEN. Amplified cDNA was separated by 1 % agarose gel-electrophoresis. Finally, desired amplicons were extracted from gels and sequenced.

Table 5: Reaction mix for RT-PCR (OneStep RT-PCR kit)

<u>Reagent</u>	<u>Volume/amount</u>	<u>Cycler conditions</u>
5x QIAGEN OneStep RT-PCR Buffer	5 µl	50 °C, 30 min, reverse transcription
dNTP Mix	2.0 µl	95 °C, 15 min, initial PCR activation
Primer fwd	0.3 µM	} 50x 94 °C, 1 min, denaturation 50 °C, 1 min, annealing 72 °C, 1 min, extension
Primer rev	0.3 µM	
QIAGEN OneStep RT-PCR Enzyme Mix	1 µl	
Isolated RNA	1 pg - 2 µg	72 °C, 10 min, final extension
RNase-free H ₂ O	ad 25 µl	

3.1.5 Real-time PCR

FFV EnvG2 or FFV/HIV-1 MPER1 or MPER2 virus titers were determined using real-time PCR (Table 6, see section 4.4.1). In contrast to primer-to-template hybridization that is assisted by polymerase, probe-to-template hybridization lacks this support. In order to increase probe-to-template hybridization, elongation-temperature and annealing-temperature were matched [102]. All PCR-runs were carried out with a Mx3005™ Real-time PCR cycler from Stratagene.

Table 6: PCR mix for real-time PCR

<u>Reagent</u>	<u>Volume/amount</u>	<u>Cycler conditions</u>
10 x buffer	2.5 µl	95 °C, 10 min
MgCl ₂	25 mM	95 °C, 30 sec, denaturation
dNTPs	0.5 µl (10 mM)	} 50x 58 °C, 1 min, annealing and elongation
5'-primer, PRE fwd	0.5 µl (10 pmol/µl)	
3'-primer, PRE 2 rev	0.5 µl (10 pmol/µl)	
AmpliTaq Gold® with GeneAmp®	0.25 µl	
Genomic DNA	100 ng	
Nuclease-free H ₂ O	ad 25 µl	

3.1.6 Subcloning with the In-Fusion® HD Protocol from Clontech

The In-Fusion® system is for subcloning DNA sequences into target vectors based on homologous recombination (Figure 14) [103]. In order to allow homologous recombination with MP71-GPRE, PCR-amplification of the FFV EnvG2, FFV EnvG2 x MPER1 and FFV EnvG2 x MPER2 sequences was performed with primers that added 5' and 3' 15 bp extensions homologous to the MP71 regions flanking the eGFP sequence (see section 3.1.1.). The amplicons were introduced into MP71 in a single reaction (Table 7) which was incubated at 50 °C for 15 min. Subsequently, NovaBlue Giga Singles were transformed with the reaction mixtures. The following day, single colonies were picked for colony-PCR.

Table 7: In-Fusion® HD mix

<u>Reagent</u>	<u>Volume/amount</u>
PCR-product	50-100 ng
linearized MP71	50-100 ng
5x Fusion Enzyme Premix	2 µl
Nuclease-free H ₂ O	ad 10 µl

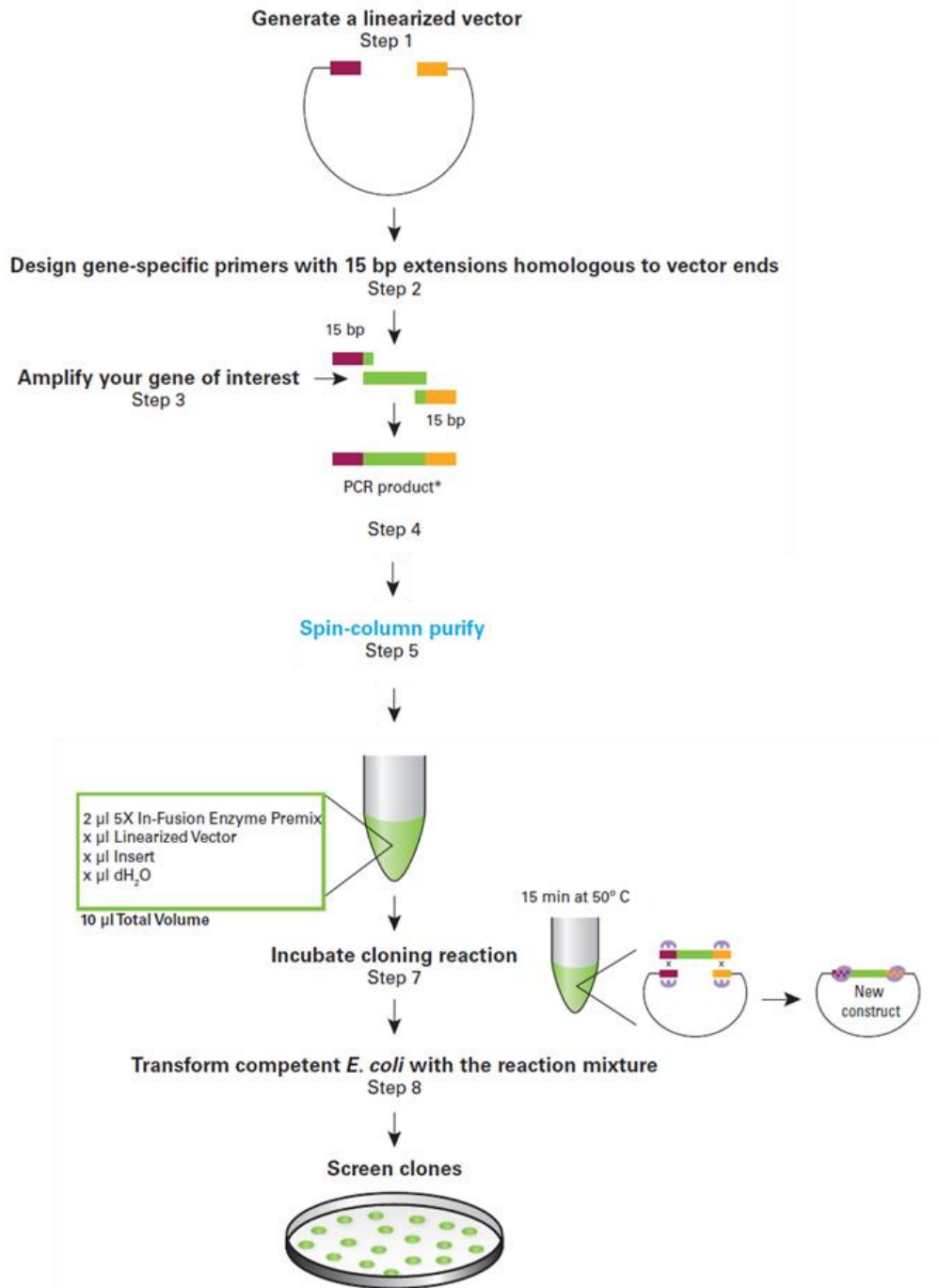


Figure 14. In-Fusion HD work-flow overview [103]

The EnvG2, EnvG2 x MPER1 and EnvG2 x MPER2 sequences were PCR-amplified using the primers FFV Env Fusion1 and FFV Env Fusion2 that added 5' and 3' 15 bp extensions homologous to linearized MP71. After separation with 1 % agarose gel-electrophoresis, the desired amplicons were eluted from gel pieces by spin-column purification. In a single reaction, the sequences were introduced into MP71 by homologous recombination. Afterwards, NovaBlue Giga Singles were transformed with the reaction mixture.

3.1.7 Ligation and self-circularization

T4 DNA ligase enzyme was used for self-circularization (Table 8) of linear plasmids that were amplified by mutagenesis-PCR. Reaction mixtures were incubated at 37 °C for 1 hour, before transformation into NovaBlue GigaSingles™ Competent Cells.

Table 8: Self-circularization of a linear vector amplicon

<i>Reagent</i>	<i>Volume/amount</i>
Linear plasmid DNA	10-20 ng
10x ligase buffer	2 µl
T4 ligase (5 U/µl)	1 µl
Nuclease-free H ₂ O	ad 20 µl

3.1.8 Restriction digestion

Restriction digestion of DNA was either performed for analytical or subcloning purposes. All restriction enzymes were purchased as FastDigest enzymes from Thermo Scientific with 100 % activity in the universal FastDigest Buffer and FastDigest Buffer Green. Therefore, double-digestions in single reactions are possible, regardless of the enzymes used. For analytical control digests, FastDigest Buffer Green was applied because it allows direct loading of reaction mixtures onto agarose gels. According to the manufacturer, FastDigest enzymes are optimized to digest 1 µg DNA in 5 - 15 min. For cloning purposes, reactions were incubated up to 1 hour at 37 °C to assure complete digestion.

3.1.9 Isolation of plasmid DNA from *E.coli*

For isolation of plasmid DNA from *E.coli*, the Invisorb® Spin Plasmid Mini Kit Two (250), Plasmid Midi/MaxiKit or Nucleobond® AX was used. The procedure of isolation was performed according to the protocols of the manufacturers.

3.1.10 Isolation of genomic DNA from eukaryotic cells

For isolation of genomic DNA from transduced cells, the DNeasy® Blood & Tissue Kit (250) from QIAGEN was used. The procedure of isolation was performed according to the protocols of the manufacturer. Genomic DNA was subjected to real time-PCR for determination of virus titers (see section 4.4.1).

3.1.11 Isolation of RNA from eukaryotic cells

For isolation of RNA from transfected cells, the RNeasy® Mini Kit (250) from QIAGEN was used. The procedure of isolation was performed according to the protocol of the manufacturer. Isolated RNA was subjected to reverse transcription-PCR.

3.1.12 Determination of DNA concentrations

Concentrations of purified DNA solutions were spectrometrically determined at 260 nm with a NanoDrop® device from peqLab.

3.1.13 Sequencing and analysis of cloned plasmid constructs

Sequencing of cloned plasmid constructs was performed according to Sanger. In Table 9 the amounts for a single sequencing PCR mix are shown. After PCR, reaction mixtures were handed over to the sequencing laboratory of the Robert Koch-Institute for compilation of the sequencing data. The obtained data were evaluated with the DNASTAR Lasergene SeqMan Pro software.

Table 9: PCR mix for sequencing

<u>Reagent</u>	<u>Volume/amount</u>
Primer	0.5 µl
Big Dye 3.1	2 µl
5x Buffer	1 µl
Template DNA	150-300 µl
Nuclease-free H ₂ O	ad 10 µl

3.1.14 Agarose gel-electrophoresis

DNA fragments were separated according to their lengths in 1 % agarose gels. Agarose was dissolved in 1x TAE buffer by boiling in a microwave. After cooling the agarose solution to a moderate temperature, 0.001 % (v/v) ethidium bromide was added to allow subsequent visualization of DNA fragments by exposure to UV light. Mixtures were poured into an electrophoresis chamber and incubated until full polymerization. Gels were placed in a gel apparatus containing TAE buffer. Before loading, DNA samples were mixed with 6x Orange Loading Dye. Separations were performed at 130 V. Gels were visualized and documented with a transilluminator system and software from Biorad.

3.1.15 Extraction and purification of DNA fragments from agarose gels

After gel-electrophoresis, DNA bands with the intended size were excised from gels under UV-exposure for visualization. DNA was extracted and purified from the gel slices using the Invisorb® Spin DNA Extraction Kit (250). The procedure of DNA purification was performed according to the protocol of the manufacturer.

3.1.16 Transformation of competent bacteria

For plasmid amplification, DNA was delivered into competent NovaBlue GigaSingles™ Competent Cells by heat shock. Competent bacteria kept at -80 °C were thawed on ice. 1 - 10 ng plasmid DNA or 10 µl self-circularization reaction mixture were added to 50 µl of bacterial suspension. After incubation on ice for 10 min, bacteria were heat shocked at 42 °C for 30 sec. and further incubated on ice for 2 min. Then 250 µl pre-warmed S.O.C.-medium were added. Before plating on agar-plates supplemented with ampicillin for positive selection, transformed bacteria were incubated shaking at 37 °C for 10 min.

3.1.17 Preparation of glycerol stocks of single clones for long-term storage

Single colonies of positive clones were stored as glycerol stocks. For this purpose, 900 µl of bacterial overnight-culture were mixed with 600 µl of 50 % sterile-filtered glycerol. Tubes containing bacterial suspensions were immediately put into liquid nitrogen. Finally, the stocks were stored at -80 °C.

3.2 Cell cultural methods

3.2.1 Thawing and establishing of eukaryotic cells

Frozen cells in cryo-tubes stored in liquid nitrogen were thawed in a water bath. When only a small piece of ice was visible, cell suspensions were immediately transferred into fresh culture medium in order to mitigate toxic effects of the DMSO-supplemented freezing medium. DMSO was completely removed by pelleting cells and discarding the supernatant. Cells were resuspended in fresh culture medium and seeded in cell culture flasks at an appropriate density.

3.2.2 Subculturing of cells

About every second to third day, confluent adherent cell cultures (HEK293T, Plat-GP) or suspension cultures (293F, C8166) with a density of 1×10^6 - 3×10^6 cells/ml were split at ratios of 1:2 to 1:10, depending on the confluency or cell density of cultures. Suspension cultures were split by resuspending pelleted cells in an appropriate amount of culture medium and diluting the cell suspensions. Adherent cell cultures first had to be detached with trypsin. For this purpose, culture medium was removed and cells were washed with 10 - 15 ml 1x PBS. Subsequently, 2 - 5 ml trypsin/EDTA solution was added. Trypsin digest was incubated at 37 °C for up to 5 min until cells were floating. Cells were resuspended in culture medium and split at a desired ratio.

3.2.3 Determination of cell numbers and viabilities

In order to define cell numbers and viabilities of cell suspensions, the Guava® ViaCount® assay from Millipore was used. For this purpose cell suspensions were prepared as described above. 20 µl cell suspension with unknown cell density were mixed with 180 µl Guava® ViaCount® reagent (1:10-dilution) in a 1.5 ml reaction tube. Subsequently, the tube was immediately placed in the retainer of the Guava PCA analysis system for analysis with the Guava ViaCount application of the CytoSoft software. The Guava® ViaCount® assay differs between viable and dead cells. The Guava® ViaCount® reagent is composed of two different fluorescent dyes. Nucleated cells are stained with a membrane-permeable DNA-binding dye, while dead cells are stained with a dye that can only penetrate membranes with impaired integrity. The fluorescence signal emitted from the DNA-binding dye is detected by the photomultiplier 2 (PM2) of the Guava PCA analysis system. The dead cell stain is detected by PM1. Each signal leads to a counted event if the corresponding forward scattered signal (FSC) intensity is appropriate for a nucleated cell [104]. Before data acquisition, the system settings were adjusted with the Guava ViaCount application. If necessary, the voltage settings were changed so that live and dead populations could be distinguished on the plots (PM1/FSC, PM2/PM1). The FSC threshold was moved to exclude cell debris from detected cells and the PM2 threshold was shifted to separate the live and dead cell populations. After data acquisition of standardly 1000 events, the CytoSoft software calculated the viability and the cell density of the undiluted cell suspension considering the dilution factor.

3.2.4 Freezing cells

For freezing cells, 2 ml of a cell suspension (up to 1×10^7 cells/ml) in freezing medium were transferred into cryo-tubes. Then, tubes were put into a cryo-container which allows slow cooling of cells to -80 °C at a rate of -1 °C/min. The following day, tubes were transferred into liquid nitrogen for long-term storage.

3.2.5 Transfection of cells

Cells were transiently transfected using polyethylenimine (PEI). The day before transfection, adherent cells were seeded to 30 % confluency. In order to find optimal transfection conditions to produce virus, 0.5 µg, 1 µg or 2 µg plasmid DNA and various DNA/PEI-ratios were tested in parallel, as described in detail in section 4.2.1.

For pseudotyping of MP71 vectors with vesicular stomatitis virus protein G (VSV-G), the packaging cell line Platinum-GP was co-transfected with MP71 expression plasmid and VSV-G-encoding vector; the relative amount was 2:1.

VSV-G pseudotyped pLenti vectors were produced by co-transfection of HEK293T cells with pLenti expression plasmid and Gag/Pol-, Rev- and VSV-G-encoding plasmids; the relative amount was 5:3.75:1.5:1.

Transfection mixtures were vigorously vortexed and evenly distributed onto cell cultures after incubation at room temperature for 15 min. Culture media were replaced 5 hours later. After additional 24 hours, culture media were supplemented with different amounts of histone deacetylase-inhibitors, valproic acid or Na-butyrate, in order to test their influence on transgene expression or virus production (see section 4.2.2).

3.2.6 Transduction of cells

The day before transduction, adherent cells were seeded to 20 - 30 % confluency. Suspension cultures were diluted to a density of 5×10^5 cells/ml at the time of transduction. Concentrated virus was added to cultures. Different conditions for enhancement of infection were tested by supplementation of media with 8 µg/µl polybrene, by centrifugation of infected cultures at 1000 g at 30 °C for 1 hour or by combination of both where polybrene was added before centrifugation (see section 4.3). Media were replaced 24 hours later to reduce toxic effects of polybrene.

3.2.7 Concentration of virus particles

Cell culture supernatants were harvested 48 and 72 hours after transfection. After pooling both supernatants, they were centrifuged at 4000 rpm for 5 min and filtered through a 0.45 µm filter in order to remove residual cells and cell material. Virus was concentrated either by polyethylene glycol precipitation according to the protocol of Tiscornia et al. [105] or pelleted by centrifugation with an Avanti™ J-20XP centrifuge at 75500 g at 4 °C for 2 hours. Subsequently, culture media were quickly decanted. Tubes were incubated upside down on a filter paper to allow draining of residual liquid. Dried virus pellets were resuspended in PBS as 50 - 100x concentrates of the initial cell culture supernatant. Viral concentrates were used for infection or stored at -80 °C.

3.2.8 Concentration of cell culture supernatants containing subviral particles

Cell culture supernatants supposed to contain subviral particles (SVPs) were harvested 48 hours after transduction. Supernatants were centrifuged at 4000 rpm for 5 min and filtered through a 0.45 µm filter in order to remove residual cells and cell material. Cell-free supernatants were stored at 4 °C or applied to ultracentrifugation on a 20 % sucrose/1x PBS cushion in a SW41, SW32 or Type19 rotors, depending on the volume of the supernatant. The volume of 20 % sucrose/1x PBS was one-fifth of the tube's maximum liquid capacity. Centrifugation was performed at 28000 rpm (SW41, SW32) or 19000 (Type19) for 2 or 5 hours, respectively. Subsequently, culture media and sucrose cushions were decanted. Tubes were incubated upside down on a filter paper to allow draining of residual liquid. Dried pellets were resuspended in either 1x PBS containing protease inhibitor or sample buffer as 200 - 1000x concentrates of the initial cell culture supernatant. Concentrates were directly applied to SDS-PAGE, electron microscopy, immunoprecipitation or stored at 4 °C.

3.2.9 Large-scale production of subviral particles

Transduced cell cultures were first expanded into four T-160 flasks before large-scale production of subviral particles (SVPs). For further experiments, Corning® HYPER-Flask® Cell Culture Vessels were applied to avoid space constraints in the incubator and allow easy handling of large amounts of cells. Therefore, transduced cell cultures were pooled and 1×10^7 cells were transferred into 500 ml of DMEM with high glucose (DMEM HG). Each HYPERFlask® was completely filled with cell suspension.

After 48 hours, cell culture supernatants were harvested and stored at 4 °C or concentrated. Cells were washed with 100 ml of 1xPBS and detached by adding 50 ml trypsin solution. Before retrieval from HYPERFlasks®, 50 ml of fresh culture medium were added. 1×10^7 cells were transferred into 500 ml fresh DMEM HG to start another round of large-scale production of SVPs.

3.3 Biochemical and immunological methods

3.3.1 Preparation of cell lysates

Cell culture media were removed from transiently transfected HEK293T or Plat-GP cell cultures. Cells were washed once with 1x PBS and scraped from culture dishes. Cell suspensions were transferred to 1.5 ml reaction tubes and pelleted by centrifugation. Supernatants were subsequently discarded. Suspension cells were directly pelleted in appropriate tubes to separate them from culture media. In order to degrade genomic DNA and other nucleic acids during lysis, 1 µl Benzoase was added to the cell pellets and incubated at 37 °C for 5 - 10 min. Cells were lysed with 100 - 250 µl lysis buffer at room temperature for 5 - 10 min. Lysates were put on ice before proceeding with the Pierce™ BCA Protein Assay or stored at -20 °C.

3.3.2 Determination of protein concentrations

In order to determine protein concentrations of cell lysates, the Pierce™ BCA Protein Assay was applied. In 96-well plates, 4 µl sample per well were mixed with 200 µl of a 1:50-mixture of BCA Reagent B/BCA Reagent A. BCA standard dilutions and ddH₂O served as reference solutions. All standards and samples were prepared in triplicate. Plates were incubated for 30 min at 37 °C before spectrometric measurement at 562 nm using a Multiskan™ GO UV/Vis microplate spectrophotometer from Thermo Scientific.

3.3.3 SDS-PAGE

Proteins were separated according to their molecular weight by sodium dodecyl sulfate polyacrylamide gel-electrophoresis (SDS-PAGE) using 4 % stacking gels and 10 % separation gels (Table 10). Protein samples (25 - 50 µg) were mixed with 10 µl 2x sample buffer before loading onto gels. Gel-electrophoresis was performed at 130 V.

Table 10: SDS-gels

<i>Reagent</i>	<i>4 % stacking gel</i>	<i>10 % separation gel</i>
SDS-Gel buffer	2 ml	5 ml
ddH ₂ O	3.2 ml	5 ml
Acrylamide	0.8 ml	5 ml
APS	100 µl	100 µl
TEMED	10 µl	10 µl

3.3.4 Immunoblot

Proteins separated by SDS-PAGE were transferred onto nitrocellulose membranes by semi-dry blot transfer. Nitrocellulose membranes as well as gels containing separated protein samples were equilibrated in transfer buffer before use. Two layers of filter paper were soaked with transfer buffer and placed onto the anode of the blotting chamber. Then one piece of wet membrane was put onto the filter paper, followed by the gel and another two layers of transfer buffer-soaked filter paper. The upper layer was supposed to be in direct contact with the cathode on top of the chamber. Finally, the blotting chamber was closed and transfer was performed at 20 V for 30 min.

After transfer to a nitrocellulose membrane, bound antigens were detected immunologically by specific primary antibodies or antisera and horseradish peroxidase-coupled (HRP) secondary antibodies. For this purpose, unspecific binding sites were first blocked with blocking solution at room temperature for 1 hour. Afterwards, membranes were incubated with primary antibody or antiserum diluted in 1.5 % milk in 1x PBS-Tween at room temperature for 1 hour. Unbound antibodies were removed by washing the membrane three times with washing solution shaking for 5 min. For detection of bound antibodies, membranes were incubated with HRP-coupled secondary antibodies diluted in 1.5 % milk in 1x PBS-Tween at room temperature for 1 hour. Unbound antibodies were washed away with washing solution three times shaking for 5 min. Membranes were covered with ECL solution for detection of bound HRP-coupled secondary antibodies. Emitted light was visualized by a transilluminator system and software from Biorad.

3.3.5 Blot stripping

To allow *de novo* immunoblotting of already probed nitrocellulose membranes, bound antibodies had to be removed first. For this purpose, membranes were incubated in stripping buffer under rotation at 60 °C for 1 hour. Subsequently, membranes were

washed three times for 5 min before subjecting them to another round of immunoblotting.

3.3.6 Immunoprecipitation of subviral particles

Subviral particles (SVP) in concentrated cell culture supernatants were immunoprecipitated with Protein G Sepharose by GE Healthcare. For this purpose, 400 μ l of Protein G Sepharose were twice washed with 1 ml 1x PBS and centrifuged at 1000 g for 3 min after each washing step. Residual liquid was completely removed. 80 μ l drained Protein G Sepharose was supplemented with 165 μ g mAb 2F5, mAb 4E10 or goat348 α -TM serum. Antibody-protein G complexes were incubated on an overhead shaker at room temperature for 45 min. Subsequently, complexes were washed twice with 1 ml 1x PBS and centrifuged at 1000 g for 3 min after each washing step. Drained antibody-protein G complexes were supplemented with 50 μ l concentrated cell culture supernatant. 1 ml 1x PBS was added to antigen-antibody-protein G complexes and incubated on an overhead shaker at 4 °C over night. The following day, complexes were washed four times with 1x PBS and centrifuged at 1000 g for 3 min after every washing step. Last washing fractions (W4) were saved as controls for immunoblotting. Drained complexes were supplemented with 60 μ l sample buffer and boiled at 95 °C for 5 min in order to elute immunoprecipitated antigens. Antigen-free beads were removed by centrifugation at maximum speed for 10 min. Supernatants containing immunoprecipitated antigens were directly applied to SDS-PAGE.

3.4 Negative staining electron microscopy

Concentrated cell culture supernatants that were supposed to contain subviral particles were applied to transmission electron microscopy. Electron micrographs (Figure 31) were generated and kindly provided by Michael Laue and Gudrun Holland of the Robert Koch-Institute.

Samples were adsorbed to Pioloform-coated, carbon-stabilized and alcianblue-treated copper grids. The adherent particles were washed three times with distilled water. After negative staining with 1 % uranyl acetate, the samples were analyzed using a transmission electron microscope (EM 902, Zeiss, Oberkochen, Germany) at 80 kV and the images were taken using a slow scan CCD-camera (Proscan, Scheuring, Germany).

4 Results

4.1 Subcloning of the FFV EnvG2 and chimeric FFV/HIV-1 EnvG2 x MPER1 and MPER2 DNA sequences into a retroviral vector

The FV *env* gene sequence encodes a splice donor-acceptor pair (SD/SA) flanking the membrane-spanning domain (MSD) of the transmembrane envelope protein (gp48). By that splice event, *tas* and *bet* are generated, while the MSD is deleted. Excision of the MSD results in synthesis of soluble Env protein that is C-terminally truncated and not incorporated into the cellular membrane. Thereby, subviral particle (SVP) formation is impaired due to reduced expression of membrane-bound Env protein after transient transfection of HEK293T cells with pBCenv constructs coding for FFV Env protein [95]. In order to increase incorporation of Env protein into the cellular membrane, the active SD/SA-pair was knocked out by silent mutagenesis [95]. The corresponding expression construct, pBCenv Δ SASD, promoted increased incorporation of Env protein into the membrane and secretion of SVPs [95]. Additionally, two unique restriction sites recognized by BspEI and SgrAI were silently introduced adjacent to the membrane proximal external region (MPER). Similarly, two unique restriction sites recognized by BlnI and Bst1107I flanking the fusion peptide proximal region (FPPR) were silently introduced. The new pBCenv Δ SASD backbone with those additional restriction sites was designated pBC EnvG2 (G2 = generation 2). The pBC EnvG2 backbone was used to replace the adjacent immunogenic regions in the FFV MPER (Figure 11) by the HIV MPER which naturally carries the 2F5 and 4E10 epitopes. Two expression constructs, MPER1 x pBC EnvG2 and MPER2 x pBC EnvG2 were cloned that differ by a three amino acid-shift (Figure 15). That was based on the idea that altering the position in the predicted alpha-helical domain might increase the accessibility of the 2F5 and 4E10 epitopes [95].

For simplification, hybrid MPER1 x EnvG2 and MPER2 x EnvG2 will be referred to as MPER1 and MPER2, respectively, in the following sections.

FFV MPER	YPEWLQLLGEATKDVWPTISNFVSGIGNFIKDTAGGIFGTAFS
FFV/HIV MPER1	YPQELLELDKWASLWNWFNITNWLWYIKFIKDTAGGIFGTAFS
FFV/HIV MPER2	YPEWLQELLELDKWASLWNWFNITNWLWYIKDTAGGIFGTAFS
	<div style="display: flex; justify-content: space-around; margin-top: 10px;"> <u>2F5</u> <u>4E10</u> </div>

Figure 15. Amino acid sequences of the wild-type FFV MPER and chimeric FFV/HIV-1 MPER1 and MPER2 proteins generated by Anne Bleiholder [95]

The first line shows the C-terminal part of FFV TM (grey) with the epitopes identified by FFV TM epitope mapping (red) and the N-terminal part of the membrane-spanning domain (green). Below, the FFV/HIV-1 MPER1 and MPER2 sequences with the integrated HIV MPER (blue) sequence naturally carrying the 2F5 and 4E10 epitopes (underlined) are displayed.

The EnvG2, MPER1 and MPER2 expression constructs were characterized as described in the introduction section (Figure 12) [95]. After transient transfection of HEK293T cells, the EnvG2, MPER1 and MPER2 proteins were expressed and processed as shown by the detection of gp130, gp48 and cell lysate-associated TM^{CL}. The presence of the 2F5 and 4E10 epitopes in the MPER1 and MPER2 chimeras was confirmed by immunoprecipitation with both antibodies. The EnvG2, MPER1 and MPER2 constructs did not allow marker gene transfer but were released into cell culture supernatants as SVPs.

Two different retroviral transfer plasmids served as target vectors for the EnvG2 and hybrid MPER1 and MPER2 DNA sequences: MP71-GFP [90] and pLenti-GFP naturally containing eGFP (Figure 16).

MP71-GFP is optimized for strong protein expression in lymphotropic cell lines [90]. Protein expression is promoted by an improved 5'LTR derived from murine embryonic stem cell virus (Figure 16A) [96]. Transgene expression is enhanced by an intron sequence located 5' of the transgene sequence and flanked by a SD/SA-pair that assists nuclear export of transgene mRNA. Protein expression is further increased by a woodchuck hepatitis virus post-transcriptional regulatory element (PRE) positioned 3' of the transgene sequence. The PRE acts in *cis* by accumulation of mRNA levels and inhibition of mRNA degradation in the cytoplasm [106, 107]. In order to produce MP71 replication-incompetent viruses, Platinum-GP packaging cells were co-transfected with MP71 expression plasmids and pMD2.G coding for vesicular stomatitis virus protein G (VSV-G). Platinum-GP cells are grown in the presence of blasticidin for selection of cells stably expressing *gag* and *pol*.

pLenti-GFP on the other hand, is a HIV-based lentiviral transfer plasmid [108]. In pLenti, protein expression is promoted by a strong CMV promoter (Figure 16B). Like MP71, pLenti also contains a PRE for increasing the steady-state level of transgene mRNA. Pseudotyping is enabled by a psi-packaging signal and further supported by the HIV-1 Rev-response element (RRE) which allows HIV-1 Rev-mediated transportation of viral mRNA to the cytoplasm. pLenti belongs to the 3rd generation packaging system that requires co-transfection of 4 plasmids in total for virus production [108]: a transfer plasmid (pLenti CMV GFP Puro (658-5)), an envelope plasmid (pMD2.G coding for VSV-G) and 2 packaging plasmids expressing Gag and Pol protein from one packaging vector (pMDLg/pRRE) and Rev protein from another (pRSV-Rev).

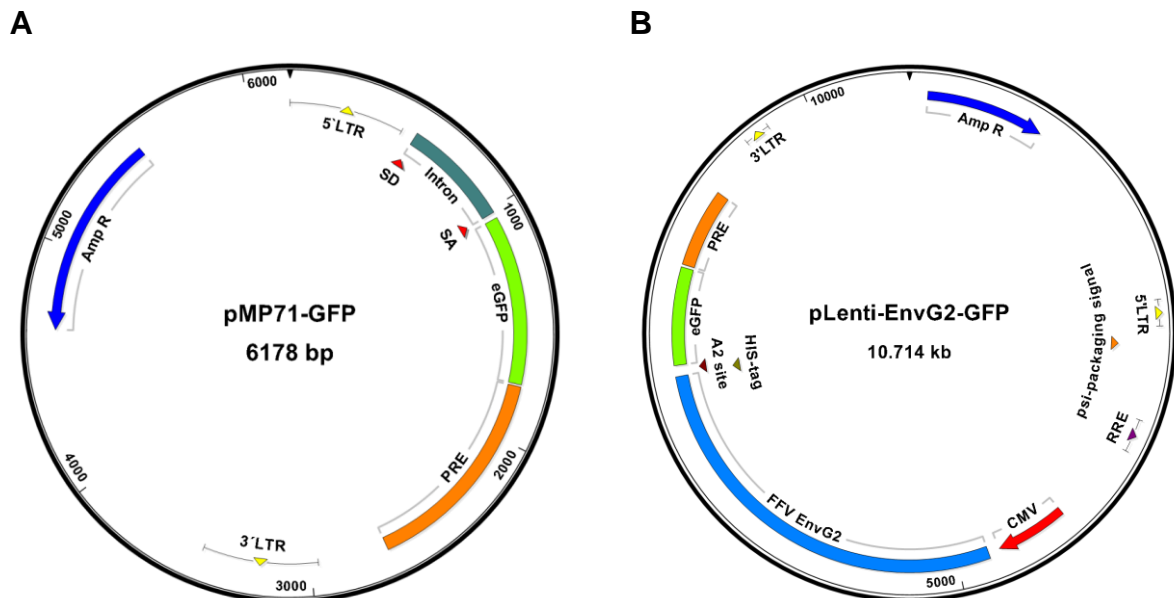


Figure 16. Retroviral vector maps of unmodified MP71-GFP (A) and lentiviral pLenti with the incorporated FFV EnvG2 gene (B)

LTR: long terminal repeat, SD: splice donor, SA: splice acceptor, eGFP: enhanced green fluorescent protein, PRE: post-transcriptional regulatory element, AmpR: prokaryotic ampicillin resistance selection marker, CMV: cytomegalovirus promoter sequence, RRE: Rev-response element, A2 site: A2-cleavage site, His-tag: histidin-tag. Subcloning of the chimeric FFV EnvG2 sequences into MP71 was done by homologous recombination replacing the eGFP gene, while insertion into pLenti was 5' of the eGFP gene sequence by restriction digestion and ligation (the pLenti expression constructs were kindly provided by Kerstin Hoffmann from the Berlin-Brandenburg Center for Regenerative Therapies - Charité University Medicine).

Another feature of the pLenti system is the production of fusion proteins originating from the transgene sequence and the eGFP gene sequence linked via an A2-site (Figure 17). During processing by the cell machinery, the dipeptide is auto-cleaved at the A2-cleavage site generating FFV EnvG2, FFV/HIV-1 MPER1 or MPER2 protein and functional eGFP. As a consequence, the fluorescence signal emitted by eGFP directly correlates with transgene expression.

The pLenti FFV EnvG2 and chimeric pLenti FFV/HIV-1 MPER1 and MPER2 expression plasmids were generated and kindly provided by Kerstin Hoffmann of the Berlin-Brandenburg Center for Regenerative Therapies - Charité University Medicine.

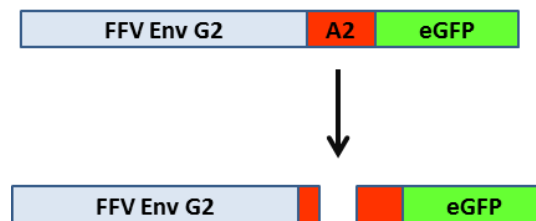


Figure 17. Principle of transgenic protein expression promoted by pLenti

Transgenic FFV EnvG2 protein and eGFP are translated as a dipeptide that is later auto-cleaved at the A2-site. Therefore, the fluorescence signal of eGFP is proportional to transgene expression.

4.1.1 Generation of MP71 FFV EnvG2 and chimeric MP71 FFV/HIV-1 MPER1 and MPER2 expression plasmids

Subcloning of the FFV EnvG2 and chimeric FFV/HIV-1 MPER1 and MPER2 DNA sequences into MP71 was done by homologous recombination replacing the eGFP gene in MP71-GFP.

For this purpose, MP71-GFP was linearized with the restriction enzyme EcoRI. To enable homologous recombination, the FFV EnvG2 and chimeric FFV/HIV-1 MPER1 and MPER2 DNA sequences were PCR-amplified using the primers FFV Env Fusion1 and FFV Env Fusion2. Those primers were designed to add 15 bp-extensions 5' and 3' homologous to vector regions confining the eGFP gene in MP71-GFP. The pBC EnvG2, pBC MPER1 and pBC MPER2 expression plasmids [95] served as templates. After separation of the PCR mixtures by 1 % agarose gel-electrophoresis, the corresponding amplicons were extracted from gel slices. The linear amplicons were

introduced into MP71 in a single reaction utilizing the In-Fusion® Kit from Clontech (see section 3.1.6). Subsequently, the reaction mixtures were transformed into NovaBlue GigaSingles™ Competent Cells for cloning. The following day, random colonies were picked for colony-PCR. The primers FFV TMH fwd and FFV Int sequencing primer rev were used resulting in amplicons of the N-terminal part of the FFV TM sequence with 491 bp in size. Analysis with 1 % agarose gel-electrophoresis revealed that most of the colonies were positive for the amplicons (Figure 18A). Five clones of each construct (EnvG2, MPER1 and MPER2) were chosen for a control digest with EcoRI that was supposed to cut in the MP71 vector region and the SU sequence of the FFV Env gene. Clones that revealed one fragment with 360 bp in length after separation by 1 % agarose gel-electrophoresis were considered positive (Figure 18B). Sequencing according to Sanger confirmed successful subcloning into MP71.

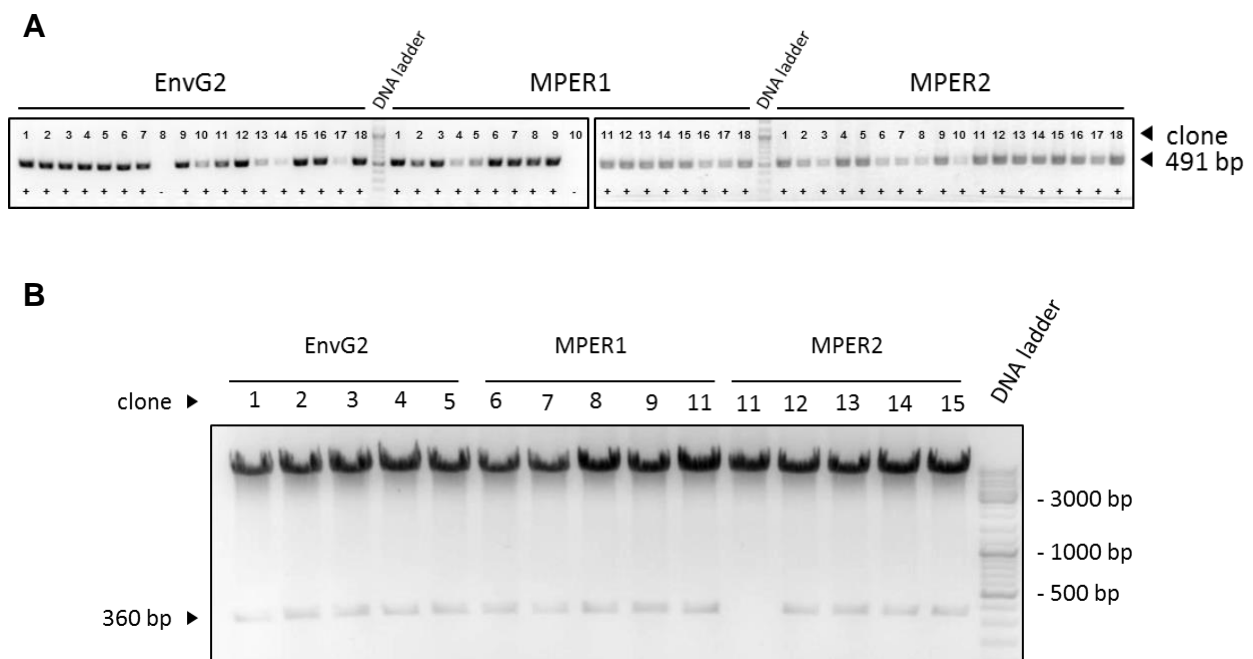


Figure 18. Subcloning into MP71

A) Colony-PCR for screening of positive clones. Colony-PCR mixtures were directly applied to 1 % agarose gel-electrophoresis. Clones resulting in amplicons with 491 bp in length were considered positive (+) for either MP71 EnvG2 or chimeric MP71 MPER1 or MPER2, respectively. **B)** EcoRI-control digest of clones that were positive after colony-PCR. Digested clones with a 360 bp-insert were assumed to carry the EnvG2, MPER1 or MPER2 gene sequence. Finally, sequencing was applied to confirm subcloning into MP71.

4.1.2 Testing the FFV EnvG2 and chimeric FFV/HIV-1 MPER1 and MPER2 expression constructs for protein expression

After successful subcloning, all FFV EnvG2 and hybrid FFV/HIV-1 MPER1 and MPER2 expression plasmids (pBC, pLenti, MP71) were tested for transgene expression. Therefore, HEK293T cells were transiently transfected with 1 µg pBC (positive control), 1 µg MP71 or 2 µg pLenti expression plasmid (EnvG2, MPER1, MPER2), 2 µg pCF7 (infectious molecular clone of FFV, positive control) or 1 µg pEGFP-N3 (negative control) using PEI as transfection reagent (see section 3.2.5). Cell lysates were prepared 48 hours after transfection and equal amounts applied to immunoblotting using goat348 α-TM serum for antigen detection (Figure 19). After blot stripping, hybrid FFV/HIV-1 MPER1 and MPER2 antigens were reprobed with mAb 2F5 or mAb 4E10.

All expression constructs (pBC, MP71, pLenti) promoted wild-type FFV EnvG2 and hybrid FFV/HIV-1 MPER1 and MPER2 protein expression and processing as shown by the detection of gp130 and furin-cleaved gp48. As described by Bleiholder et al. before [95], the chimeric MPER1 and MPER2 expression constructs showed reduced protein expression and processing in comparison to the EnvG2 expression plasmids. Goat348 α-TM serum also detected a cell lysate-associated form of gp48 (TM^{CL}) of 35 - 40 kDa in length. It was found that TM^{CL} is glycosylated but yet absent in viral and subviral particles. This might be explained by a possible loss of the C-terminus including the membrane-spanning domain that serves as a membrane anchor [95].

Gp130 and processed gp48 were running above the 130 kDa and 48 kDa marker bands that is an indication for proper glycosylation of Env [95]. In order to verify glycosylation of EnvG2, MPER1 and MPER2 proteins expressed by the pBC constructs, Bleiholder et al. treated cell lysates of transiently transfected HEK293T cells with Endoglycosidase H (EndoH) [95]. Deglycosylation decreased the molecular weight with the result that gp130 was running at approximately 130 kDa and gp48 below 50 kDa, respectively [95]. In this way, the reduced electrophoretic mobilities of untreated gp130 and gp48 were ascribed to glycosylation.

The fact that hybrid FFV/HIV-1 MPER1 and MPER2 proteins were recognized by mAb 2F5 and mAb 4E10 indicates that the HIV-1 MPER peptide naturally carrying the respective epitopes is present in all chimeric constructs. In comparison to MPER2, binding of 2F5 to MPER1 was stronger. 2F5 was also able to detect pro-

cessed MPER1 gp48 but not MPER2 gp48. Likewise, detection of MPER1 by 4E10 was stronger compared to MPER2. In contrast to 2F5, 4E10 also allowed detection of MPER2 gp48. Detection of MPER2 protein by 2F5 or 4E10 was weakest when expression was promoted by the pLenti MPER2 expression construct.

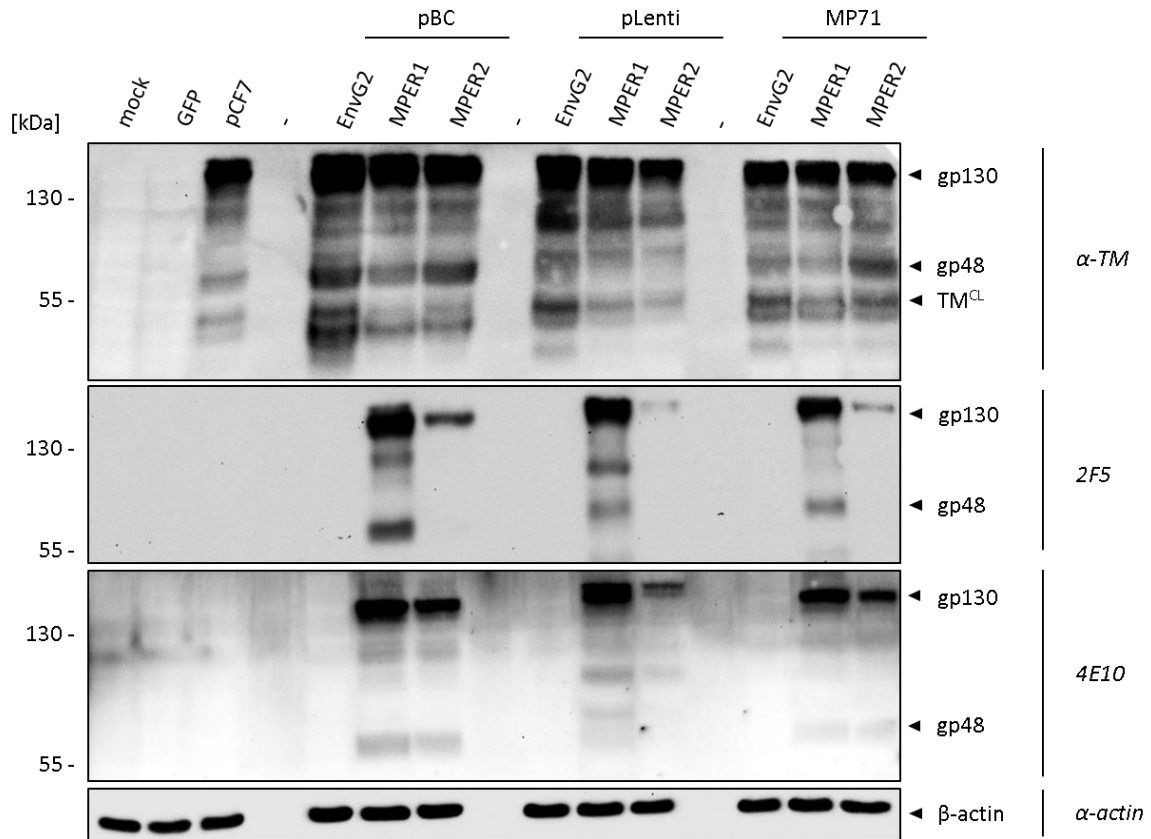


Figure 19. FFV EnvG2 and chimeric FFV/HIV-1 MPER1 and MPER2 protein expressions are promoted by the pLenti and MP71 expression plasmids.

1.6×10^5 HEK293T cells were transfected with $1 \mu\text{g}$ pBC (positive control) [95] or MP71 expression plasmid (EnvG2, MPER1, MPER2), with $2 \mu\text{g}$ pLenti expression plasmid (EnvG2, MPER1, MPER2) or pCF7 (positive control) or $1 \mu\text{g}$ pEGFP-N3 as second negative control in addition to mock (no DNA). 48 hours after transfection, cell lysates were prepared and analyzed by immunoblotting. Detection of antigens was performed either with goat348 α -TM serum, mAb 2F5 or mAb 4E10. Detection of β -actin with anti-actin antibody confirmed equal loading onto the SDS-gel. FFV EnvG2 or hybrid FFV/HIV-1 MPER1 or MPER2 proteins were expressed and processed to different degrees, as shown by the detection of gp130, gp48 and TM^{CL} . The reduced electrophoretic mobilities of gp130 and gp48 in comparison to the 130 kDa and 55 kDa marker bands, respectively, indicated proper glycosylation. Chimeric MPER1 and MPER2 proteins were recognized by 2F5 and 4E10; whereas overall detection of MPER1 protein was stronger compared to MPER2 protein.

4.2 Establishment of efficient protocols for virus production

In order to generate cell lines stably expressing FFV EnvG2 or hybrid FFV/HIV-1 MPER1 or MPER2 protein, single-round viruses for transduction had to be produced. Above all, transduction efficiencies correlate with virus titers. Therefore, transfection, virus production and concentration had to be optimized. For all experimental procedures, the parental vectors MP71-GFP and pLenti-GFP were used to allow an easy read-out based on the detection of the fluorescence signal emitted by GFP.

4.2.1 Transfection optimization for virus production

Viral titers primarily depend on transfection efficiencies. Therefore, different amounts of MP71-GFP or pLenti-GFP plasmid DNA (pDNA) and different concentrations of transfection reagent, polyethylenimine (PEI), were tested in parallel; the assay included DNA/PEI-ratios of 1:1, 1:2, 1:4 and 1:8. In this project, viral MP71 or pLenti transgene mRNA was pseudotyped with VSV-G. The high tropism of VSV-G [109] would allow screening of various target cells in further experiments (see section 4.3 and 4.5.1).

Platinum-GP packaging cells or HEK293T cells were seeded in separate 12-well plates with 40 % confluency. The following day, cells were transfected with 0.5 µg, 1 µg and 2 µg MP71-GFP or pLenti-GFP. Platinum-GP cells stably expressing *gag* and *pol* were co-transfected with MP71-GFP and pMD2.G (VSV-G) in a ratio of 2:1; whereas HEK293T cells were co-transfected with pLenti-GFP, pMDLg/pRRE (*gag* and *pol*), pRSV-Rev (*rev*) and pMD2.G (VSV-G) in a ratio of 5:3.75:1.5:1. The cell viabilities were examined 48 hours after transfection (Figure 20A). Subsequently, cell lysates were prepared and analyzed by immunoblotting detecting GFP expression with α-GFP HRP antibody (Figure 20B). The unconcentrated cell culture supernatants were directly used for transduction of HEK293T cells to allow determination of the relative virus productions in dependence of the transfection efficiencies (Figure 20C).

The viability-assay of the transfected cells revealed increased dying at higher concentrations of PEI (Figure 20A). When transfection was performed with 2 µg pDNA that clearly requires more PEI for transfection (DNA/PEI), viabilities were drastically reduced at DNA/PEI-ratios of 1:4 and 1:8. Viabilities of Platinum-GP cultures were more considerably impaired by PEI.

Higher amounts of MP71-GFP DNA increased transfection efficiencies in Platinum-GP cells as shown by stronger detection of GFP (Figure 20B). Detected GFP bands of Platinum-GP cell lysates were most distinct when transfection was with 0.5 µg, 1 µg or 2 µg MP71-GFP and a DNA/PEI-ratio of 1:8, 1:4 or 1:2, respectively. In HEK293T cells, higher amounts of pLenti-GFP reduced the required concentration of PEI as shown by increased binding of GFP. Transfection with 2 µg pLenti-GFP and a DNA/PEI-ratio of 1:2 to 1:8 resulted in strongest GFP expression.

Based on those results, transfections were carried out with 5 µg pDNA/ 1.6×10^6 cells and a DNA/PEI-ratio of 1:8 in further experiments on virus production.

Results

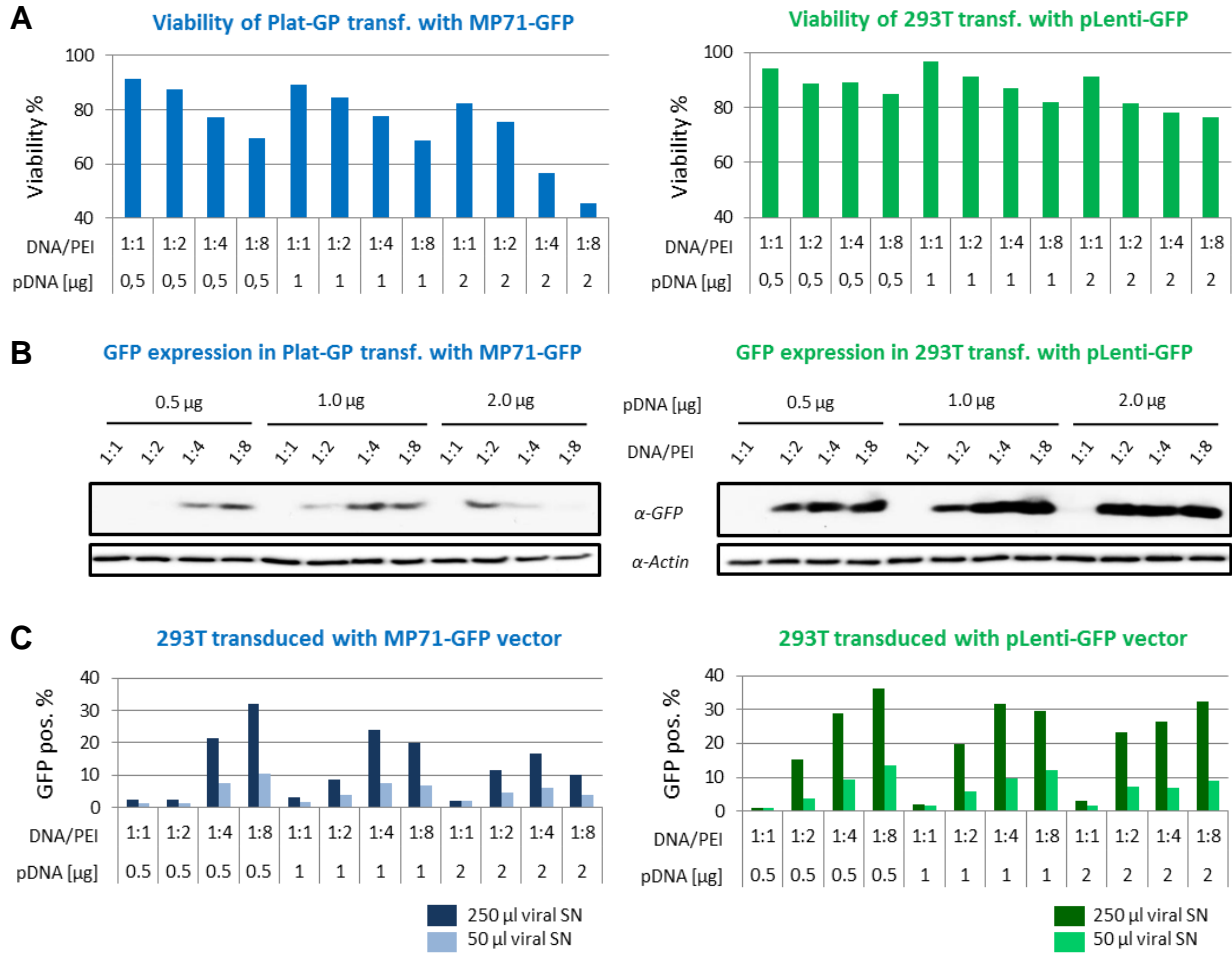


Figure 20. Screening transfection conditions for optimal virus production

1.6×10^5 Platinum-GP cells or HEK293T cells were co-transfected with different amounts of MP71-GFP or pLenti-GFP plasmid DNA (pDNA), respectively, and vectors required for virus production. For transfection with polyethyleneimine (PEI), various ratios of DNA/PEI were tested in parallel, as indicated. **A**) Viabilities depend on the amount of transfected pDNA and the DNA/PEI-ratio used for transfection. 48 hours after transfection, viabilities were determined as described in the method section. The bars represent viabilities of Platinum-GP (blue) and HEK293T cells (green). Increasing concentrations of PEI reduced viabilities. Platinum-GP cultures were more sensitive to PEI than HEK293T cells. **B**) Transfection efficiencies depend on the amount of transfected pDNA and the DNA/PEI-ratio. 48 hours after transfection, cell lysates were prepared and analyzed by immunoblotting. Relative transfection efficiencies were assessed by detection of GFP with α -GFP HRP antibody. Detection of β -actin with anti-actin antibody confirmed equal loading of the cell lysates. In the case of MP71, equal transfection efficiencies with 0.5 μ g, 1 μ g and 2 μ g MP71-GFP pDNA could be observed when the DNA/PEI-ratios were 1:8, 1:4 and 1:2, respectively. Transfection with pLenti-GFP was most effective with 2 μ g pDNA and a DNA/PEI-ratio of 1:2 to 1:8. **C**) Transduction efficiencies depend on the amount of transfected pDNA and the DNA/PEI-ratio used for virus production. 48 hours after transfection, supernatants were harvested. 250 μ l or 50 μ l of unconcentrated supernatant (SN) were used for transduction of HEK293T cells in a 96-well plate. 72 hours after infection, transduction efficiencies (GFP pos. %) were determined by FACS. GFP pos. % $\hat{=}$ % of events with FITC-height > lg 1. The bars represent the values of one experiment that directly correlated with the rate of virus production. Infection with MP71-GFP or pLenti-GFP virus is indicated in blue or green, respectively. The best virus production was by transfection with 0.5 μ g MP71-GFP or pLenti-GFP pDNA and a DNA/PEI-ratio of 1:8.

4.2.2 Testing additives for enhanced virus production

For maximizing virus production, two histone-deacetylase inhibitors, Na-butyrate and valproic acid, were tested as supplements in cell culture media.

For this purpose, 1.6×10^5 Platinum-GP or HEK293T cells per well of two 24-well plates were transiently transfected with 0.5 μg MP71-GFP or pLenti-GFP and a DNA/PEI-ratio of 1:8 (see section 4.2.1). 24 hours after transfection, the culture media were supplemented with 1, 2, 5, 10, 15, 20, 30 or 50 mM (final concentrations) Na-butyrate or valproic acid. Viral culture supernatants were harvested after further 48 hours and 50 μl unconcentrated aliquots directly used to infect 1.6×10^5 HEK293T cells. Transduction efficiencies were measured by FACS 72 hours after infection (Figure 21).

MP71-GFP and pLenti-GFP virus production correlated nonlinearly with the tested concentrations of Na-butyrate and valproic acid. Compared to Na-butyrate, valproic acid was less effective in enhancing virus production. A 1.7-fold increase of transduction efficiency could be obtained by infection with MP71-GFP virus produced in the presence of 2 mM Na-butyrate (Figure 21A). On the other hand, transduction efficiencies by pLenti-GFP virus increased 4-fold after supplementation with 50 mM Na-butyrate (Figure 21B).

According to those results, 2 mM and 50 mM Na-butyrate were applied 24 hours after transfections for productions of MP71 and pLenti viruses, respectively.

Results

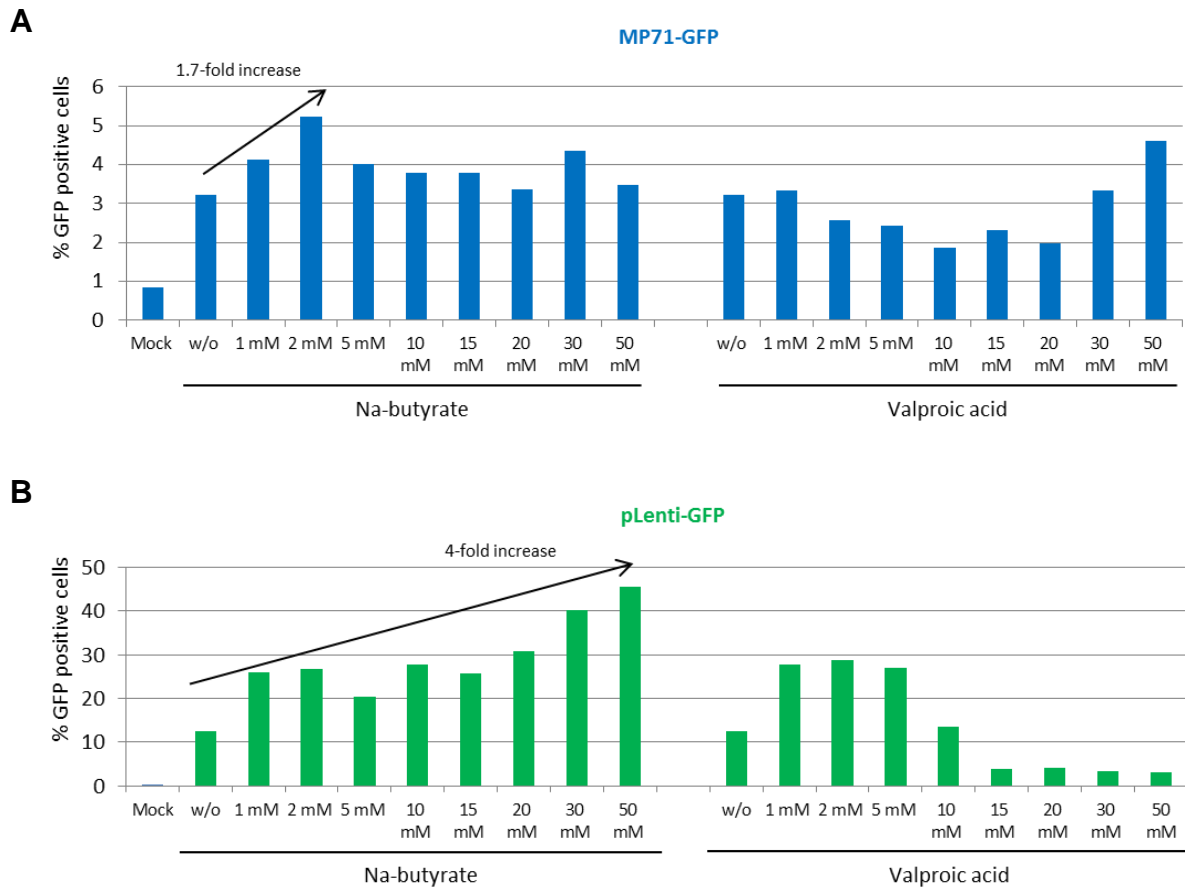


Figure 21. Testing Na-butyrate and valproic acid for increased virus production

0.5 μg MP71-GFP or pLenti-GFP were PEI-transfected (DNA/PEI-ratio was 1:8) into 1.6×10^5 Platinum-GP or HEK293T cells, respectively. 24 hours after transfection, Na-butyrate and valproic acid were added to the culture medium in various concentrations, as indicated. After further 48 hours, 50 μl of unconcentrated viral culture supernatant were used to infect 1.6×10^5 293T cells. 72 hours after infection, transduction efficiencies (% GFP positive cells) were determined by FACS. % GFP positive cells \triangleq % of events with FITC-height $> \lg 1$. The bars represent the values of one experiment that directly correlated with the rate of virus production. Mock: no DNA, w/o: no additive. **A)** A significant correlation between production of MP71 virus and concentration of Na-butyrate or valproic acid was absent. The best virus production was achieved with 2 mM Na-butyrate that resulted in a 1.7-fold increase of transduction efficiency. **B)** Valproic acid significantly enhanced the pLenti virus production when concentrations were 1 to 5 mM. However, 50 mM Na-butyrate led to best virus production as the transduction efficiency was 4-fold increased.

4.2.3 Testing methods to concentrate virus

After having found optimal conditions for the production of MP71-GFP and pLenti-GFP virus, two methods for concentrating virus were tested: polyethylene glycol (PEG) precipitation according to the protocol of Tiscornia et al. [105] and centrifugation.

For this purpose, 1.6×10^7 Platinum-GP or HEK293T cells were transiently transfected with 26 μg MP71-GFP or pLenti-GFP and a DNA/PEI-ratio of 1:8 (see section 4.2.1). Two days after transfection, 18 ml viral culture supernatants were harvested and filtered through a 0.45 μm filter. 7.5 ml cell-free supernatant were applied to PEG precipitation, 7.5 ml were centrifuged at 75500 g for 2 h and the residual 3 ml were stored at $-20\text{ }^\circ\text{C}$. 150x virus concentrates were prepared by resuspending the respective pellets in 100 μl 1x PBS. 1.6×10^5 HEK293T cells in 24-well plates were infected with 10 μl unconcentrated cell-free viral supernatant or 10 μl virus concentrate obtained by PEG or centrifugation. 48 hours after infection, the relative success of virus concentration was determined based on the transduction efficiencies measured by FACS (Figure 22).

PEG precipitation seemed to be most suitable for concentrating MP71-GFP viruses since the transduction efficiency was approximately 13 % higher when compared to the centrifugation method. However, centrifugation was more promising for concentration of pLenti-GFP virus because the transfection efficiency was 5 % higher in comparison to PEG precipitation.

Those results did not show decisive differences between PEG precipitation and centrifugation for virus concentration. Therefore, the method of centrifugation was applied in further experiments, since it is more feasible and yields virus pellets with higher purity [110].

Results

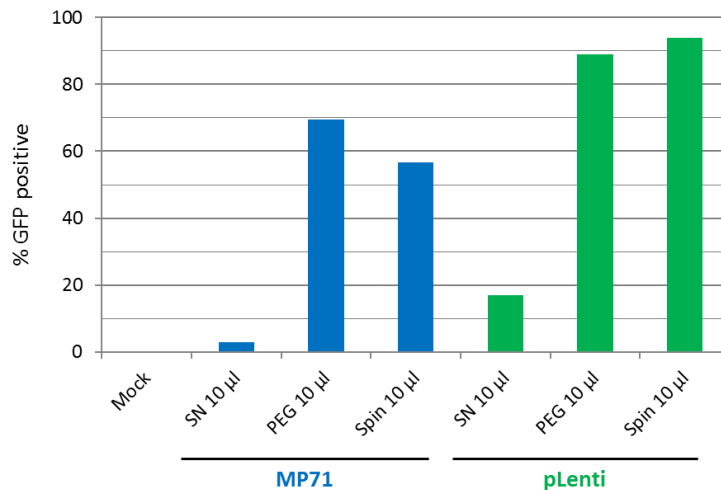


Figure 22. Testing polyethylene glycol precipitation and centrifugation at 75500 g for virus concentration

MP71-GFP or pLenti-GFP virus was produced by transfecting 1.6×10^7 Platinum-GP or HEK293T cells with 26 µg MP71-GFP or pLenti-GFP, respectively, and a DNA/PEI-ratio of 1:8. 48 hours after transfection, viral culture supernatants were harvested. 7.5 ml of cell-free viral supernatant were applied to polyethyleneglycol (PEG) precipitation or centrifuged at 75500 g for 2 h (Spin). Pelleted virus was resuspended in 100 µl 1x PBS. 1.6×10^5 HEK293T cells were infected with 10 µl unconcentrated cell-free viral supernatant (SN) or virus concentrate, as indicated. 48 hours later, transduction efficiencies (% GFP positive) were determined by FACS. % GFP positive \triangleq % of events with FITC-height > Ig 1. The bars represent the values of one experiment that directly correlated with virus titers. Infection with MP71-GFP or pLenti-GFP virus is indicated in blue or green, respectively. Concentration of MP71 virus by PEG precipitation was by 13 % more effective than centrifugation. On the other hand, pLenti-GFP virus led to a 5 % higher transduction rate when centrifugation was applied.

4.3 Optimization of retroviral infection

Vectors pseudotyped with vesicular stomatitis virus protein G (VSV-G) have a broad host range [109]. However, infection rates may vary dependent on the target cell line. In order to find a target cell line that allows high transduction rates achieved by infection with VSV-G pseudotyped MP71 or pLenti virus, four different cell lines were tested in parallel:

- HEK293T cells that were used by Anne Bleiholder et al. for the production of subviral particles (SVPs) (Figure 12D) [95]. They served as a kind of reference cell line.

- 293F cells that are suspension cells derived from 293 cells. They are adapted to be cultured in serum-free expression media (e.g., FreeStyle™ 293 Expression Medium). Their characteristics would be advantageous because transduced suspension 293F cells would constitute a larger culture surface releasing SVPs into serum-free medium. This could significantly simplify purification of SVPs.
- Lymphotropic C8166 cells that are grown in suspension. That feature turns them into interesting target cells because transduced C8166 cells would constitute a high culture surface releasing SVPs (see 293F cells). Furthermore, their lymphotropic character could be advantageous when transduction was with MP71 vectors since MP71 is optimized for protein expression in lymphotropic cell lines [96].
- CRFK cells that are feline kidney cells. They were tested because main parts of the epitope scaffold/the SVPs originate from feline foamy virus (FFV). Expression of FFV Env protein could be increasingly promoted in CRFK cells due to possible evolutionary adaption of FFV to its natural host, the cat [58].

Additionally, four infection conditions were tested in parallel for further optimization of retroviral infection with MP71 and pLenti virus:

- infection with concentrated virus
- polybrene added to the medium (8 µl/ml) (PB)
- spinoculation at 1000 g at 37 °C for 1 hour (Spin)
- polybrene added to the medium (8 µl/ml) and spinoculation at 1000 g at 37 °C for 1 hour (PB+Spin)

For this purpose, 1.6×10^7 Platinum-GP or HEK293T cells were transiently transfected with 26 µg MP71-GFP or pLenti-GFP and a DNA/PEI-ratio of 1:8 (see section 4.2.1). 48 hours after transfection, viral supernatants were harvested and filtered through a 0.45 µm filter. Virus was concentrated hundred-fold by centrifugation at 75500 g for 2 h and resuspending the viral pellets in an appropriate volume of 1x PBS.

In order to test the four infection conditions mentioned above, 1×10^5 HEK293T, 293F, C8166 or CRFK cells were infected with MP71-GFP or pLenti-GFP virus concentrate in 24-well plates. The volumes of virus concentrates were adapted so that estimated multiplicities of infections (MOI) were 1. One day after infection, the culture media were changed in order to mitigate toxic side-effects of polybrene. After further 48 hours, FACS analysis of the transduced cells allowed comparison and evaluation of the infection conditions on the basis of the respective transduction efficiencies (Figure 23A) and mean fluorescence intensities (MFI) that indicate GFP expression per cell and correlate with integrated proviral copy numbers (Figure 23B).

The highest transduction efficiencies and MFIs of HEK293T, C8166 and CRFK cells were obtained when PB + Spin was applied. However, MFIs of C8166 cells transduced with MP71-GFP virus remained unaffected after assisted infection in any of the tested condition.

Infection of 293F cells with MP71-GFP and pLenti-GFP virus resulted in diverse transduction efficiencies and MFIs, when compared to all other tested cell lines. Even though the transduction efficiency of MP71-GFP infection was increased by PB + Spin, MFIs could not be improved by any infection condition. As it was the case for the other cell lines, pLenti-GFP infection of 293F cells was more efficient than MP71-GFP infection. However, neither polybrene nor spinoculation resulted in increased transduction efficiencies in 293F cells; only spinoculation elevated the MFI.

Infection optimization by adding polybrene to the medium (8 μ l/ml) in combination with spinoculation at 1000 g at 37 °C for 1 hour led to highest transduction efficiencies and MFIs of 3 of the 4 tested cell lines. Therefore, PB+Spin was used for infection enhancement in further experiments.

Results

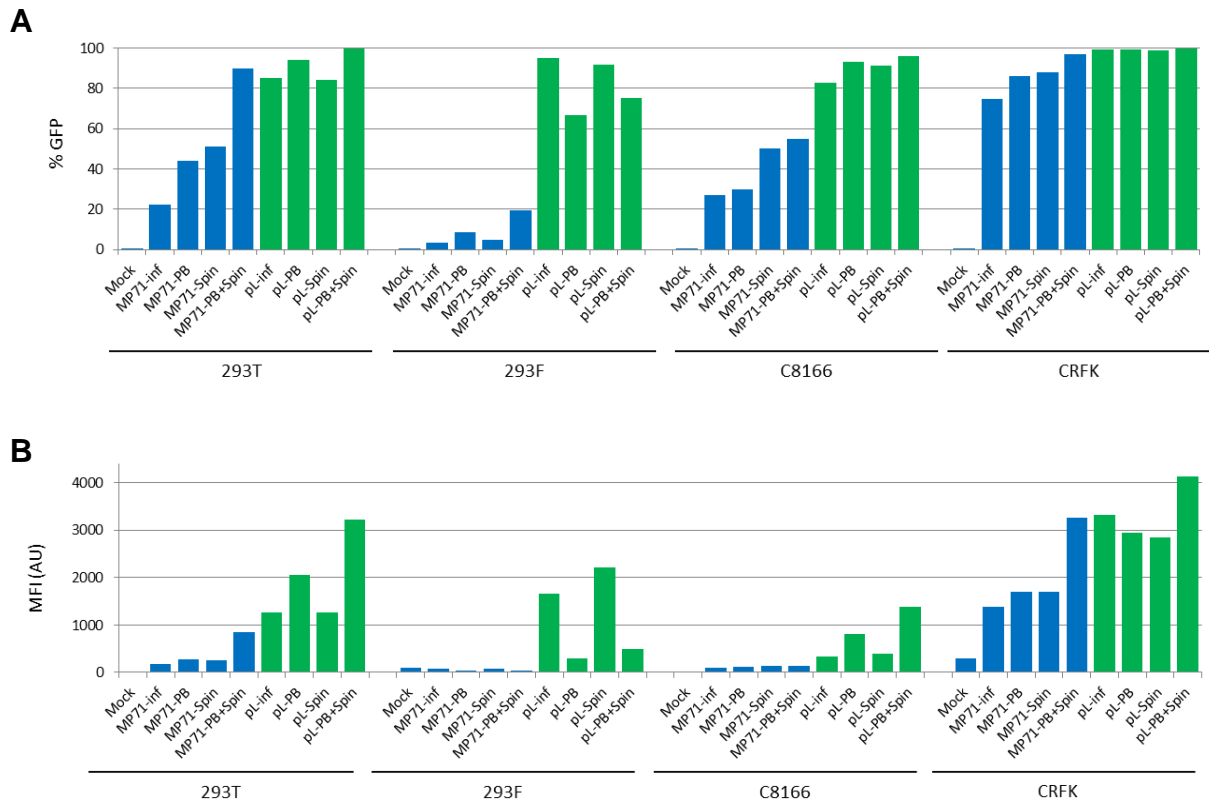


Figure 23. Transduction optimization

1 x 10⁵ HEK293T, 293F, C8166 or CRFK cells were transduced with concentrated MP71-GFP (blue bars) or pLenti-GFP (green bars, pL) virus as indicated. Estimated multiplicities of infections (MOI) were 1. Four infection conditions were tested in parallel: infection with concentrated virus, inf; infection in the presence of polybrene (8 µl/ml), PB; centrifugation at 1000 g at 37 °C for 1 h, Spin; combination of polybrene (8 µl/ml) and centrifugation at 1000 g at 37 °C for 1 h, PB+Spin. 24 h after infection, the culture media were replaced. After a further 48 hours, transduced cells were analyzed by FACS. **A**) Transduction efficiencies (% GFP) in dependence of different infection conditions and cell lines. % GFP ≙ % of events with FITC-height > lg 1. The bars represent the values of one experiment. The highest transduction efficiencies of HEK293T, C8166 and CRFK cells after infection with MP71-GFP and pLenti-GFP virus were obtained when PB+Spin was used. 293F cells were the exception because the transduction efficiency with pLenti-GFP virus was highest when infection was performed with virus concentrate only. Infection of 293F cells with MP71-GFP virus was best when PB+Spin was used, but very inefficient when compared to transduction efficiencies of the other tested cell lines. **B**) Mean fluorescence intensities (MFIs) in dependence of different infection conditions and cell lines. MFIs correlated with average GFP expression per cell and multiple integrations of proviral DNA copies into the target genomes. MFI ≙ mean of FITC-heights > lg 1. AD: arbitrary units. The bars represent the values of one experiment. MFIs of pLenti-infected HEK293T, C8166 and CRFK cells were highest when PB+Spin was used. 293F cells transduced with pLenti-GFP virus resulted in highest MFI after centrifugation. Infection with MP71-GFP virus led to higher MFIs of CRFK cells when compared to the other tested cell lines. Distinct increases in MFIs of MP71-infected 293F and C8166 cells after supported infections could not be achieved.

4.4 Testing the established protocols for virus production and infection for applicability on the FFV EnvG2 and chimeric FFV/HIV-1 MPER1 and MPER2 constructs

4.4.1 Real-time PCR for determination of virus titers

In order to determine virus titers of MP71- and pLenti-FFV EnvG2 and hybrid FFV/HIV-1 MPER1 and MPER2 viruses, real-time PCR was applied. Since all MP71 and pLenti vectors incorporate the PRE into target genomes, a real-time PCR program was established that amplifies a short sequence of the PRE (Figure 16). Therefore, the probe PRE2 Probe fwd and the primers PRE fwd and PRE2 rev were designed to bind a sequence with 142 bp in length within the PRE sequence. Several concentrations of MgCl₂ were tested for optimizing the sensitivity of the real-time PCR. An optimal condition and program was found (see section 3.1.5) which allowed detection of down to 10¹ initial plasmid DNA (pDNA) copies within 35 PCR-cycles (C_T) (Figure 24A).

The established protocol for real-time PCR was used to deduce two correlation curves (Figure 24B and 25) needed for calculations of virus titers:

- C_T / log copies of pDNA
- Transduction efficiency / proviral copies

For this purpose, plasmid standard dilution series of MP71-GFP and pLenti-GFP pDNA with 10⁶, 10⁵, 10⁴, 10³, 10², 10¹ and 10⁰ copies/3 µl were prepared. Real-time PCR amplification of the dilution series (Figure 24A) allowed establishment of the standard curve C_T / log copies pDNA (Figure 24B) based on equation (1).

$$C_T = k \cdot \log \text{copies} + d \tag{1}$$

C_T Cycle threshold; defined as the number of cycles required for the fluorescence signal to cross the fixed threshold [111].
 k Gradient; change of C_T -value per copies.
 copies Initial plasmid copy number
 d Regressor

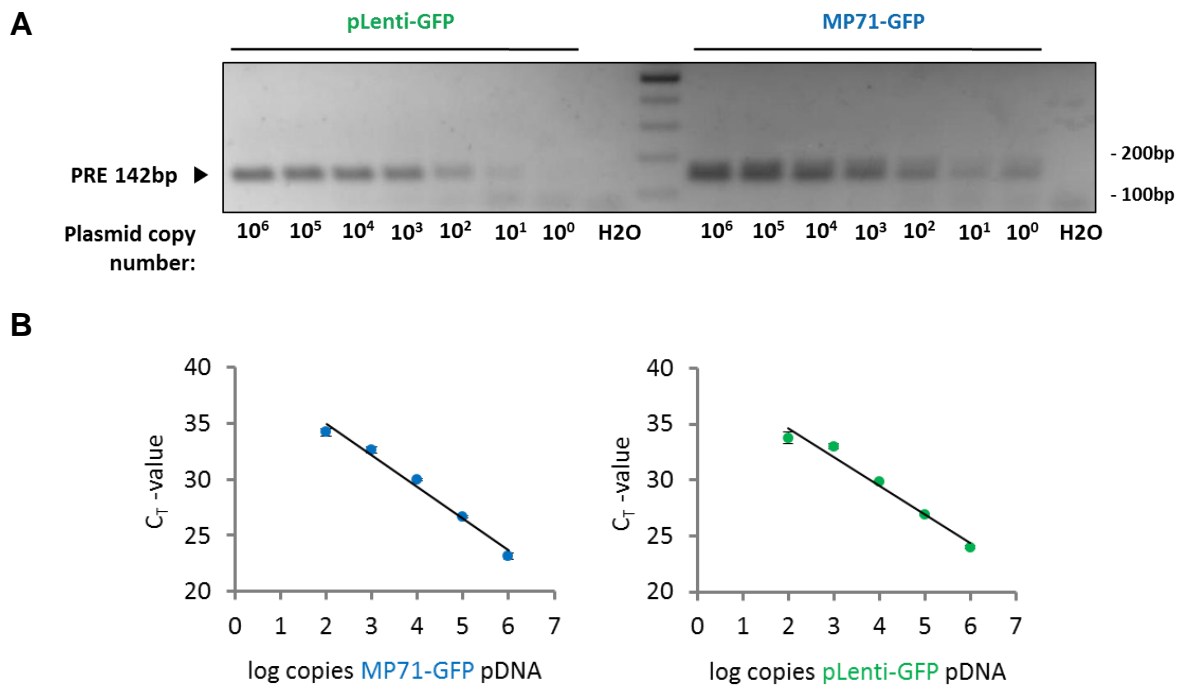


Figure 24. Real-time PCR of the MP71-GFP and pLenti-GFP dilution series

Real-time PCR of MP71- or pLenti-GFP plasmid DNA dilution series with initial plasmid copy numbers of 10^6 down to 10^0 was performed as described in section 3.1.5. **A)** Analytical agarose gel-electrophoresis of the real-time PCR-amplified pLenti-GFP and MP71-GFP dilution series. **B)** C_T / log copy number-correlations of the MP71-GFP (blue) and pLenti-GFP (green) plasmid DNA dilution series.

In order to establish the second calibration curve (transduction efficiency / proviral copies), transduction efficiencies and the corresponding C_T -values of cells transduced with MP71-GFP or pLenti-GFP virus had to be determined. As MP71-GFP and pLenti-GFP vectors lead to equivalent transductions (1 PRE/provirus), it was sufficient to conduct only pLenti-GFP infections.

For this purpose, 2.8×10^5 HEK293T cells were infected with 100 μ l, 20 μ l and 4 μ l of unconcentrated cell culture supernatant containing pLenti-GFP virus with unknown titer. 72 hours after infection, transduction efficiencies were determined by FACS. Afterwards, 100 ng genomic DNA (gDNA) were applied to real-time PCR for determina-

tion of the corresponding C_T -values. Now, rearrangement of equation (1) to equation (2) allowed calculation of pLenti-GFP proviral copies integrated in 100 ng of transduced gDNA.

$$\text{copies}_{\text{proviral}} = 10^{\left(\frac{C_T - d}{k}\right)} \quad (2)$$

Together with the transduction efficiencies obtained by FACS, the correlation between transduction efficiency and proviral copy number (Figure 25) based on equation (3) could be deduced.

$$\% \text{ GFP positive} = a \cdot \text{copies}^b \quad (3)$$

% GFP positive	Percentage of transduced cells.
<i>a</i>	Gradient; change of transduction efficiency per copies.
<i>b</i>	Exponent
copies	Proviral copy number (= $\text{copies}_{\text{proviral}}$)

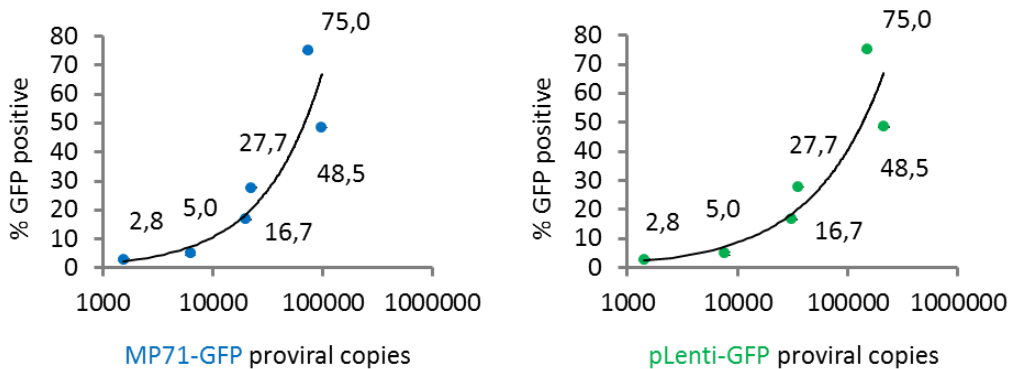


Figure 25. Calibration curves obtained by real-time PCR with transduced genomic DNA

The real-time PCR protocol was established for amplification of a short sequence of the PRE integrated into target genomes, regardless of the vector (MP71 or pLenti) used for transduction. Accordingly, it was sufficient to apply just pLenti-GFP infection for subsequent deduction of the MP71 as well as the pLenti calibration curves. Therefore, 2.8×10^5 HEK293T cells were infected with 100 μ l, 20 μ l or 4 μ l of unconcentrated pLenti-GFP viral culture supernatant with unknown titer. 72 hours after infection, transduction efficiencies (% GFP positive) were determined by FACS. % GFP positive \triangleq % of events with FITC-height > lg 1. Genomic DNA was isolated and applied to real-time PCR for triplicate determination of proviral copies integrated. Finally, the correlations between transduction efficiencies (values of one experiment) and integrated MP71- or pLenti-GFP proviral copies (mean values) were established as indicated.

In order to calculate virus titers of MP71 and pLenti FFV EnvG2 and hybrid FFV/HIV-1 MPER1 and MPER2 virus concentrates, 3.2×10^5 HEK293T cells were infected with 1 μ l virus concentrate of unknown titer. 72 hours after infection, 100 ng gDNA were applied to real-time PCR. The obtained C_T -values were used to calculate the corresponding proviral copies integrated by applying equation (2). The respective transduction efficiencies were determined with equation (3). Finally, application of equation (4) revealed virus titers (infectious units per ml) of MP71 and pLenti FFV EnvG2 and hybrid FFV/HIV-1 MPER1 and MPER2 virus concentrates.

$$\text{IU / ml} = \frac{\text{cell number} \cdot \left(\frac{\text{corr. \% GFP}}{100} \right)}{\mu\text{l of virus}} \cdot 1000 \quad (4)$$

IU	Infectious units
corr. % GFP	Corresponding transduction efficiencies calculated with equation (3).
μ l of virus	Volume of virus concentrate used for infection.

4.4.2 Applicability of the established protocols on the MP71-EnvG2 and pLenti-EnvG2 constructs

The MP71 and pLenti FFV EnvG2 and chimeric FFV/HIV-1 MPER1 and MPER2 expression plasmids differ from the MP71-GFP and pLenti-GFP plasmids by approximately 2.3 kb and 3 kb in length, respectively. Furthermore, possible toxic side-effects due to over-expression of transgenic FFV Env protein might arise. According to those facts, the protocols for virus production that were established with the MP71-GFP and pLenti-GFP plasmids needed to be tested for applicability on the EnvG2 and chimeric MPER constructs.

For this purpose, 7×10^4 Platinum-GP or HEK293T cells were transfected with 125 ng or 250 ng total amount of DNA comprising MP71-EnvG2 or pLenti-EnvG2 expression plasmid and plasmids required for virus production as described in detail in section 3.2.5. To screen for optimal PEI-transfection, different ratios of DNA/PEI (1:1, 1:2, 1:4, 1:6 and 1:8) were tested in parallel (as described for MP71-GFP and pLenti-GFP in section 4.2.1). Cell lysates were prepared 48 hours after transfection and equal aliquots analyzed by immunoblotting using goat348 α -TM serum for antigen detection (Figure 26).

In general, transfection with 250 ng DNA and the DNA/PEI-ratio of 1:8 resulted in strongest EnvG2 protein expression. Transfection with MP71-EnvG2 required fewer amounts of DNA and PEI. EnvG2 protein expression and processing promoted by MP71 could be detected after transfection with 125 ng DNA and DNA/PEI-ratios of 1:4 to 1:8, as shown by the detection of gp130, gp48 and TM^{CL} (Figure 26A). Transfection with pLenti-EnvG2 required more DNA for detectable EnvG2 protein expression. After transfection with 125 ng pDNA and DNA/PEI-ratios of 1:6 and 1:8, only weak expression of gp130 and uncleaved gp130-GFP could be detected. Although transfection with 250 ng DNA resulted in stronger detection of EnvG2 protein expression promoted by pLenti, clear bands of processed gp48 and TM^{CL} were still absent (Figure 26B). EnvG2 gp130 and gp48 expressed by MP71 or pLenti were properly glycosylated as shown by lower electrophoretic mobilities compared to the 130 kDa and 55 kDa marker bands, respectively.

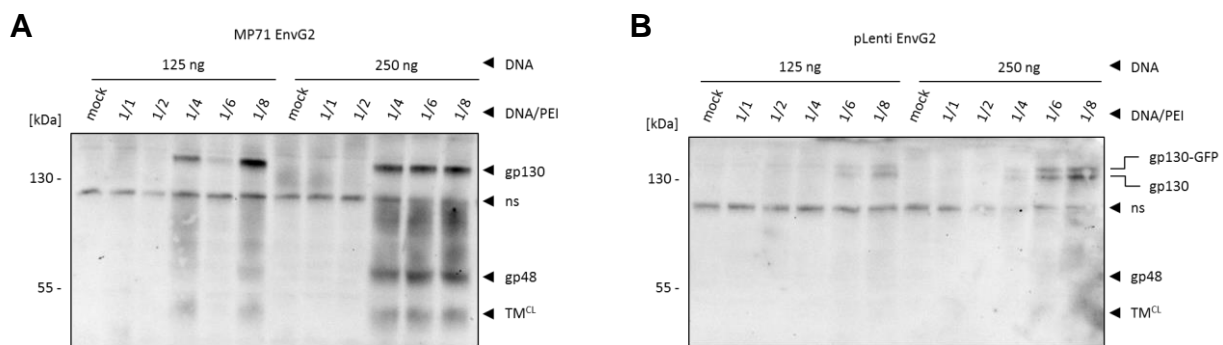


Figure 26. Transfection optimization with the MP71-EnvG2 and pLenti-EnvG2 constructs

7 x 10⁴ Platinum-GP cells or HEK293T cells were co-transfected with 125 ng or 250 ng DNA (MP71-EnvG2 or pLenti-EnvG2 pDNA and plasmids required for virus production; see section 3.2.5). For transfection with polyethyleneimine (PEI) various ratios of DNA/PEI were tested in parallel, as indicated. 48 hours after transfection, cell lysates were prepared and analyzed by immunoblotting. Detection of antigens was performed with goat348 α -TM serum. **A)** Immunoblot of Platinum-GP cells transfected with MP71-EnvG2. 250 ng DNA transfected with a DNA/PEI-ratio of 1:8 gave the best transfection efficiencies as indicated by stronger binding of gp130, gp48 and TM^{CL}. The reduced electrophoretic mobilities of gp130 and gp48 in comparison to the 130 kDa and 55 kDa marker bands, respectively, indicated proper glycosylation. ns: non-specific detection. **B)** Immunoblot of HEK293T cells transfected with pLenti-EnvG2. 250 ng DNA transfected with a DNA/PEI-ratio of 1:8 resulted in best transfection efficiencies as shown by the detection of gp130 and uncleaved gp130-GFP. However, Env protein expression was too low to allow detection of processed gp48 and TM^{CL}. The reduced electrophoretic mobilities of gp130, gp130-GFP and gp48 in comparison to the 130 kDa and 55 kDa marker bands, respectively, indicated proper glycosylation. ns: non-specific detection.

200 µl of unconcentrated viral supernatant obtained from the cultures transfected with 250 ng DNA were used to transduce 3.2×10^5 293T cells. 72 hours after infection, genomic DNA was isolated and used for real-time PCR. Virus titers (IU/ml) were determined as described in detail in section 4.4.1.

Transfection with the MP71-EnvG2 and pLenti-EnvG2 expression plasmids in a DNA/PEI ratio of 1:8 resulted in best virus titers (Figure 27), just as it was previously the case for MP71-GFP and pLenti-GFP virus production.

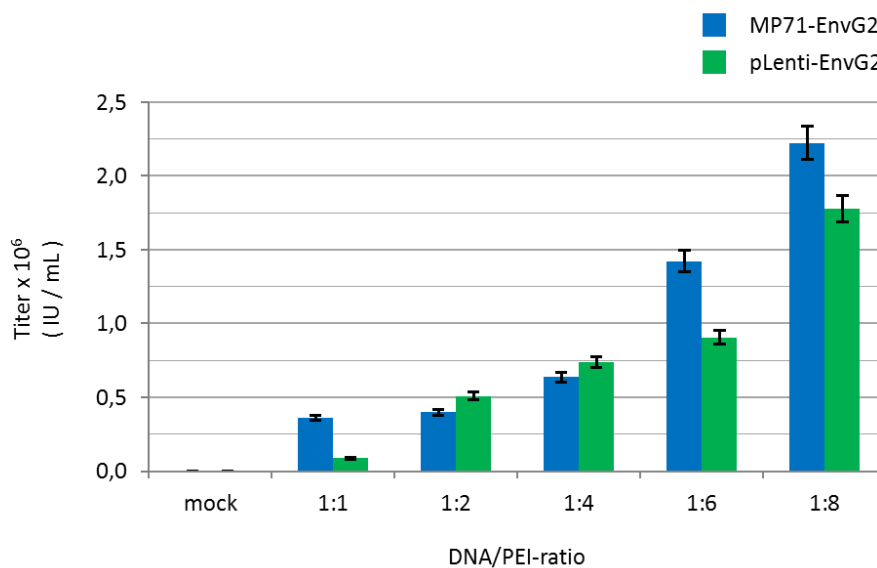


Figure 27. Virus titers of FFV Env expression vectors in dependence of DNA/PEI-ratios

7×10^4 Platinum-GP or HEK293T cells were transfected with 250 ng MP71-EnvG2 or pLenti-EnvG2 and various DNA/PEI-ratios, as indicated, in order to find an optimal condition for virus production. 48 hours after transfection, 200 µl of unconcentrated viral culture supernatant were used to transduce 3.2×10^5 293T cells. 72 hours after infection, virus titers were determined in triplicate by applying real-time PCR (see section 4.4.1). The mean values and standard deviations of one experiment are shown. The bars represent the MP71-EnvG2 (blue) and the pLenti-EnvG2 (green) virus titers. Transfection with a DNA/PEI-ratio of 1:8 resulted in highest virus titers.

Those data indicated that the protocols for virus production established with the MP71-GFP and pLenti-GFP vectors are generally applicable for the MP71- and pLenti-EnvG2 and MPER constructs; albeit, twice as much DNA is required for transfection.

4.5 Production of subviral particles

4.5.1 Finding a suitable target cell line for stable FFV EnvG2 and chimeric FFV/HIV-1 MPER1 and MPER2 protein expression

After having established protocols for the production of MP71 and pLenti viruses, a cell line that is most suitable for transduction and stable FFV EnvG2 and chimeric FFV/HIV-1 MPER1 and MPER2 protein expression needed to be found. In that experiment, the HEK293T, 293F, C8166 and CRFK cell lines were screened because of their characteristics mentioned in section 4.3.

For this purpose, 1.6×10^7 Platinum-GP or HEK293T cells were transfected with 26 µg MP71- or pLenti-EnvG2, MPER1 or MPER2, MP71-GFP or pLenti-GFP and a DNA/PEI-ratio of 1:8. 24 hours after transfection, 2 mM or 50 mM Na-butyrate were added to the Platinum-GP or HEK293T cultures, respectively. After a further 24 hours, viral culture supernatants were harvested. The Platinum-GP or HEK293T cultures were provided with fresh culture medium supplemented with 2 mM or 50 mM Na-butyrate, respectively. 24 hours later (72 hours after transfection), viral culture supernatants were harvested again. The 48 and 72 hours-supernatants were filtered through a 0.45 µm filter. Virus was concentrated hundred-fold by centrifugation at 75500 g for 2 h and resuspending the viral pellets in an appropriate volume of 1x PBS. Related 48 and 72 hours-virus concentrates were pooled and stored at -20 °C. Afterwards, 50 µl of concentrated MP71- or pLenti-EnvG2, MPER1 or MPER2 virus or MP71-GFP or pLenti-GFP virus (negative controls) were used for infection of 1.4×10^5 293F, C8166, 293T or CRFK cells. Cell lysates were prepared 72 hours after infection and applied to immunoblotting detecting antigens with goat348 α-TM serum. Cell lysates of cells earlier transfected with pCF7 served as positive control (Figure 28).

293F cells transduced with MP71- or pLenti-EnvG2, MPER1 or MPER2 virus expressed Env protein as shown by weak detection of gp130 (Figure 28A). The expression of gp130 and uncleaved gp130-GFP proteins by pLenti MPER1 and MPER2 was very low. Processing of Env protein could not be shown, since gp48 and TM^{CL} remained undetected. However, proper glycosylation of gp130 and gp130-GFP was indicated by their reduced electrophoretic mobility compared to the 130 kDa marker band.

Env protein expression in infected C8166 cells was completely absent (Figure 28B).

Env protein expression was not promoted in pLenti-infected HEK293T cells. In contrast, MP71-infected HEK293T cells expressed EnvG2, MPER1 or MPER2 protein as shown by the detection of gp130 (Figure 28C). Expression of EnvG2 gp130 protein was stronger than MPER1 and MPER2 gp130 protein so that processing of EnvG2 could also be shown as indicated by the detection of gp48 and TM^{CL}. Furthermore, gp130 was running above the 130 kDa marker band, indicating proper glycosylation. However, the protein smear of processed EnvG2 might be a result of differential and incomplete glycosylation levels.

CRFK cells transduced with MP71-EnvG2, MPER1 and MPER2 virus showed strong expression and processing of Env protein as indicated by detection of distinct protein bands of gp130, gp48 and TM^{CL} (Figure 28D). Proper glycosylation of Env was verified by the presence of only low protein smear but sharp protein bands of gp130 and gp48 running above the 130 kDa and 55 kDa marker bands, respectively. Again, Env protein expression in pLenti-infected CRFK cells remained undetectable.

Those results suggested that CRFK cells infected with MP71-EnvG2, MPER1 or MPER2 virus are most suitable for FFV Env protein expression when compared to infected 293F, C8166 and HEK293T cells. Consequently, the MP71-transduced CRFK cultures were expanded for further experiments on subviral particle production.

Results

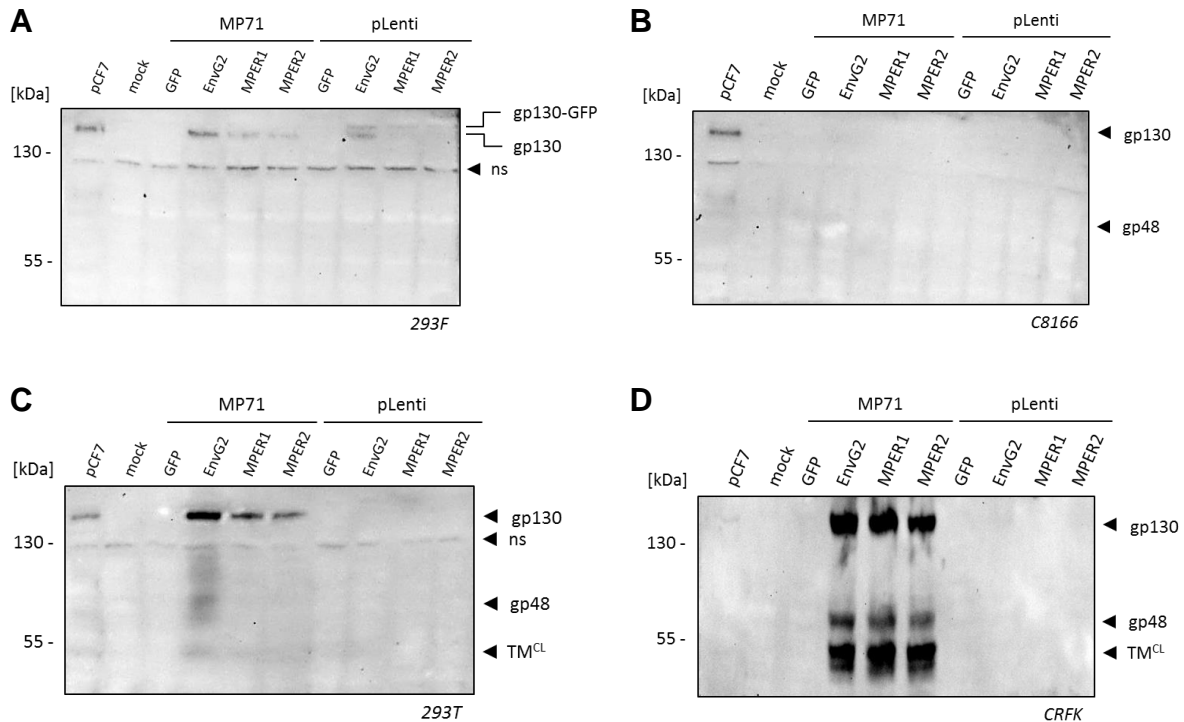


Figure 28. Screening various cell lines for stable expression of FFV EnvG2 and chimeric FFV/HIV-1 MPER1 and MPER2 protein

1.4×10^5 293F, C8166, HEK293T or CRFK cells were infected with 50 μ l of concentrated MP71- or pLenti-EnvG2, MPER1 or MPER2 virus or MP71-GFP or pLenti-GFP virus (negative controls) as indicated. 72 hours after infection, cell lysates were prepared and analyzed by immunoblotting, along with cell lysates of pCF7-transfected cells as positive control. Detection of antigens was performed with goat348 α -TM serum. **A)** Immunoblot of transduced 293F cells. All constructs promoted FFV EnvG2 and hybrid FFV/HIV-1 MPER1 and MPER2 protein expression as shown by the detection of gp130 and uncleaved gp130-GFP encoded by the pLenti constructs. The reduced electrophoretic mobilities of gp130 and gp130-GFP in comparison to the 130 kDa marker band indicated proper glycosylation. Expression of processed gp48 and TM^{CL} was absent. ns: non-specific detection. **B)** Immunoblot of transduced C8166 cells. Expression by all MP71 and pLenti constructs was absent. **C)** Immunoblot of transduced 293T cells. Expression of FFV Env protein by the pLenti constructs was absent. All MP71 constructs promoted FFV EnvG2 protein and hybrid FFV/HIV-1 MPER1 and MPER2 protein expression as shown by the detection of gp130. FFV EnvG2 protein was stronger expressed than MPER1 and MPER2 proteins. Weak bands of processed FFV EnvG2 gp48 and TM^{CL} could be detected. The reduced electrophoretic mobilities of gp130 and gp48 in comparison to the 130 kDa and 55 kDa marker bands, respectively, indicated proper glycosylation. ns: non-specific detection. **D)** Immunoblot of transduced CRFK cells. Expression of FFV Env protein by the pLenti constructs was absent. All MP71 constructs promoted strong FFV EnvG2 and hybrid FFV/HIV-1 MPER1 and MPER2 protein expression and processing as shown by the detection of distinct bands of gp130, gp48 and TM^{CL}. The reduced electrophoretic mobilities of gp130 and gp48 in comparison to the 130 kDa and 55 kDa marker bands, respectively, indicated proper glycosylation.

4.5.2 CRFK cells transduced with MP71-EnvG2, MPER1 and MPER2 virus release subviral particles

CRFK cells that were transduced with MP71-EnvG2, MPER1 and MPER2 virus seem to be suitable for strong expression of FFV EnvG2 and hybrid FFV/HIV-1 MPER1 and MPER2 protein (Figure 28D). Next, they had to be tested for subviral particle-release (SVP).

For this purpose, 8 ml cell culture supernatant of confluent CRFK cultures infected with MP71-EnvG2, MPER1 or MPER2 virus were harvested. The cell-free supernatants that were supposed to contain SVPs were applied to ultracentrifugation on a 20 % sucrose cushion. The protein pellets were resuspended in 80 µl sample buffer and directly analyzed by immunoblotting, along with cell lysates of the corresponding transduced CRFK cells as positive controls. Goat348 α-TM serum was used for antigen detection (Figure 29).

In all supernatants of EnvG2, MPER1 or MPER2 protein-expressing CRFK cultures, processed and properly glycosylated gp48 was present as shown by the detection of sharp protein bands running above the 55 kDa marker band. EnvG2 protein was more abundant when compared to MPER1 and MPER2 protein; even precursor EnvG2 gp130 could be detected.

Those results gave a first indication that CRFK cells transduced with MP71-EnvG2, MPER1 and MPER2 virus release SVPs into supernatants.

Results

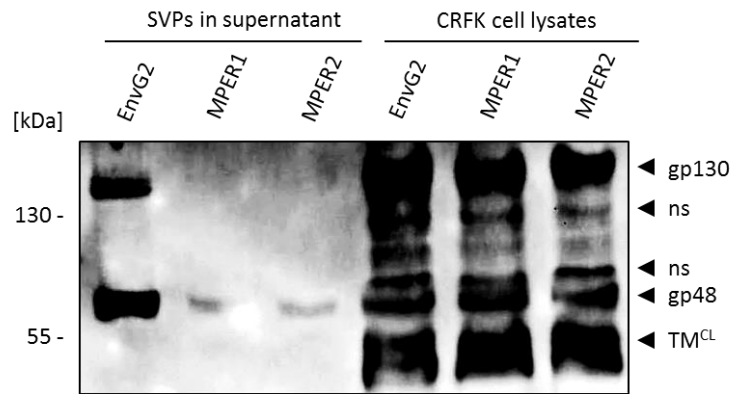


Figure 29. MP71-transduced CRFK cells release FFV EnvG2 and chimeric FFV/HIV-1 MPER1 and MPER2 subviral particles into cell culture media

Cell culture supernatants of confluent CRFK cultures transduced with MP71-EnvG2, MPER1 or MPER2 virus were harvested. 8 ml of cell-free supernatants were concentrated hundred-fold by ultracentrifugation on a 20 % sucrose cushion and analyzed by immunoblotting. Cell lysates of the corresponding transduced CRFK cells served as positive controls. Detection of antigens was performed with goat348 α -TM serum. FFV EnvG2 and chimeric FFV/HIV-1 MPER1 and MPER2 SVPs were released into the supernatants as shown by the detection of processed gp48. EnvG2 SVPs were stronger released than MPER1 and MPER2 SVPs that were present in equal amounts. The precursor gp130 of EnvG2 protein was also detected. The reduced electrophoretic mobilities of gp130 and gp48 in comparison to the 130 kDa and 55 kDa marker bands, respectively, indicated proper glycosylation. ns: non-specific detection.

4.5.3 Characterization of EnvG2, MPER1 and MPER2 subviral particles by immunoprecipitation

In order to test MP71-transduced CRFK cells on release of functional subviral particles (SVPs), immunoprecipitation was applied. To allow verification that the 2F5 and 4E10 epitopes are accessible on the surface of native MPER1 or MPER2 SVPs, mAb 2F5 and mAb 4E10 were used for immunoprecipitation.

For this purpose, cell culture supernatants of confluent CRFK cultures transduced with MP71-EnvG2, MPER1 or MPER2 virus were harvested. The cell-free supernatants that were supposed to contain SVPs were ultracentrifuged on a 20 % sucrose cushion. Subsequently, the protein pellets were resuspended in an appropriate volume of 1x PBS containing protease inhibitor for two hundred-fold concentration. The concentrates were directly applied to immunoprecipitation. For immunoprecipitation of FFV EnvG2 SVPs and antigens from pCF7-transfected HEK293T cells (positive control), goat348 α -TM serum was used. FFV MPER1 and MPER2 SVPs and 1x

PBS (negative control) were submitted to immunoprecipitation with mAb 2F5 or mAb 4E10. After washing the antigen-antibody-protein G complexes, the last washing fractions were saved as controls for immunoblotting. Immunoprecipitated antigens were eluted from protein G by boiling in sample buffer. Finally, equal aliquots of the saved washing fractions (W4) and the immunoprecipitates were analyzed by immunoblotting (Figure 30). In order to avoid cross-reactivity of secondary antibodies, Rat321-3 α -TM serum was used to detect immunoprecipitated EnvG2 SVPs; immunoprecipitated MPER1 and MPER2 SVPs were detected with goat348 α -TM serum.

Native EnvG2 SVPs present in concentrated supernatants were immunoprecipitated by goat348 α -TM serum as indicated by the presence of furin-cleaved and properly glycosylated gp48 running above the 55 kDa marker band (Figure 30A). Likewise, mAb 2F5 and mAb 4E10 were able to immunoprecipitate MPER1 and MPER2 as shown by the detection of processed gp48 (Figure 30B, C). Again, reduced electrophoretic mobility compared to the 55 kDa marker band, verified proper glycosylation of gp48. Immunoprecipitation with mAb 2F5 resulted in higher enriched MPER1 SVPs in relation to MPER2 SVPs. In return, immunoprecipitation of MPER2 SVPs was more efficient with mAb 4E10. All three immunoprecipitations could be considered very specific since antigens were completely absent in all washing fractions.

The results of immunoprecipitation indicated that CRFK cells transduced with MP71-EnvG2, MPER1 and MPER2 virus release functional SVPs with accessible 2F5 and 4E10 epitopes.

Results

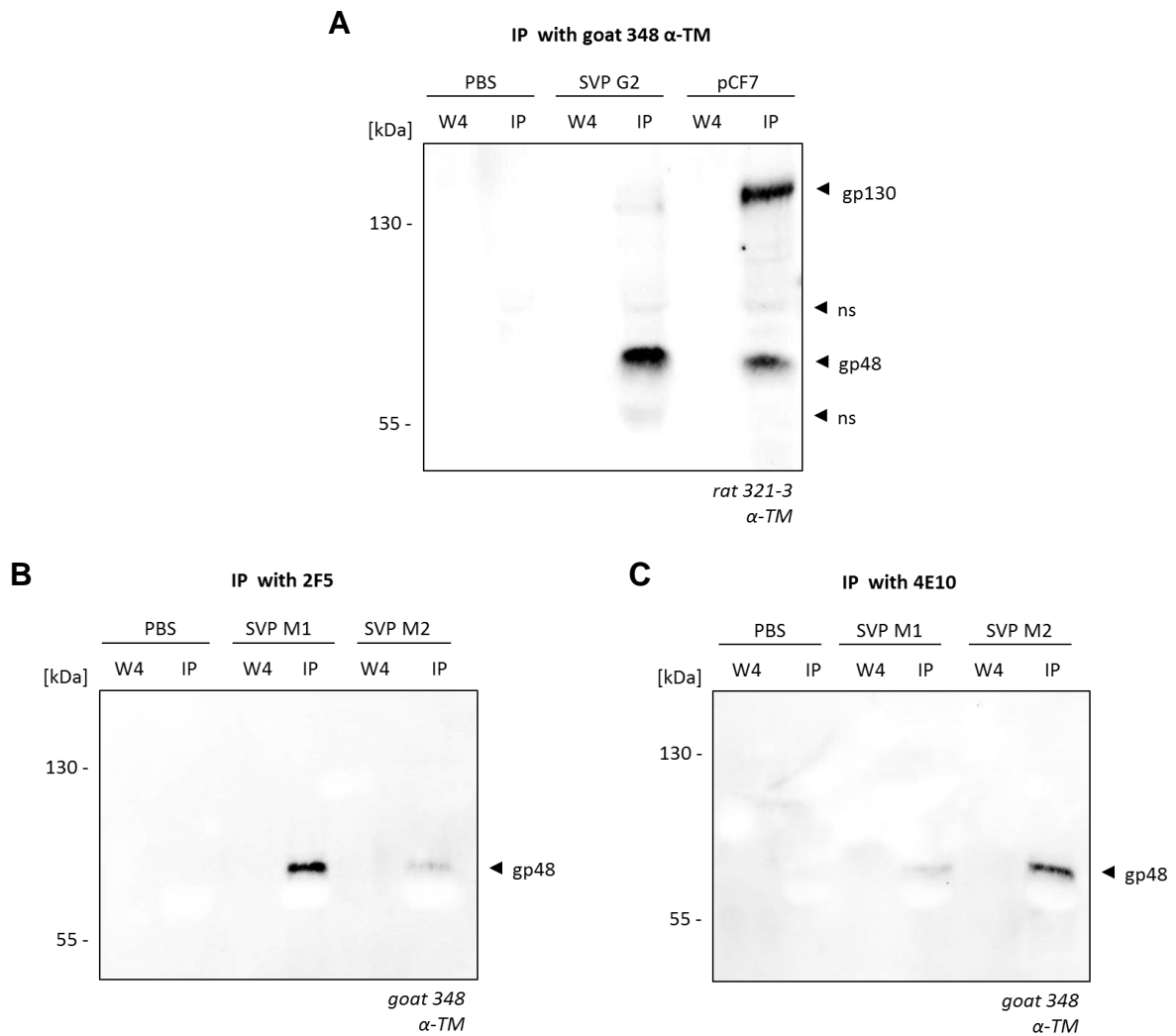


Figure 30. Immunoprecipitates of FFV EnvG2 and chimeric FFV/HIV-1 MPER1 and MPER2 sub-viral particles

Cell culture supernatants of confluent CRFK cultures transduced with MP71-EnvG2, MPER1 or MPER2 virus were harvested and concentrated two hundred-fold by ultracentrifugation on a 20 % sucrose cushion. The concentrates were applied to immunoprecipitation. **A**) Immunoprecipitation of native FFV EnvG2 SVPs, 1x PBS (negative control) and a cell lysate of pCF7-transfected HEK293T cells (positive control) with goat348 α -TM serum. The immunoprecipitates (IP) and the fourth washing fractions (W4) were analyzed by immunoblotting. Detection of antigens was performed with rat321-3 α -TM serum. FFV EnvG2 SVPs were immunoprecipitated by goat 348 α -TM serum as shown by the detection of gp48. The reduced electrophoretic mobility of gp48 in comparison to the 55 kDa marker band indicated proper glycosylation. **B, C**) Immunoprecipitation of hybrid FFV/HIV-1 MPER1 and MPER2 SVPs and 1x PBS (negative control) with mAb 2F5 (**B**) or mAb 4E10 (**C**). The immunoprecipitates (IP) and the fourth washing fractions (W4) were analyzed by immunoblotting. Detection of antigens was performed with goat348 α -TM serum. Chimeric FFV/HIV-1 MPER1 and MPER2 SVPs were immunoprecipitated by mAb 2F5 and mAb 4E10 as shown by the detection of gp48. MPER1 SVPs were more efficiently immunoprecipitated by mAb 2F5 than MPER2 SVPs (**B**); whereas MPER2 SVPs were higher enriched by mAb 4E10 than MPER1 SVPs (**C**). The reduced electrophoretic mobility of gp48 in comparison to the 55 kDa marker band indicated proper glycosylation. Immunoprecipitation was specific, since antigens were absent in all washing fractions. ns: non-specific binding

4.5.4 Transmission electron microscopy of concentrated cell culture supernatants supposed to contain subviral particles

To further indicate that subviral particles (SVPs) are present in cell culture supernatants of CRFK cultures transduced with MP71-EnvG2, MPER1 and MPER2 virus, transmission electron microscopy was applied.

For this purpose, MP71-transduced CRFK cultures (see section 4.5.2) were expanded for SVP large-scale production in Corning® HYPERFlasks®. 500 ml cell-free supernatants of confluent CRFK cultures that were supposed to release SVPs were harvested and ultracentrifuged on a 20 % sucrose cushion. Protein pellets were re-suspended in 500 µl 1x PBS containing protease inhibitor. Concentrates were analyzed by Michael Laue and Gudrun Holland of the ZBS 4 (Advanced Light and Electron Microscopy) of the Robert Koch-Institute by negative staining electron microscopy (see section 3.4) (Figure 31).

In general, two classes of particles were discovered in all samples. One class was more abundant, electron dense and about 100 nm in size. The other class was smaller in size (50 - 70 nm) with characteristic surface structures that resemble FV-typical dense glycoprotein [83]. In order to demonstrate that one of those classes of particles are FFV SVPs, it would be necessary to apply electron microscopy after the method of immunogold-labeling utilizing, for example, goat348 α-TM serum, mAb 2F5 or mAb 4E10.

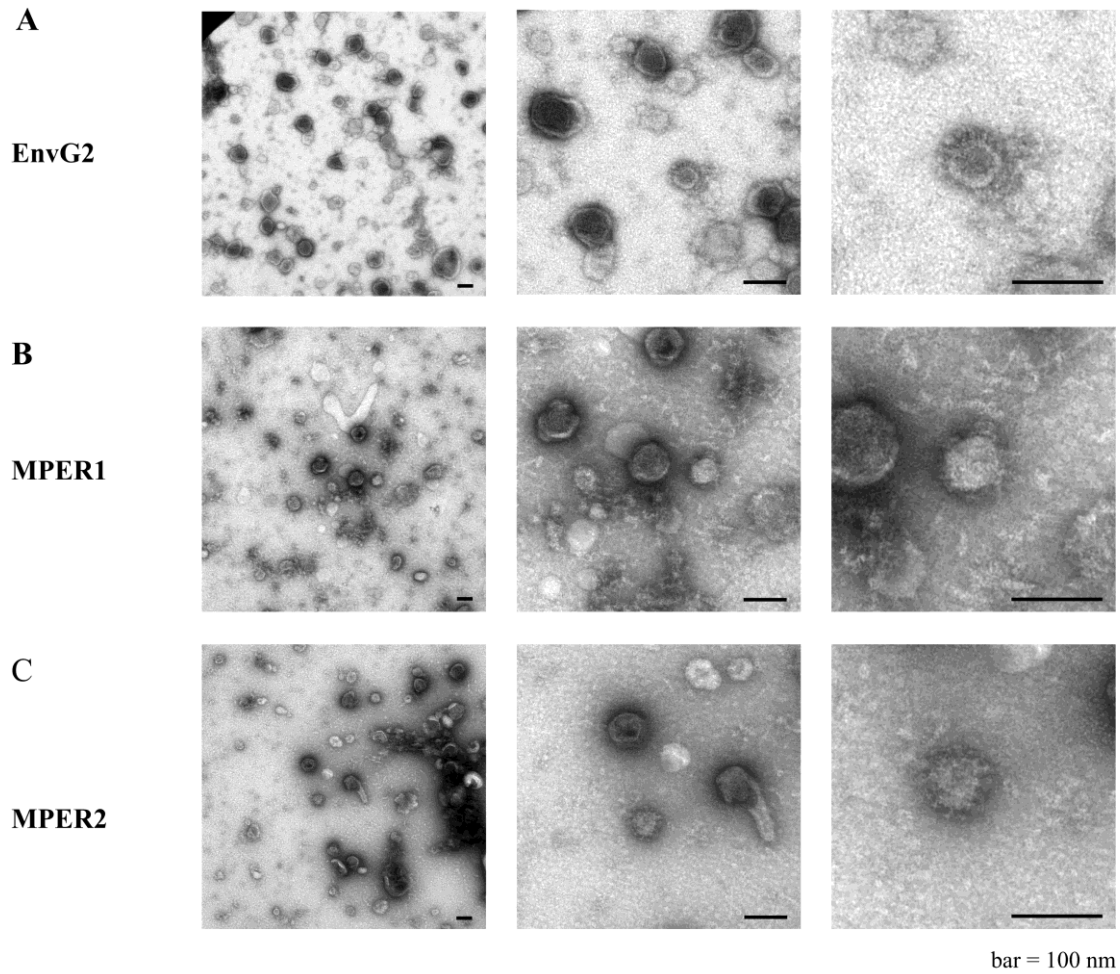


Figure 31. Electron micrographs of concentrated subviral particle-like structures

Supernatants of confluent CRFK cultures transduced with MP71-EnvG2, MPER1 or MPER2 virus were harvested and concentrated thousand-fold by ultracentrifugation on a 20 % sucrose cushion. FFV EnvG2 (**A**), FFV/HIV-1 MPER1 (**B**) and FFV/HIV-1 MPER2 (**C**). Two classes of particles could be found in all samples. One class was more abundant, electron dense and about 100 nm in size. The other class was smaller in size with characteristic surface structures that resemble glycoprotein.

4.5.5 Optimization of subviral particle production

DMEM HG was used in the experiments so far. However, the presence of 10 % FCS in cell culture supernatants could hamper SVP purification. For that reason, CRFK cells transduced with MP71-EnvG2 virus were subcultured in various commercially available serum-free expression media:

- DMEM HG, FCS-free
- RPMI, FCS-free
- FreeStyle™ 293 Expression Medium
- HyClone™ SFM4HEK293™ Medium
- EX-CELL® VPRO

Transduced CRFK cells grown in standard DMEM HG with 10 % FCS served as reference culture. 48 hours after subculturing, cells were analyzed by means of viabilities, expression and processing of EnvG2 protein and release of EnvG2 SVPs. The viability-assay revealed that HyClone™ SFM4HEK293™ Medium and EX-CELL® VPRO increased the cell viabilities 2.4- and 2.2-fold, respectively (Figure 32A).

8 ml cell-free supernatants were concentrated by ultracentrifugation on a 20 % sucrose cushion. The protein pellets were resuspended in 80 µl sample buffer. In addition, cell lysates of the corresponding cells were prepared. Concentrates and lysates were analyzed in parallel by immunoblotting using goat348 α-TM serum for antigen detection (Figure 32B).

In comparison, all tested media promoted EnvG2 protein expression and processing to similar degrees. Nevertheless, HyClone™ SFM4HEK293™ Medium and EX-CELL® VPRO resulted in highest SVP-release, as indicated by strong detection of processed and properly glycosylated gp48 in the respective concentrated cell culture supernatants.

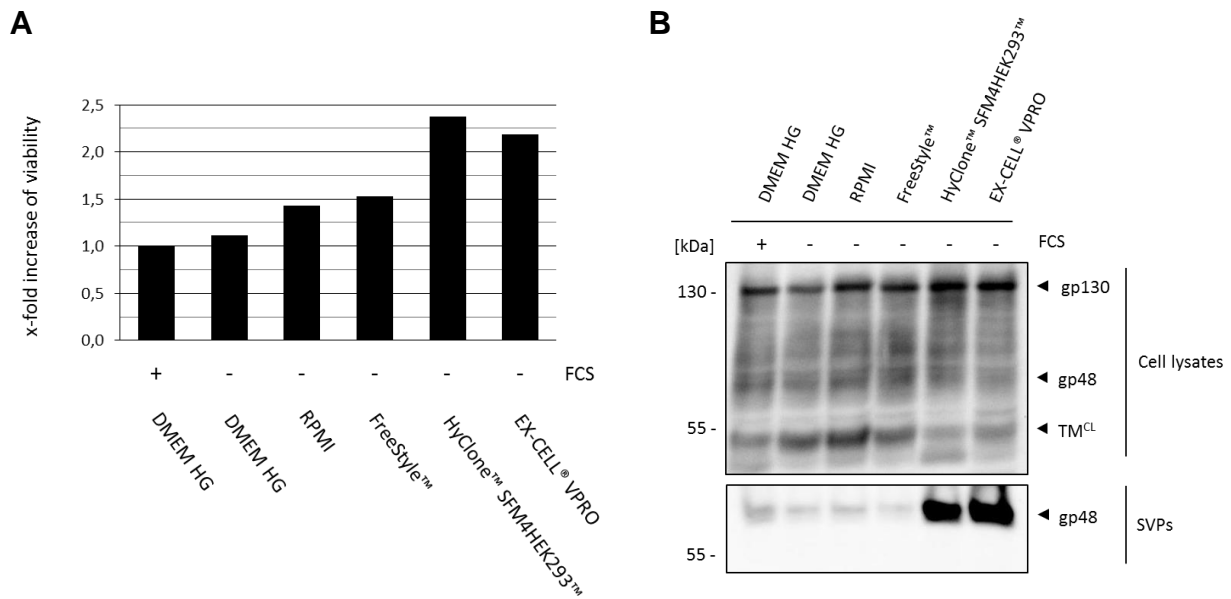


Figure 32. Testing various serum-free expression media for the purpose of large-scale production of subviral particles

CRFK cells transduced with MP71-EnvG2 virus were subcultured in various serum-free (-) culture media as indicated: DMEM HG, RPMI, FreeStyle™ 293 Expression Medium, HyClone™ SFM4HEK293™ Medium or EX-CELL® VPRO. As reference served transduced CRFK cells cultured in DMEM HG complemented with 10 % FCS (+). **A**) Viabilities in dependence of the tested expression media. 48 hours after subculturing, viabilities were determined as described in the method section. The individual viabilities were put in relation to the viability of the reference culture. The bars indicate the values of one experiment. In comparison, HyClone™ SFM4HEK293™ Medium was most supportive to cells since it resulted in a 2.4-fold increase of viability. **B**) FFV EnvG2 protein expression and FFV EnvG2 subviral particle-release (SVP) in dependence of the tested expression media. 48 hours after subculturing, the cell-free supernatants were concentrated hundred-fold by ultracentrifugation on a 20 % sucrose cushion. The concentrates were analyzed by immunoblotting, along with cell lysates of the transduced CRFK cells grown in the respective media. Detection of antigens was performed with goat348 α-TM serum. Compared to all other tested media, HyClone™ SFM4HEK293™ Medium and EX-CELL® VPRO promoted FFV EnvG2 SVP-release decisively as shown by the dominant protein bands of processed gp48 in the concentrates. The reduced electrophoretic mobilities of gp130 and gp48 in comparison to the 130 kDa and 55 kDa marker bands, respectively, indicated proper glycosylation.

Due to unknown characteristics about the stability of SVPs in cell culture supernatants, an additional experiment should reveal an optimal harvest time point. Therefore, four CRFK cultures transduced with MP71-EnvG2 virus were established in HyClone™ SFM4HEK293™ Medium. In order to find an optimal harvest time point, cell culture supernatants were harvested 24, 48, 72 or 96 hours after subculturing, respectively. 8 ml of the respective cell-free supernatants were concentrated by ultracentrifugation on a 20 % sucrose cushion. The protein pellets were resuspended in

80 µl sample buffer and directly analyzed by immunoblotting using goat348 α-TM serum for antigen detection (Figure 33). The cell lysates of the CRFK cells collected at the same time points as the corresponding cell culture supernatants served as reference.

It turned out that harvesting the cell culture supernatants at different time points did not accumulate SVPs after 24 hours as shown by equal detection of gp48. However, enriched contaminants could be observed in the 96 hour-concentrate as indicated by the detection of TM^{CL} running below gp48.

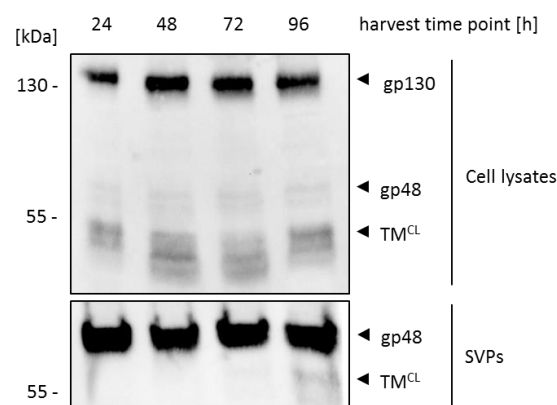


Figure 33. Amount of subviral particles in cell culture supernatants at different time points

CRFK cells transduced with MP71-EnvG2 virus were four times subcultured in HyClone™ SFM4HEK293™ Medium. 24, 48, 72 or 96 hours after subculturing, the respective cell culture supernatants were harvested and applied to ultracentrifugation on a 20 % sucrose cushion for hundred-fold concentration. The concentrates were analyzed by immunoblotting, along with the corresponding cell lysates of the subcultured CRFK cells collected at the same time points as the respective cell culture supernatants. Detection of antigens was performed with goat348 α-TM serum. Harvesting cell culture supernatants at different time points revealed no accumulation or depletion of released subviral particles as shown by equal detection of gp48 in the respective supernatants. Gp130 and gp48 had reduced electrophoretic mobilities when compared to the 130 kDa and 55 kDa marker bands, respectively, that is an indication for proper glycosylation.

The results indicated that HyClone™ SFM4HEK293™ Medium as well as EX-CELL® VPRO are very suitable expression media for large-scale production of FFV SVPs. No change in the amount of SVPs could be observed after 24 hours of subculturing. In order to avoid accumulation of contaminants, supernatants should be harvested within 24 and 72 hours. One can conclude that MP71-transduced CRFK cells cultured in HyClone™ SFM4HEK293™ Medium allow daily harvesting of SVP-containing cell culture supernatants for the purpose of large-scale production.

4.5.6 Do lysine-to-arginine mutations in FFV EIp increase SVP-release?

It is known that FV Env undergoes several post-translational modifications throughout cellular processing. Previous studies on PFV Env revealed five lysine residues (K₁₄, K₁₅, K₁₈, K₃₄ and K₅₃) located in the N-terminal part of the envelope leader peptide (EIp) that are targets for ubiquitination (Figure 34A). Those ubiquitination sites are apparently responsible for limited subviral particle-release (SVP) since lysine-to-arginine mutations of all five residues (R₁₄, R₁₅, R₁₈, R₃₄ and R₅₃) increased SVP-release more than 10-fold (Figure 34B) [87, 88].

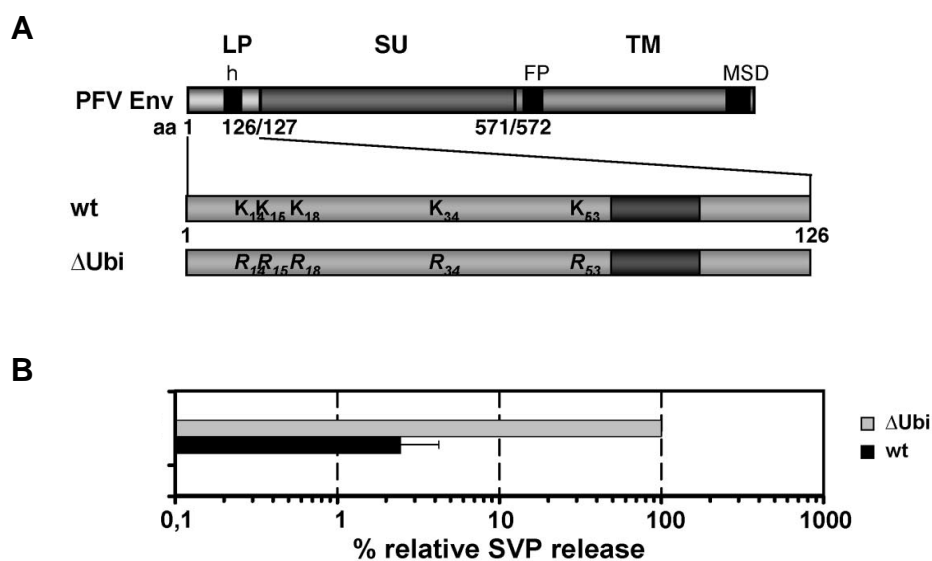


Figure 34. Deletion of the ubiquitination sites in PFV EIp leads to increased subviral particle-release [87, 88]

A) PFV Env. LP: envelope leader peptide, h: hydrophobic region, SU: surface protein, FP: fusion peptide, TM: transmembrane envelope protein, MSD: membrane spanning domain, K: lysine residue, R: arginine residue. Also shown are the approximate locations of the ubiquitination sites (K₁₄, K₁₅, K₁₈, K₃₄ and K₅₃) of the wild-type PFV LP (wt) and the inactivated ubiquitination sites (R₁₄, R₁₅, R₁₈, R₃₄ and R₅₃) of the mutated PFV LP (ΔUbi). **B)** Relative influence of the deletions of the ubiquitination sites in the PFV LP on subviral particle-release (SVP). SVP-release is increased more than 10-fold after deletion of all five ubiquitination sites.

Whether FFV EIp also carries ubiquitination sites, is currently unknown. Based on the assumption that ubiquitination does happen in FFV EIp, deletion of presumptive ubiquitination sites might also increase FFV SVP-release. By checking the sequence of the N-terminal part of FFV EIp, five lysine residues could be found (K₁₀, K₂₀, K₂₄, K₄₅ and K₄₈) (Figure 35). Those lysine residues were mutated to arginine using muta-

genesis-PCR. The expression plasmids pBC EnvG2, MPER1 and MPER2 [95] served as templates and the K-to-R mutations were introduced by the primers Elp1 fwd, Elp1 rev, Elp2 fwd and Elp2 rev. The expression plasmids carrying all five K-to-R mutations in the FFV Elp sequence were called pBC Elp-EnvG2, pBC Elp-MPER1 and pBC Elp-MPER2.

```

      14,15  18      34      53
PVF Elp wt   MAPPMTLQQWIIWKKMNKAHEALQNTTTEQQKEQIILDIQNEEVQPTRRDKFRYLL
FFV Elp wt   MEQEHVMTLKEWMEWNAHKQLQK LQSTHPELHVDIPEDIPLVPEKVPLKMRMR YRC
FFV Elp ΔUbi MEQEHVMTLREWMEWNAHRQLQR LQSTHPELHVDIPEDIPLVPERVPLRMRMR YRC
    
```

Figure 35. Amino acid sequences of PVF Elp wt, FFV Elp wt and FFV Elp ΔUbi carrying the mutations K₁₀R, K₂₀R, K₂₄R, K₄₅R and K₄₈R

The upper amino acid sequence indicates the N-terminal region of the wild-type PFV Envelope leader peptide (Elp). PFV Elp naturally contains five lysine residues that are targets of ubiquitination (red K₁₄, K₁₅, K₁₈, K₃₄ and K₅₃). Also shown are the N-terminal sequences of the wild-type FFV Elp and the mutated FFV Elp ΔUbi. The five wild-type lysine residues (Ks) are highlighted in red, while the lysine-to-arginine mutations (Rs) are depicted in blue.

In order to test the impact of the mutated FFV Elp gene sequence on EnvG2 protein expression and SVP-release, 3 x 10⁶ HEK293T cells were transfected with 15 μg pBC EnvG2, pBC Elp-EnvG2 or pCF7 Bet-His as positive control. 72 hours after transfection, two fractions of cell pellets were prepared to allow subsequent gene expression analysis by reverse transcription-PCR (RT-PCR) and immunoblotting.

One fraction was used for investigation of Elp-EnvG2 gene transcription. Therefore, cellular RNA was isolated and applied to non-quantitative RT-PCR along with pBC EnvG2, pBC Elp-EnvG2 and pCF7 Bet-His plasmid DNA (pDNA) as positive controls. For amplification of the whole Env gene sequence, the primers FFV EnvG2 fwd and FFV EnvG2 rev were used. Figure 36A shows the cDNA-amplicons separated by 1 % agarose gel-electrophoresis. RT-PCR of isolated RNA resulted in two distinct amplicons that were smaller than the single amplicons coming from the expression plasmids (pDNA). One of the two cDNA-amplicons obtained from the pCF7 Bet-His RNA-isolate (positive control) was smaller in length than the respective cDNA-amplicons of EnvG2 and Elp-EnvG2 RNA-isolates. In comparison, transcription of the Elp-EnvG2 gene seemed to be less promoted than EnvG2 gene transcription as shown by the faint detection of the Elp-EnvG2 cDNA-amplicons.

The second cell fraction was used for the preparation of cell lysates that were analyzed by immunoblotting working with goat348 α -TM serum (Figure 36B) for antigen detection. pBC Elp-EnvG2 promoted Elp-EnvG2 protein expression, processing and proper glycosylation as shown by the detection of gp130 and gp48 running above the 130 kDa and 55 kDa marker bands. Elp-EnvG2 protein expression was reduced.

In order to determine the impact of the five K-to-R mutations on SVP-release, the cell-free supernatants of the transfected HEK293T cultures were ultracentrifuged on a 20 % sucrose cushion. Subsequently, protein pellets were resuspended in an appropriate volume of sample buffer for hundred-fold concentration and directly analyzed by immunoblotting (Figure 36C) using goat348 α -TM serum for antigen detection. In comparison to EnvG2 SVPs, lower amounts of Elp-EnvG2 SVPs were released into the supernatants as shown by the weaker detection of processed gp48.

Those results indicated that the five lysine-to-arginine mutations incorporated into the N-terminal region of FFV Elp significantly decreased expression of Env protein. As a consequence, the release of Elp-EnvG2 SVPs was reduced when compared to EnvG2 SVPs. According to those observations, the pBC Elp-EnvG2, MPER1 and MPER2 expression plasmids were excluded from further experiments on SVP production.

5 Discussion

5.1 Transfection optimization for high virus titers

The experiments on transfection optimization confirmed findings of previous studies showing that the plasmid size is inversely correlated with the transfection efficiency [112] and thus detrimental to virus titers [113]. Additionally, the concentration of the transfection reagent plays a crucial role as indicated by the results of the screening for optimal transfection conditions (Figure 20). Actually, the outcome of that experiment seemed to be contradictory on first sight. Higher amounts of MP71-GFP and pLenti-GFP pDNA (2 µg/1.6 x 10⁵ cells) resulted in increased detection of GFP expression in the cell lysates (Figure 20B), but the highest virus titers were obtained with lower DNA-levels (0.5 µg/1.6 x 10⁵ cells) (Figure 20C). This might be explained by the fact that 2 µg DNA required four-fold more transfection reagent, polyethyleneimine (PEI). However, viabilities were drastically reduced at higher concentrations (Figure 20A) that is not quite surprising because PEI is known to inflict damages on cytoplasm membranes [114]. Transfection with 0.5 µg DNA per 1.6 x 10⁵ cells and a DNA/PEI-ratio of 1:8 seemed to reflect a balanced compromise between the toxicity of PEI and the required DNA amount for virus production.

The outcome of the experiment on the transferability of the transfection protocols on MP71-EnvG2 and pLenti-EnvG2 confirmed that the plasmid size is decisive for transfection efficiencies (Figure 26). For comparison: MP71-GFP is ~ 6 kb and MP71-EnvG2 is ~ 8.3 kb in length; while pLenti-GFP is ~ 8.4 kb and pLenti-EnvG2 is ~ 11.7 kb in length. When the amount of transfected DNA was doubled, EnvG2 protein expression promoted by MP71-EnvG2 (Figure 26A) and pLenti-EnvG2 (Figure 26B) was significantly increased. Probably, transfection of pLenti-EnvG2 would even require more DNA. Transfection with 250 ng DNA increased detection of gp130 and uncleaved gp130-GFP but it was still low compared to EnvG2 protein expression promoted by MP71-EnvG2; processed gp48 was not expressed. Comparison of the MP71-EnvG2 and pLenti-EnvG2 virus titers (Figure 27) further verifies the hypothesis that larger proviral DNA leads to lower virus titers. However, one must consider that the MP71 and pLenti transfer plasmids belong to different packaging systems. In contrast to MP71-vectors, pLenti-vectors require co-transfection of three additional plasmids for virus production (see section 3.2.5). Since equal pDNA-levels were trans-

ected for MP71- or pLenti virus production, comparatively lower pLenti virus titers could also be a result of less amount of pLenti-vector available for packaging.

Nevertheless, the pLenti packaging system is optimized for virus production as indicated by infections with pLenti-GFP virus. In the experiment on increasing virus production with additives, transduction efficiencies after infections with pLenti-GFP virus were between ~ 10 to 45 % compared to ~ 3 to 5 % resulting from MP71-GFP virus infections (Figure 21). The efficiency of pLenti-GFP virus infection was further indicated by the data obtained from transduction optimization through assisted infection; ~ 70 to 100 % transduction efficiencies could be obtained (Figure 23A). Presumably, those results display the fact that the pLenti packaging system works with a protocol that is established and optimized for virus production. While the pLenti packaging system uses three plasmids expressing Gag, Pol and accessory proteins at predefined ratios, MP71 virus production was performed with a packaging cell line. In this project, Platinum-GP cells were used which constantly express the packaging factors *gag* and *pol* at default rates. Accordingly, diverse transduction efficiencies between MP71- and pLenti-infected cell cultures are not surprising. Platinum-GP cells are also 293 cells but, regarding their comparably reduced viabilities, it has to be added that they need to be grown under blasticidin-selection in order to maintain gene expression of *gag* and *pol*. Drug selection might constitute a substantial burden that could hamper virus production and increase their vulnerability to PEI (Figure 20). Furthermore, the cytotoxicity of VSV-G [115, 116] should also be taken into account of which comparatively higher amounts were applied for pseudotyping MP71-vectors (see section 3.2.5).

Interestingly, supplementation with Na-butyrate and valproic acid, that also have clear cytotoxic properties [117-119], showed to be supportive in virus production at completely different concentrations (Figure 21). Obviously, MP71-GFP and pLenti-GFP virus production was less supported by valproic acid than Na-butyrate even though valproic acid was shown to be superior in promoting protein expression after transient transfection of 293 cells [120]. Additionally, virus production was non-linear with increasing concentrations of Na-butyrate or valproic acid. That might be explained by the fact that both chemicals interfere in biochemical pathways regulating the cell-cycle by directly and/or indirectly activating and/or de-activating several regulatory proteins [117, 119]. Therefore, it can be speculated that those diverse results are a phenomenon of biochemical homeostasis.

5.2 MP71-infection of CRFK cells seemed to be most suitable for the establishment of cell lines stably expressing EnvG2, MPER1 and MPER2 protein

In a previous study, it was shown that polybrene and spinoculation enhance lentiviral transduction efficiencies [121]. Accordingly, it was not surprising that polybrene and spinoculation in combination resulted in enhanced infections as shown by the results of the transduction optimization experiments (Figure 23). As already mentioned above, infection with pLenti-GFP virus seems to be more feasible, presumably due to high virus titers. Infection of 293T, C8166 and CRFK cells with virus concentrate only resulted in transduction efficiencies between 80 and 100 %. Therefore, infection enhancement by polybrene and spinoculation was insignificant. In contrast, MP71-GFP virus infections could be considerably boosted by polybrene and spinoculation. Using polybrene or spinoculation alone resulted in 20 to 30 % increase of transduction efficiencies in 293T, C8166 and CRFK cells. When polybrene and spinoculation were used in combination, the transduction efficiency in 293T cells could even be increased by approximately 70 %.

Efficacy of polybrene and spinoculation was further confirmed by determination of the mean fluorescence intensities (MFI) that were considered to correlate with multiple integrations of retroviral vectors (Figure 23B). MFIs in 293T, C8166 and CRFK cells could be increased by several 100 to 2000 arbitrary units (AU) when polybrene and spinoculation were used in combination during infection with MP71-GFP or pLenti-GFP virus. However, a change of MFIs in C8166 cells after assisted infection with MP71-GFP virus could not be observed.

Interestingly, the four tested infection conditions led to diverse results in 293F cells. Transduction with MP71-GFP virus could be improved by a maximum of 18 % when polybrene and spinoculation were used in combination. However, the highest transduction efficiency with pLenti-GFP virus was achieved with virus concentrate only. As it was the case for C8166 cells, any of the tested conditions did not increase MFIs after infection with MP71-GFP virus; whereas MFI was significant higher after pLenti-GFP virus infection with spinoculation. The results of that experiment showed that infection efficiencies depend on the target cell line. Nevertheless, it was surprising that transduction of 293F cells was inconsistent with the infection rates of the other tested cell lines. 293F cells are 293 cells adapted to be grown in suspension but 293F cells

also tended to adhere onto the bottom of culture plates during incubation and spinoculation (data not shown). Accordingly, 293F cultures would rather resemble 293T cultures. 293F cells are standardly grown in serum-free FreeStyle™ 293 Expression Medium. It can be speculated that some unknown factors supplemented to the medium are possibly detrimental to infections with VSV-G pseudotyped vectors. However, it has to be considered that the experiment and measurements were each conducted only once. Repetitions might allow more convincing insights on infections of 293F cells.

Surprisingly, when infections were performed with MP71 FFV EnvG2 or hybrid FFV/HIV-1 MPER1 or MPER2 virus, 293F cells seemed to be more suitable compared to C8166 cells (Figure 28A, B). While 293F cells showed weak expression of precursor gp130, Env protein expression was even entirely absent in C8166 cells. At least Env protein expression promoted by the MP71 expression vectors was expected because MP71 vector is optimized for protein expression in lymphotropic cell lines like C8166 [96]. In comparison to both suspension cell lines, infections of the adherent 293T and CRFK cells with MP71 viruses were more effective (Figure 28C, D). Especially CRFK cells showed very strong Env protein expression. Presumably, MP71 virus titers were too low to obtain comparable transduction efficiencies in the suspension cell lines 293F and C8166; that would be in line with previous reports about transduction of suspension cells [122]. When infection was performed with pLenti FFV EnvG2 or hybrid FFV/HIV-1 MPER1 or MPER2 virus, 293F cells were the only cell line in the panel that showed Env protein expression. This and the fact that Env protein expression promoted by pLenti vectors was totally absent in adherent 293T and CRFK cells (Figure 28C, D) are in stark contrast to transduction efficiencies obtained with pLenti-GFP virus (Figure 23). It has to be considered that the titer of pLenti EnvG2 virus was lower than the titer of MP71 EnvG2 virus (Figure 27). Presumably, the titers of pLenti viruses were too low for detectable transductions. Another reason for those observations could be possible degradation of the gp130-GFP fusion peptide. This cannot be excluded because gp130-GFP is more complex than gp130 expressed by the MP71 expression constructs. Misfolding might influence correct processing of the A2-site of gp130-GFP (Figure 17) and target the fusion peptide to proteasomal degradation.

5.3 Transduced CRFK cells release chimeric FFV/HIV-1 MPER1 and MPER2 SVPs that are recognized by 2F5 and 4E10

In her PhD thesis, Anne Bleiholder demonstrated distinct levels of FFV EnvG2 and FFV/HIV-1 MPER1 and MPER2 protein expression and subviral particle release upon transient transfection of HEK293T cells. Compared to MPER1 and MPER2 protein, release of EnvG2 protein into supernatants was greater promoted (Figure 12) [95]. In this project, her findings were confirmed by parallel transfection of HEK293T cells with the pBC, pLenti and MP71 EnvG2 and MPER expression constructs (Figure 19); although transduced CRFK cells revealed equal protein expression (Figure 28D, 29). Analysis of the supernatants obtained from the transduced CRFK cultures verified reduced MPER1 and MPER2 SVP-release (Figure 29). It was suggested that replacing the respective DNA sequence in FFV TM with the HIV-1 MPER DNA sequence might result in mRNA transcripts with reduced stability or enhanced misfolding of Env protein which is subsequently targeted for degradation [95].

Interestingly, detection of MPER1 protein expression with mAb 2F5 and mAb 4E10 was stronger when compared to MPER2 protein, as it was already previously shown with mAb 2F5 [95]. In an earlier study it was demonstrated that 2F5 and 4E10 recognize their respective epitopes in linear form after denaturation by SDS-PAGE [123-125]. Thus, different detection of MPER1 and MPER2 protein was quite surprising, since both chimeras carry the very same HIV-1 MPER sequences. It can be speculated that more stringent denaturing conditions would have been necessary in order to resolve unknown remaining secondary structures or dimerization products caused by the three amino acid shift that might reduce the accessibilities of both epitopes. However, mAb 2F5 and mAb 4E10 were able to bind the respective epitopes in native conformation as shown by immunoprecipitation. Both antibodies specifically recognized and precipitated MPER1 and MPER2 SVPs present in concentrated cell culture supernatants (Figure 30B, C). Successful immunoprecipitation thus confirmed the accessibility of the 2F5 and 4E10 epitopes on the surface of the released hybrid MPER1 and MPER2 SVPs that is key for binding by B-cell receptors. However, it should be mentioned that B-cell activation depends on activation by T-cells which are, in turn, activated by B-cells as antigen-presenting cells. B-cells introduce antigens as small peptides bound to class II major histocompatibility complex proteins to T-cells [126]. Accordingly, T-cell receptors have to recognize the 2F5 and 4E10

epitopes in the absence of a lipid environment (see section 1.1.4 and 1.3) in order to allow successful induction of immune responses against the HIV-1 MPER.

After immunoprecipitation of EnvG2 SVPs, the precursor protein gp130 was weakly detected (Figure 30A). By contrast, gp130 was completely absent in the MPER1 and MPER2 precipitates. It was previously demonstrated that FFV EnvG2 protein, unlike chimeric FFV/HIV-1 MPER1 and MPER2 proteins, mediates cell fusion upon transient transfection of 293T cells [95]. Fusogenic activities or cytopathic effects (CPE) (Figure 9) result in release of free gp130 protein due to cell lysis. Accordingly, Bleiholder's findings would explain the detection of co-precipitated gp130.

Negative staining electron microscopy of EnvG2, MPER1 and MPER2 SVP concentrates revealed two classes of particles present in concentrated cell culture supernatants (Figure 31). One class was more electron-dense and about 100 nm in size. The other class was smaller and had a surface with characteristics resembling glycoprotein. The member of the electron microscopy department assumed that the smaller particles are probably SVPs; whereas the larger particles would be too dense for SVPs which do not contain Gag. The morphological appearance of the larger particles thus suggests the presence of virus or virus-like particles (containing Gag and Env) in cell culture supernatants. As a matter of fact, it was previously demonstrated that CRFK cells produce an endogenous virus [127, 128]. Concerning immunization studies, it would be advantages to gain more insight on the characteristics of the larger particles before immunization because their presence in SVP concentrates could potentially influence the outcome of the immunization studies.

5.4 Some expression media increase EnvG2 protein expression

For the purpose of successful immunization studies using subviral particles (SVPs), several micrograms of antigen should be available in high purity. Hence, large-scale production of SVPs needed to be optimized in order to increase the yield after ensuing purification. Different commercially available serum-free expression media were tested that should facilitate later large-scale production and purification. The results displayed in Figure 32 demonstrated significant support of culture viability together with high release of EnvG2 protein into supernatants by the application of HyClone™ SFM4HEK293™ Medium or EX-CELL® VPRO. In fact, viability was boosted 2.4- or 2.2-fold by HyClone™ SFM4HEK293™ Medium or EX-CELL® VPRO, respectively.

As depicted in Figure 32B, EnvG2 protein expression was apparently only minimally stronger promoted by HyClone™ SFM4HEK293™ Medium or EX-CELL® VPRO, whereas processing even seemed to be reduced when compared to the other tested media. However, together with the strong detection of gp48 in the concentrated culture supernatants, it can be assumed that SVP-release was considerably enhanced. High concentration of gp48 in the supernatants due to fusogenic activity of EnvG2 could be excluded, since no TM^{CL} was detected [95].

Harvesting cell culture supernatants at different time points revealed no accumulation of SVPs (Figure 33) that was different than expected. It is unclear if the HyClone™ SFM4HEK293™ Medium that was used for culturing the transduced CRFK cells leads to reduced stability of SVPs. Presumably, the boosted viability and SVP-release by HyClone™ SFM4HEK293™ Medium is only short-term before cells eventually start dying. This would also explain the detection of TM^{CL} in the 96-hour supernatant (Figure 33). Accordingly, cell culture supernatants should be concentrated between 24 and 72 hours after subculturing. If the harvest time point is later, accumulations of undesired TM^{CL} occur.

5.5 Lysine-to-arginine mutations in FFV Elp decrease subviral particle release

Introduction of five lysine-to-arginine mutations (K-to-R) in the N-terminal region of the FFV envelope leader peptide (Elp) (Figure 35) clearly reduced EnvG2 protein expression (Figure 36). Those results indicated that the ubiquitination sites of PFV Elp are not conserved in FFV Elp. While deletion of the ubiquitination sites by K-to-R mutations in PFV Elp increased PFV subviral particle (SVP) release (Figure 34), equivalent mutations in the FFV Elp DNA sequence obviously decreased stability of Env mRNA transcripts (Figure 36A).

Why RT-PCR with isolated RNA resulted in two amplicons is still unexplained (Figure 36A). The primers that were used should allow amplification of the full-length Env gene sequence as demonstrated by parallel RT-PCR-amplification of the respective plasmids. Interestingly, even RNA from cells transfected with the infectious molecular clone of FFV (pCF7) led to two cDNA-amplicons. However, the smaller fragment of pCF7 was apparently shorter in length than the smaller fragments of EnvG2 or Elp-EnvG2. Analysis of the respective cell lysates by immunoblotting proved that Env protein was still expressed and processed (Figure 36B). Sequencing revealed that

those amplicons partially correspond to the SU and the TM DNA sequences. Hence, the fact that pCF7 resulted in still two but one smaller cDNA-amplicon, could be due to the fact that pCF7 encodes unmodified Env; the SD/SA-pair of the Env gene sequence is deleted in pBC EnvG2 and pBC Elp-EnvG2 [95]. As a consequence, spliced mRNA transcripts of the EnvG2 gene encoded by pCF7 are actually expected to be shorter. Nevertheless, those results showed that R-to-K mutations in FFV Elp result in decreased SVP-release (Figure 36C) because of reduced EnvG2 protein expression (Figure 36A, B).

5.6 Immunization studies will reveal the potential of hybrid FFV/HIV-1 SVPs to induce neutralizing antibodies against HIV-1

In this project, an efficient protocol for the production of FFV-based subviral particles (SVPs) carrying the HIV-1 MPER sequence was established. The protocol is based on the strategy of generating cell lines stably expressing FFV EnvG2 or hybrid FFV/HIV-1 MPER1 or MPER2 protein after retroviral infection.

The respective coding sequences were subcloned from the pBC EnvG2, pBC MPER1 and pBC MPER2 expression plasmids [95] into two different retroviral transfer plasmids (MP71 and pLenti). Afterwards, generation of single-round viruses and infection of target cells was optimized. Stably transduced CRFK cells were then used to optimize the large-scale production of EnvG2, MPER1 and MPER2 SVPs. It was finally shown that the MPER1 and MPER2 SVPs carry the 2F5 and 4E10 epitopes that are accessible to the respective antibodies.

Further experiments will give rise to efficient protocols for large-scale purification of SVPs. The antigens should be eventually confirmed by transmission electron microscopy using the method of immunogold-labeling. Final immunization studies utilizing the hybrid FFV/HIV-1 MPER1 or MPER2 SVP antigens in a DNA-prime/SVP-boost regimen will evaluate their potential for the induction of 2F5 and 4E10-like antibodies against HIV-1.

6 Zusammenfassung

Durchschnittlich 2,5 Jahre nach einer HIV-Infektion entwickeln ungefähr 10 - 30 % der infizierten Patienten breitneutralisierende Antikörper. Zwei solcher Antikörper sind 2F5 und 4E10, die die membrannahe externe Region (MPER) des transmembranen Hüllproteins gp41 binden. Studien haben ergeben, dass das nichtpathogene Retrovirus feline foamy virus (FFV), ähnlich der 2F5 und 4E10-Epitope, ebenfalls immunogene Regionen im membrannahen Bereich von TM (gp48) mit zweiteiliger Anordnung aufweist. Anders als bei anderen Retroviren, ist das FFV Env-Protein in der Lage sich ohne weitere Virusproteine als subviraler Partikel (SVP) von der Zytoplasmamembran abzuschneiden. In einer vorangegangenen Arbeit wurden durch Ersetzen der äquivalenten Sequenzen die 2F5 und 4E10-Epitope in die FFV Env-kodierende Gensequenz eingefügt. Nach Transfektion von HEK293T-Zellen, wurden hybride FFV/HIV-1 SVPs, auf deren Oberfläche die 2F5 und 4E10 Epitope exponiert sind, in die Zellkulturüberstände abgegeben. Um jedoch deren Potential als Impfstoff gegen Infektionen durch HIV-1 mittels Immunisierungsstudien in Ratten bestimmen zu können, sind größere Mengen dieser chimären SVP-Antigene erforderlich. Im Rahmen dieser Masterarbeit wurden effiziente Protokolle zur Großproduktion von SVPs etabliert. Zuerst wurden die entsprechenden Sequenzen in retrovirale Transfervektoren subkloniert. Um diese mit Vesicular stomatitis virus-Protein G zu pseudotypisieren, wurden anschließend die Produktion und das Konzentrieren von infektiösen Viren systematisch optimiert, um möglichst hohe virale Titer zu erhalten. Verschiedene Zelllinien wurden dann testweise für die Produktion von SVPs stabil transduziert, wobei sich CRFK-Zellen als optimale SVP-Produzenten erwiesen. Nachdem durch Immunopräzipitation der Antigene mit den monoklonalen Antikörpern 2F5 und 4E10 gezeigt wurde, dass die entsprechenden Epitope zugänglich sind, wurde die erfolgreiche SVP-Produktion mittels Transmissionselektronenmikroskopie nach "Negativkontrastierung" bestätigt. Schließlich wurde die Produktion von SVPs nochmalig durch das Testen einer Reihe kommerzieller Expressionsmedien optimiert, wobei erstmals durch das Anwenden von Corning® HYPERFlasks® SVPs im größeren Maßstab produziert wurden. Durch die hier etablierten Protokolle für die Großproduktion von hybriden FFV/HIV-1 SVPs, die die 2F5 und 4E10 Epitope an ihrer Oberfläche präsentieren, kann diese neuartige FFV-basierende rekombinante Strategie für ein Antigen als potentieller HIV-Impfstoff getestet werden.

7 References

1. Walker LM, Burton DR. Rational antibody-based HIV-1 vaccine design: current approaches and future directions. *Curr Opin Immunol*. 2010 Jun;22(3):358-66.
2. Girard MP, Osmanov S, Assossou OM, Kieny MP. Human immunodeficiency virus (HIV) immunopathogenesis and vaccine development: a review. *Vaccine*. 2011 Aug 26;29(37):6191-218.
3. Girard MP, Koff WC. 51 – Human Immunodeficiency Virus Vaccines. In 'Vaccines'. 6th edition. Edited by Plotkin SA, Orenstein W, Offit PA. Philadelphia: Saunders; 2012. 1097-121.
4. Haase AT. Targeting early infection to prevent HIV-1 mucosal transmission. *Nature*. 2010 Mar 11;464(7286):217-23.
5. Douek DC, Picker LJ, Koup RA. T cell dynamics in HIV-1 infection. *Annu Rev Immunol*. 2003;21:265-304.
6. Haase AT. Early events in sexual transmission of HIV and SIV and opportunities for interventions. *Annu Rev Med*. 2011;62:127-39.
7. Grossman Z, Meier-Schellersheim M, Paul WE, Picker LJ. Pathogenesis of HIV infection: what the virus spares is as important as what it destroys. *Nat Med*. 2006 Mar;12(3):289-95.
8. Mens H, Kearney M, Wiegand A, Shao W, Schønning K, Gerstoft J, Obel N, Maldarelli F, Mellors JW, Benfield T, Coffin JM. HIV-1 continues to replicate and evolve in patients with natural control of HIV infection. *J Virol*. 2010 Dec;84(24):12971-81.
9. Iwami S, Nakaoka S, Takeuchi Y. Viral diversity limits immune diversity in asymptomatic phase of HIV infection. *Theor Popul Biol*. 2008 May;73(3):332-41.
10. Global situation and trends. World Health Organization, HIV/AIDS, Global Health Observatory (GHO) 2011. [<http://www.who.int/gho/hiv/en/>]
11. Emerman M, Malim MH. HIV-1 regulatory/accessory genes: keys to unraveling viral and host cell biology. *Science*. 1998 Jun 19;280(5371):1880-4.
12. Karn J, Stoltzfus CM. Transcriptional and posttranscriptional regulation of HIV-1 gene expression. *Cold Spring Harb Perspect Med*. 2012 Feb;2(2):a006916.

References

13. Manninen A, Saksela K. HIV-1 Nef interacts with inositol trisphosphate receptor to activate calcium signaling in T cells. *J Exp Med.* 2002 Apr 15;195(8):1023-32.
14. James CO, Huang MB, Khan M, Garcia-Barrio M, Powell MD, Bond VC. Extracellular Nef protein targets CD4+ T cells for apoptosis by interacting with CXCR4 surface receptors. *J Virol.* 2004 Mar;78(6):3099-109.
15. Lenassi M, Cagney G, Liao M, Vaupotic T, Bartholomeeusen K, Cheng Y, Krogan NJ, Plemenitas A, Peterlin BM. HIV Nef is secreted in exosomes and triggers apoptosis in bystander CD4+ T cells. *Traffic.* 2010 Jan;11(1):110-22.
16. Casartelli N, Di Matteo G, Potestà M, Rossi P, Doria M. CD4 and major histocompatibility complex class I downregulation by the human immunodeficiency virus type 1 nef protein in pediatric AIDS progression. *J Virol.* 2003 Nov;77(21):11536-45.
17. Yu X, Yu Y, Liu B, Luo K, Kong W, Mao P, Yu XF. Induction of APOBEC3G ubiquitination and degradation by an HIV-1 Vif-Cul5-SCF complex. *Science.* 2003 Nov 7;302(5647):1056-60.
18. Bishop KN, Holmes RK, Sheehy AM, Malim MH. APOBEC-mediated editing of viral RNA. *Science.* 2004 Jul 30;305(5684):645.
19. Sakai K, Dimas J, Lenardo MJ. The Vif and Vpr accessory proteins independently cause HIV-1-induced T cell cytopathicity and cell cycle arrest. *Proc Natl Acad Sci U S A.* 2006 Feb 28;103(9):3369-74.
20. Neil SJ, Zang T, Bieniasz PD. Tetherin inhibits retrovirus release and is antagonized by HIV-1 Vpu. *Nature.* 2008 Jan 24;451(7177):425-30.
21. Willey RL, Maldarelli F, Martin MA, Strebel K. Human immunodeficiency virus type 1 Vpu protein induces rapid degradation of CD4. *J Virol.* 1992 Dec;66(12):7193-200.
22. Douek DC, Brenchley JM, Betts MR, Ambrozak DR, Hill BJ, Okamoto Y, Casazza JP, Kuruppu J, Kunstman K, Wolinsky S, Grossman Z, Dybul M, Oxenius A, Price DA, Connors M, Koup RA. HIV preferentially infects HIV-specific CD4+ T cells. *Nature.* 2002 May 2;417(6884):95-8.
23. Hartley O, Klasse PJ, Sattentau QJ, Moore JP. V3: HIV's switch-hitter. *AIDS Res Hum Retroviruses.* 2005 Feb;21(2):171-89.
24. Wilen CB, Tilton JC, Doms RW. HIV: cell binding and entry. *Cold Spring Harb Perspect Med.* 2012 Aug 1;2(8):pii: a006866.

References

25. Swanstrom R, Wills JW. Synthesis, Assembly, and Processing of Viral Proteins. In 'Retroviruses'. Edited by Coffin JM, Hughes SH, Varmus HE. Cold Spring Harbor (NY): Cold Spring Harbor Laboratory; 1997.
26. Replication Cycle of HIV, Entry of HIV into cells. More on How HIV Causes AIDS. U.S. Department of Health and Human Services, NIAID. 2009. [<http://www.niaid.nih.gov/topics/hivaids/understanding/howhivcausesaids/Pages/howhiv.aspx>]
27. Poignard P, Saphire EO, Parren PW, Burton DR. gp120: Biologic aspects of structural features. *Annu Rev Immunol*. 2001;19:253-74.
28. Wyatt R, Sodroski J. The HIV-1 envelope glycoproteins: fusogens, antigens, and immunogens. *Science*. 1998 Jun 19;280(5371):1884-8.
29. Hallenberger S, Bosch V, Angliker H, Shaw E, Klenk HD, Garten W. Inhibition of furin-mediated cleavage activation of HIV-1 glycoprotein gp160. *Nature*. 1992 Nov 26;360(6402):358-61.
30. Checkley MA, Luttgé BG, Freed EO. HIV-1 envelope glycoprotein biosynthesis, trafficking, and incorporation. *J Mol Biol*. 2011 Jul 22;410(4):582-608.
31. Burton DR. Scaffolding to build a rational vaccine design strategy. *Proc Natl Acad Sci U S A*. 2010 Oct 19;107(42):17859-60.
32. Bunnik EM, Pisas L, van Nuenen AC, Schuitemaker H. Autologous neutralizing humoral immunity and evolution of the viral envelope in the course of subtype B human immunodeficiency virus type 1 infection. *J Virol*. . 2008 Aug;82(16):7932-41.
33. Johnson WE, Desrosiers RC. Viral persistence: HIV's strategies of immune system evasion. *Annu Rev Med*. 2002;53:499-518.
34. Doria-Rose NA, Klein RM, Daniels MG, O'Dell S, Nason M, Lapedes A, Bhattacharya T, Migueles SA, Wyatt RT, Korber BT, Mascola JR, Connors M. Breadth of human immunodeficiency virus-specific neutralizing activity in sera: clustering analysis and association with clinical variables. *J Virol*. 2010 Feb;84(3):1631-6.
35. Simek MD, Rida W, Priddy FH, Pung P, Carrow E, Laufer DS, Lehrman JK, Boaz M, Tarragona-Fiol T, Miiro G, Birungi J, Pozniak A, McPhee DA, Manigart O, Karita E, Inwoley A, Jaoko W, Dehovitz J, Bekker LG, Pitisuttithum P, Paris R, Walker LM, Poignard P, Wrin T, Fast PE, Burton DR, Koff WC. Human immunodeficiency virus type 1 elite neutralizers: individuals with broad and potent neutralizing activity identified by using a high-throughput neutralization assay together with an analytical selection algorithm. *J Virol*. 2009 Jul;83(14):7337-48.

References

36. Scheid JF, Mouquet H, Feldhahn N, Seaman MS, Velinzon K, Pietzsch J, Ott RG, Anthony RM, Zebroski H, Hurley A, Phogat A, Chakrabarti B, Li Y, Connors M, Pereyra F, Walker BD, Wardemann H, Ho D, Wyatt RT, Mascola JR, Ravetch JV, Nussenzweig MC. Broad diversity of neutralizing antibodies isolated from memory B cells in HIV-infected individuals. *Nature*. 2009 Apr 2;458(7238):636-40.
37. Verkoczy L, Kelsoe G, Moody MA, Haynes BF. Role of immune mechanisms in induction of HIV-1 broadly neutralizing antibodies. *Curr Opin Immunol*. 2011 Jun;23(3):383-90.
38. Mikell I, Sather DN, Kalams SA, Altfeld M, Alter G, Stamatatos L. Characteristics of the earliest cross-neutralizing antibody response to HIV-1. *PLoS Pathog*. 2011 Jan 13;7(1):e1001251.
39. Salzwedel K, West JT, Hunter E. A conserved tryptophan-rich motif in the membrane-proximal region of the human immunodeficiency virus type 1 gp41 ectodomain is important for Env-mediated fusion and virus infectivity. *J Virol*. 1999 Mar;73(3):2469-80.
40. Kwong PD, Mascola JR, Nabel GJ. Broadly neutralizing antibodies and the search for an HIV-1 vaccine: the end of the beginning. *Nat Rev Immunol*. 2013 Sep;13(9):693-701.
41. Montero M, van Houten NE, Wang X, Scott JK. The membrane-proximal external region of the human immunodeficiency virus type 1 envelope: dominant site of antibody neutralization and target for vaccine design. *Microbiol Mol Biol Rev*. 2008 Mar;72(1):54-84.
42. Binley JM, Cayanan CS, Wiley C, Schülke N, Olson WC, Burton DR. Redox-triggered infection by disulfide-shackled human immunodeficiency virus type 1 pseudovirions. *J Virol*. 2003 May;77(10):5678-84.
43. Crooks ET, Moore PL, Richman D, Robinson J, Crooks JA, Franti M, Schülke N, Binley JM. Characterizing anti-HIV monoclonal antibodies and immune sera by defining the mechanism of neutralization. *Hum Antibodies*. 2005;14(3-4):101-13.
44. de Rosny E, Vassell R, Jiang S, Kunert R, Weiss CD. Binding of the 2F5 monoclonal antibody to native and fusion-intermediate forms of human immunodeficiency virus type 1 gp41; implications for fusion-inducing conformational changes. *J Virol*. 2004 Mar;78(5):2627-31.
45. Denner J. Towards an AIDS vaccine: the transmembrane envelope protein as target for broadly neutralizing antibodies. *Hum Vaccin*. 2011 Jan-Feb;7:Suppl:4-9.

References

46. Bellamy-McIntyre AK, Lay CS, Baär S, Maerz AL, Talbo GH, Drummer HE, Pombourios P. Functional links between the fusion peptide-proximal polar segment and membrane-proximal region of human immunodeficiency virus gp41 in distinct phases of membrane fusion. *The Journal of Biological Chemistry*. 2007 Aug 10;282(32):23104-16.
47. Fiebig U, Schmolke M, Eschricht M, Kurth R, Denner J. Mode of interaction between the HIV-1-neutralizing monoclonal antibody 2F5 and its epitope. *AIDS*. 2009 May 15;23(8):887-95.
48. Vincent N, Genin C, Malvoisin E. Identification of a conserved domain of the HIV-1 transmembrane protein gp41 which interacts with cholesteryl groups. *Biochim Biophys Acta*. 2002 Dec 23;1567(1-2):157-64.
49. Cardoso RM, Zwick MB, Stanfield RL, Kunert R, Binley JM, Katinger H, Burton DR, Wilson IA. Broadly neutralizing anti-HIV antibody 4E10 recognizes a helical conformation of a highly conserved fusion-associated motif in gp41. *Immunity*. 2005 Feb;22(2):163-73.
50. Zwick MB, Komori HK, Stanfield RL, Church S, Wang M, Parren PW, Kunert R, Katinger H, Wilson IA, Burton DR. The long third complementarity-determining region of the heavy chain is important in the activity of the broadly neutralizing anti-human immunodeficiency virus type 1 antibody 2F5. *J Virol*. 2004 Mar;78(6):3155-61.
51. Ofek G, Tang M, Sambor A, Katinger H, Mascola JR, Wyatt R, Kwong PD. Structure and mechanistic analysis of the anti-human immunodeficiency virus type 1 antibody 2F5 in complex with its gp41 epitope. *J Virol*. 2004 Oct;78(19):10724-37.
52. Kunert R, Wolbank S, Stiegler G, Weik R, Katinger H. Characterization of molecular features, antigen-binding, and in vitro properties of IgG and IgM variants of 4E10, an anti-HIV type 1 neutralizing monoclonal antibody. *AIDS Res Hum Retroviruses*. 2004 Jul;20(7):755-62.
53. Spira AI, Marx PA, Patterson BK, Mahoney J, Koup RA, Wolinsky SM, Ho DD. Cellular targets of infection and route of viral dissemination after an intravaginal inoculation of simian immunodeficiency virus into rhesus macaques. *J Exp Med*. 1996 Jan 1;183(1):215-25.
54. Bomsel M, Heyman M, Hocini H, Lagaye S, Belec L, Dupont C, Desgranges C. Intracellular neutralization of HIV transcytosis across tight epithelial barriers by anti-HIV envelope protein dIgA or IgM. *Immunity*. 1998 Aug;9(2):277-87.
55. Ho J, Uger RA, Zwick MB, Luscher MA, Barber BH, MacDonald KS. Conformational constraints imposed on a pan-neutralizing HIV-1 antibody epitope result in increased antigenicity but not neutralizing response. *Vaccine*. 2005 Feb 18;23(13):1559-73.

References

56. Kim M, Qiao Z, Yu J, Montefiori D, Reinherz EL. Immunogenicity of recombinant human immunodeficiency virus type 1-like particles expressing gp41 derivatives in a pre-fusion state. *Vaccine*. 2007 Jun 28;25(27):5102-14.
57. Zhai Y, Zhong Z, Zariffard M, Spear GT, Qiao L. Bovine papillomavirus-like particles presenting conserved epitopes from membrane-proximal external region of HIV-1 gp41 induced mucosal and systemic antibodies. *Vaccine*. 2013 Nov 4;31(46):5422-9.
58. Switzer WM, Salemi M, Shanmugam V, Gao F, Cong ME, Kuiken C, Bhullar V, Beer BE, Vallet D, Gautier-Hion A, Tooze Z, Villinger F, Holmes EC, Heneine W. Ancient co-speciation of simian foamy viruses and primates. *Nature*. 2005 Mar 17;434(7031):376-80.
59. Switzer WM, Bhullar V, Shanmugam V, Cong ME, Parekh B, Lerche NW, Yee JL, Ely JJ, Boneva R, Chapman LE, Folks TM, Heneine W. Frequent simian foamy virus infection in persons occupationally exposed to nonhuman primates. *J Virol*. 2004 Mar;78(6):2780-9.
60. Herchenröder O, Turek R, Neumann-Haefelin D, Rethwilm A, Schneider J. Infectious proviral clones of chimpanzee foamy virus (SFVcpz) generated by long PCR reveal close functional relatedness to human foamy virus. *Virology*. 1995 Dec 20;214(2):685-9.
61. Herchenröder O, Renne R, Loncar D, Cobb EK, Murthy KK, Schneider J, Mergia A, Luciw PA. Isolation, cloning, and sequencing of simian foamy viruses from chimpanzees (SFVcpz): high homology to human foamy virus (HFV). *Virology*. 1994 Jun;201(2):187-99.
62. Linial M. Why aren't foamy viruses pathogenic? *Trends Microbiol*. 2000 Jun;8(6):284-9.
63. Lindemann D, Rethwilm A. Foamy virus biology and its application for vector development. *Viruses*. 2011 May;3(5):561-85.
64. Alke A, Schwantes A, Zemba M, Flügel RM, Löchelt M. Characterization of the humoral immune response and virus replication in cats experimentally infected with feline foamy virus. *Virology*. 2000 Sep 15;275(1):170-6.
65. Meiering CD, Linial ML. Historical perspective of foamy virus epidemiology and infection. *Clin Microbiol Rev*. 2001 Jan;14(1):165-76.
66. Trobridge G, Josephson N, Vassilopoulos G, Mac J, Russell DW. Improved foamy virus vectors with minimal viral sequences. *Mol Ther*. 2002 Sep;6(3):321-8.

References

67. Fischer N, Heinkelein M, Lindemann D, Enssle J, Baum C, Werder E, Zentgraf H, Müller JG, Rethwilm A. Foamy virus particle formation. *J Virol.* 1998 Feb;72(2):1610-5.
68. Pietschmann T, Heinkelein M, Heldmann M, Zentgraf H, Rethwilm A, Lindemann D. Foamy virus capsids require the cognate envelope protein for particle export. *J Virol.* 1999 Apr;73(4):2613-21.
69. Lindemann D, Pietschmann T, Picard-Maureau M, Berg A, Heinkelein M, Thurow J, Knaus P, Zentgraf H, Rethwilm A. A particle-associated glycoprotein signal peptide essential for virus maturation and infectivity. *J Virol.* 2001 Jul;75(13):5762-71.
70. Wilk T, Geiselhart V, Frech M, Fuller SD, Flügel RM, Löchelt M. Specific interaction of a novel foamy virus Env leader protein with the N-terminal Gag domain. *J Virol.* 2001 Sep;75(17):7995-8007.
71. Shaw KL, Lindemann D, Mulligan MJ, Goepfert PA. Foamy virus envelope glycoprotein is sufficient for particle budding and release. *J Virol.* 2003 Feb;77(4):2338-48.
72. Löchelt M, Flügel RM, Aboud M. The human foamy virus internal promoter directs the expression of the functional Bel 1 transactivator and Bet protein early after infection. *J Virol.* 1994 Feb;68(2):638-45.
73. Keller A, Partin KM, Löchelt M, Bannert H, Flügel RM, Cullen BR. Characterization of the transcriptional trans activator of human foamy retrovirus. *J Virol.* 1991 May;65(5):2589-94.
74. Löchelt M, Aboud M, Flügel RM. Increase in the basal transcriptional activity of the human foamy virus internal promoter by the homologous long terminal repeat promoter in cis. *Nucleic Acids Res.* 1993 Sep 11;21(18):4226-30.
75. Löchelt M, Romen F, Bastone P, Muckenfuss H, Kirchner N, Kim YB, Truyen U, Rösler U, Battenberg M, Saib A, Flory E, Cichutek K, Münk C. The antiretroviral activity of APOBEC3 is inhibited by the foamy virus accessory Bet protein. *Proc Natl Acad Sci U S A.* 2005 May 31;102(22):7982-7.
76. Perkovic M, Schmidt S, Marino D, Russell RA, Stauch B, Hofmann H, Kopietz F, Kloke BP, Zielonka J, Ströver H, Hermle J, Lindemann D, Pathak VK, Schneider G, Löchelt M, Cichutek K, Münk C. Species-specific inhibition of APOBEC3C by the prototype foamy virus protein bet. *J Biol Chem.* 2009 Feb 27;284(9):5819-26.
77. Münk C, Hechler T, Chareza S, Löchelt M. Restriction of feline retroviruses: lessons from cat APOBEC3 cytidine deaminases and TRIM5alpha proteins. *Vet Immunol Immunopathol.* 2010 Mar 15;134(1-2):14-24.

References

78. Geiselhart V, Schwantes A, Bastone P, Frech M, Löchelt M. Features of the Env leader protein and the N-terminal Gag domain of feline foamy virus important for virus morphogenesis. *Virology*. 2003 Jun 5;310(2):235-44.
79. Duda A, Stange A, Lüftenegger D, Stanke N, Westphal D, Pietschmann T, Eastman SW, Linial ML, Rethwilm A, Lindemann D. Prototype foamy virus envelope glycoprotein leader peptide processing is mediated by a furin-like cellular protease, but cleavage is not essential for viral infectivity. *J Virol*. 2004 Dec;78(24):13865-70.
80. Geiselhart V, Bastone P, Kempf T, Schnölzer M, Löchelt M. Furin-mediated cleavage of the feline foamy virus Env leader protein. *J Virol*. 2004 Dec;78(24):13573-81.
81. Pietschmann T, Zentgraf H, Rethwilm A, Lindemann D. An evolutionarily conserved positively charged amino acid in the putative membrane-spanning domain of the foamy virus envelope protein controls fusion activity. *J Virol*. 2000 May;74(10):4474-82.
82. Lüftenegger D, Picard-Maureau M, Stanke N, Rethwilm A, Lindemann D. Analysis and function of prototype foamy virus envelope N glycosylation. *J Virol*. 2005 Jun;79(12):7664-72.
83. Wilk T, de Haas F, Wagner A, Rutten T, Fuller S, Flügel RM, Löchelt M. The intact retroviral Env glycoprotein of human foamy virus is a trimer. *J Virol*. 2000 Mar;74(6):2885-7.
84. Wang G, Mulligan MJ. Comparative sequence analysis and predictions for the envelope glycoproteins of foamy viruses. *J Gen Virol*. 1999 Jan;80(Pt 1):245-54.
85. Goepfert PA, Shaw KL, Ritter GD Jr, Mulligan MJ. A sorting motif localizes the foamy virus glycoprotein to the endoplasmic reticulum. *J Virol*. 1997 Jan;71(1):778-84.
86. Goepfert PA, Shaw K, Wang G, Bansal A, Edwards BH, Mulligan MJ. An endoplasmic reticulum retrieval signal partitions human foamy virus maturation to intracytoplasmic membranes. *J Virol*. 1999 Sep;73(9):7210-7.
87. Stanke N, Stange A, Lüftenegger D, Zentgraf H, Lindemann D. Ubiquitination of the prototype foamy virus envelope glycoprotein leader peptide regulates subviral particle release. *J Virol*. 2005 Dec;79(24):15074-83.
88. Stange A, Lüftenegger D, Reh J, Weissenhorn W, Lindemann D. Subviral particle release determinants of prototype foamy virus. *J Virol*. 2008 Oct;82(20):9858-69.

References

89. Klein F, Diskin R, Scheid JF, Gaebler C, Mouquet H, Georgiev IS, Pancera M, Zhou T, Incesu RB, Fu BZ, Gnanapragasam PN, Oliveira TY, Seaman MS, Kwong PD, Bjorkman PJ, Nussenzweig MC. Somatic mutations of the immunoglobulin framework are generally required for broad and potent HIV-1 neutralization. *Cell*. 2013 Mar 28;153(1):126-38.
90. Reynaud CA, Garcia C, Hein WR, Weill JC. Hypermutation generating the sheep immunoglobulin repertoire is an antigen-independent process. *Cell*. 1995 Jan 13;80(1):115-25.
91. Wagner SD, Milstein C, Neuberger MS. Codon bias targets mutation. *Nature*. 1995 Aug 31;376(6543):732.
92. Mühle M, Bleiholder A, Kolb S, Hübner J, Löchelt M, Denner J. Immunological properties of the transmembrane envelope protein of the feline foamy virus and its use for serological screening. *Virology*. 2011 Apr 10;412(2):333-40.
93. Bleiholder A, Mühle M, Hechler T, Bevins S, vandeWoude S, Denner J, Löchelt M. Pattern of seroreactivity against feline foamy virus proteins in domestic cats from Germany. *Vet Immunol Immunopathol*. 2011 Oct 15;143(3-4):292-300.
94. Romen F, Pawlita M, Sehr P, Bachmann S, Schröder J, Lutz H, Löchelt M. Antibodies against Gag are diagnostic markers for feline foamy virus infections while Env and Bet reactivity is undetectable in a substantial fraction of infected cats. *Virology*. 2006 Feb 20;345(2):502-8.
95. Bleiholder A. Evaluation of the Feline Foamy Virus Envelope Glycoprotein as Scaffold for the Presentation of Epitope Sequences targeted by the HIV-1 broadly neutralizing antibodies 2F5 and 4E10. PhD thesis. Ruperto-Carola University of Heidelberg, Combined Faculties for the Natural Sciences and for Mathematics; 2012.
96. Engels B, Cam H, Schüler T, Indraccolo S, Gladow M, Baum C, Blankenstein T, Uckert W. Retroviral vectors for high-level transgene expression in T lymphocytes. *Hum Gene Ther*. 2003 Aug 10;14(12):1155-68.
97. Bastone P, Romen F, Liu W, Wirtz R, Koch U, Josephson N, Langbein S, Löchelt M. Construction and characterization of efficient, stable and safe replication-deficient foamy virus vectors. *Gene Ther*. 2007 Apr;14(7):613-20.
98. Stiegler G, Kunert R, Purtscher M, Wolbank S, Voglauer R, Steindl F, Katinger H. A potent cross-clade neutralizing human monoclonal antibody against a novel epitope on gp41 of human immunodeficiency virus type 1. *AIDS Res Hum Retroviruses*. 2001 Dec 10;17(18):1757-65.

References

99. Buchacher A, Predl R, Strutzenberger K, Steinfellner W, Trkola A, Purtscher M, Gruber G, Tauer C, Steindl F, Jungbauer A, Katinger H. Generation of human monoclonal antibodies against HIV-1 proteins; electrofusion and Epstein-Barr virus transformation for peripheral blood lymphocyte immortalization. *AIDS Res Hum Retroviruses*. 1994 Apr;10(4):359-69.
100. Purtscher M, Trkola A, Grassauer A, Schulz PM, Klima A, Döpfer S, Gruber G, Buchacher A, Muster T, Katinger H. Restricted antigenic variability of the epitope recognized by the neutralizing gp41 antibody 2F5. *AIDS*. 1996 Jun;10(6):587-93.
101. Purtscher M, Trkola A, Gruber G, Buchacher A, Predl R, Steindl F, Tauer C, Berger R, Barrett N, Jungbauer A, Katinger H. A broadly neutralizing human monoclonal antibody against gp41 of human immunodeficiency virus type 1. *AIDS Res Hum Retroviruses*. 1994 Dec;10(12):1651-8.
102. Schild TA. Einführung in die Real-Time TaqMan™ PCR-Technologie. Applied Biosystems GmbH, Weiterstadt. 2.1:1-118.
103. The In-Fusion HD Protocol Overview. Protocol No. PT5162-1; Version No. 072012. [www.clontech.com]
104. Ho J, Platz D, Liu B, Helsel C, Yokobata K. Assaying Sf9 Insect Cells with Guava® ViaCount® Flex: A Validation Study. Guava Technologies, Inc. 25801 Industrial Blvd., Hayward, CA 94545 USA. 2003;
105. Tiscornia G, Singer O, Verma IM. Production and purification of lentiviral vectors. *Nat Protoc*. 2006;1(1):241-5.
106. Huang ZM, Yen TS. Hepatitis B virus RNA element that facilitates accumulation of surface gene transcripts in the cytoplasm. *J Virol*. 1994 May;68(5):3193-9.
107. Donello JE, Loeb JE, Hope TJ. Woodchuck hepatitis virus contains a tripartite posttranscriptional regulatory element. *J Virol*. 1998 Jun;72(6):5085-92.
108. Lentiviral Packaging Plasmids. Addgene, Lentiviral Plasmids. [http://www.addgene.org/lentiviral/packaging/]
109. Cronin J, Zhang XY, Reiser J. Altering the tropism of lentiviral vectors through pseudotyping. *Curr Gene Ther*. 2005 Aug;5(4):387-98.
110. Sanyal D, Kudesia G, Corbitt G. Comparison of ultracentrifugation and polyethylene glycol precipitation for concentration of hepatitis B virus (HBV) DNA for molecular hybridisation tests and the relationship of HBV-DNA to HBe antigen and anti-HBe status. *J Med Microbiol*. 1991 Nov;35(5):291-3.

References

111. Real-time PCR Ct-values. WVDL, Wisconsin Veterinary Diagnostic Laboratory. CL-RES-18:1/27/14. [<http://www.wvdl.wisc.edu/>]
112. Yin W, Xiang P, Li Q. Investigations of the effect of DNA size in transient transfection assay using dual luciferase system. *Anal Biochem.* 2005 Nov 15;346(2):289-94.
113. Kumar M, Keller B, Makalou N, Sutton RE. Systematic determination of the packaging limit of lentiviral vectors. *Hum Gene Ther.* 2001 Oct 10;12(15):1893-905.
114. Fischer D, Bieber T, Li Y, Elsässer HP, Kissel T. A novel non-viral vector for DNA delivery based on low molecular weight, branched polyethylenimine: effect of molecular weight on transfection efficiency and cytotoxicity. *Pharm Res.* 1999 Aug;16(8):1273-9.
115. Burns JC, Friedmann T, Driever W, Burrascano M, Yee JK. Vesicular stomatitis virus G glycoprotein pseudotyped retroviral vectors: concentration to very high titer and efficient gene transfer into mammalian and nonmammalian cells. *Proc Natl Acad Sci U S A.* 1993 Sep 1;90(17):8033-7.
116. Yee JK, Miyanojara A, LaPorte P, Bouic K, Burns JC, Friedmann T. A general method for the generation of high-titer, pantropic retroviral vectors: highly efficient infection of primary hepatocytes. *Proc Natl Acad Sci U S A.* 1994 Sep 27;91(20):9564-8.
117. Chateauvieux S, Morceau F, Dicato M, Diederich M. Molecular and therapeutic potential and toxicity of valproic acid. *J Biomed Biotechnol.* 2010;2010:p11: 479364.
118. Kim MS, Blake M, Baek JH, Kohlhagen G, Pommier Y, Carrier F. Inhibition of histone deacetylase increases cytotoxicity to anticancer drugs targeting DNA. *Cancer Res.* 2003 Nov 1;63(21):7291-300.
119. Jeng JH, Kuo MY, Lee PH, Wang YJ, Lee MY, Lee JJ, Lin BR, Tai TF, Chang MC. Toxic and metabolic effect of sodium butyrate on SAS tongue cancer cells: role of cell cycle deregulation and redox changes. *Toxicology.* 2006 Jun 15;223(3):235-47.
120. Backliwal G, Hildinger M, Kuettel I, Delegrange F, Hacker DL, Wurm FM. Valproic acid: a viable alternative to sodium butyrate for enhancing protein expression in mammalian cell cultures. *Biotechnol Bioeng.* 2008 Sep 1;101(1):182-9.
121. Spencer A. Enhancing lentiviral transduction efficiency. Sigma-Aldrich. 2011;LSI Edition 25:5. [<http://www.sigmaaldrich.com/technical-documents/articles/life-science-innovations/enhancing-lentiviral.html>]

122. Cui Y, Chang LJ. Detection and Selection of Lentiviral Vector-Transduced Cells. In 'Lentivirus Gene Engineering Protocols (Methods in Molecular Biology). Volume 229'. 1st edition. Edited by Federico M. Humana Press; 2003. 69-85.
123. Zwick MB, Labrijn AF, Wang M, Spenlehauer C, Saphire EO, Binley JM, Moore JP, Stiegler G, Katinger H, Burton DR, Parren PW. Broadly neutralizing antibodies targeted to the membrane-proximal external region of human immunodeficiency virus type 1 glycoprotein gp41. *J Virol.* 2001 Nov;75(22):10892-905.
124. Brunel FM, Zwick MB, Cardoso RM, Nelson JD, Wilson IA, Burton DR, Dawson PE. Structure-function analysis of the epitope for 4E10, a broadly neutralizing human immunodeficiency virus type 1 antibody. *J Virol.* 2006 Feb;80(4):1680-7.
125. Zwick MB, Jensen R, Church S, Wang M, Stiegler G, Kunert R, Katinger H, Burton DR. Anti-human immunodeficiency virus type 1 (HIV-1) antibodies 2F5 and 4E10 require surprisingly few crucial residues in the membrane-proximal external region of glycoprotein gp41 to neutralize HIV-1. *J Virol.* 2005 Jan;79(2):1252-61.
126. Abbas AK, Lichtman AH, Pillai S. B Cell Activation and Antibody Production. In 'Cellular and Molecular Immunology'. 6th edition. Philadelphia: Saunders; 2007. 566.
127. Baumann JG, Günzburg WH, Salmons B. CrFK feline kidney cells produce an RD114-like endogenous virus that can package murine leukemia virus-based vectors. *J Virol.* 1998 Sep;72(9):7685-7.
128. Yoshikawa R, Sato E, Igarashi T, Miyazawa T. Characterization of RD-114 virus isolated from a commercial canine vaccine manufactured using CRFK cells. *J Clin Microbiol.* 2010 Sep;48(9):3366-9.

Curriculum vitae

Personal data:

Name: **Gerald Schneikart**
Date of birth: **xxx**
Address: **xxx**
xxx
Marital status: **unmarried**

School education:

1995 - 1999 Elementary school, Sta. Christiana, Wiener Neustadt, Austria
1999 - 2007 Humanistic high school, BG Babenbergerring, Wiener Neustadt, Austria
June 2007 Secondary school leaving examination:
Matura at Bundesgymnasium Babenbergerring, Wiener Neustadt, Austria
Written examinations: German, math, Latin, computer science
Oral examinations: English, German, biology

Language study trips:

August 2004 Eastbourne, United Kingdom
March 2005 Malta

Basic military service:

July 2007 – January 2008

Summer jobs:

2006, 2008 - 2011 Employee at the community of Neudörfel, Burgenland, Austria

Education:

2008 - 2011 Completed Bachelor's degree in Molecular Biology, University of Vienna
March 2011 Tutorial assistant at a chemistry exercise, University of Vienna
March 2013 Tutorial assistant at a biochemistry exercise, University of Vienna
2011 - 2014 Master study course in Molecular Medicine, University of Vienna
2013 Master's thesis at the Robert Koch-Institute in Berlin, Germany
Fachgebiet 18, „Zentrum für HIV und andere Retroviren“

Semester abroad:

Sept. - Dec. 2012 Department of Biochemistry, University of Oulu, Finland

Additional knowledge:

English: Classes in Finland were taken in English
Completed class in Writing and speaking scientific English
MS Office: Word, Excel, PowerPoint, Outlook; ECDL Core

Personal interests:

Nutrition and fitness training